

Novel Microfluidic Devices for Diagnosis and Treatment of Blood Disorders in Vulnerable
Pediatric Populations

by
Dalia L. Lezzar

A dissertation submitted to the Department of Biomedical Engineering
Cullen College of Engineering
in partial fulfillment of the requirements for the degree of

Doctor of Philosophy
in Biomedical Engineering

Chair of Committee: Dr. Sergey S. Shevkoplyas

Committee Member: Dr. Fong W. Lam

Committee Member: Dr. Sheereen Majd

Committee Member: Dr. Chandra Mohan

Committee Member: Dr. Tianfu Wu

University of Houston
August 2021

Copyright 2021, Dalia L. Lezzar

This work is dedicated to my Uyghur and Palestinian brothers and sisters

I will keep fighting for you

ACKNOWLEDGMENTS

First, I would like to thank my advisor, Dr. Sergey Shevkoplyas, for his support and guidance throughout my graduate school career. I thank you for all your feedback and for always pushing me to work smarter and to always take step back and think of the bigger picture.

Next, I want to thank Dr. Fong Lam for his mentorship, clinical insights, and for showing me how truly invaluable a good and kind collaborator is for any endeavor. Thank you for showing me how my research could have a real-world and positive impact on peoples' lives.

I would like to thank my committee members, Dr. Shereen Majd, Dr. Chandra Mohan, and Dr. Tianfu Wu for giving me their time and their valued insights and advice to make my research the best that it can be. I thank you for your continual support and guidance throughout my graduate school process, from my time in your classes, to my qualifying exam, and to my final defense.

I would also like to thank Dr. Metin Akay and Dr. Yasemin Akay for their continuous personal support and encouragement throughout my time in the Biomedical Engineering Department. Your kind words have always been greatly appreciated.

I want to thank all my lab members, past and present, that I have had the opportunity to work with over the years. I thank you for helping to push my projects forward and for allowing me grow both as a mentee as well as a mentor.

I would like to show my sincere gratitude and a very special thank you to my friend and lab mate Madeleine. You have been my mentor, my counselor, my cheerleader, my partner in crime, but most importantly, my friend. Your constant support and encouragement every step of the way have meant the world to me, and I genuinely could not have done it without you.

Last, but certainly not least, I would like to express my eternal gratitude to my family and friends for their constant and wholehearted love and support throughout my entire life and through this graduate school journey. Thank you for always standing beside me, propping me up, and reminding me of what is truly important. Without you, none of this would have ever been possible; my success is your success.

ABSTRACT

Blood is a complex suspension made up of four main components: plasma, platelets (PLT), red blood cells (RBC), and white blood cells (WBC). The ability to separate blood into its individual parts is a critical first step for blood analysis, clinical diagnosis, and biological research. Conventional blood separation techniques typically require bulky instrumentation and complex procedures at prohibitive costs, making them less widely available in resource-limited settings with underdeveloped healthcare infrastructure and to some populations of high-risk pediatric patients. To address these limitations, this work focuses on the development of two novel microfluidic technologies capable of processing blood for diagnostic and treatment purposes.

This dissertation first reports on a paper-based microfluidic device designed to enable universal newborn screening and rapid diagnosis of sickle cell anemia (SCA), a common inherited blood disorder causing lifelong morbidities. Our diagnostic device takes advantage of the structural difference between diseased hemoglobin, found within sickle RBC, and healthy hemoglobin to provide a distinct visual diagnosis for SCA rapidly and at a fraction of the cost of conventional approaches. The test kit can be prepared with easily accessible food-grade ingredients and has a long shelf-life, enabling its deployment even in remote resource-limited settings.

The efficient and high-throughput separation of WBC directly from whole blood—typically performed using a process called leukapheresis—is crucial in many areas of medicine, including life-saving leukodepletion procedures and many novel cell therapies. Unfortunately, this established treatment method is not available to neonates and low-weight infants due to the large extracorporeal volume of the machines and

significant risks associated with the procedures. This dissertation presents a small, microfluidic device capable of removing WBC from blood recirculating through a closed-loop circuit, with a separation efficiency and volumetric throughput on par with conventional, centrifugation-based leukapheresis. This device could provide a viable treatment alternative for underserved pediatric patients with leukemia, a common blood cancer for which leukapheresis is indicated.

If adopted, the microfluidic tools discussed in this dissertation could drastically improve the quality and accessibility of clinical care for millions of individuals worldwide, regardless of socioeconomic status or patient size.

TABLE OF CONTENTS

Acknowledgments	iv
Abstract.....	vi
Table of Contents	viii
List of Tables	ix
List of Figures.....	x
Chapter 1: Background.....	1
Chapter 2: Paper-based microfluidic device for newborn screening for rapid diagnosis of sickle cell anemia	12
OVERVIEW	12
INTRODUCTION	13
METHODS	16
RESULTS	22
DISCUSSION	31
Chapter 3: Recent advances towards passive microfluidic technologies for high throughput leukapheresis of whole blood ..	36
OVERVIEW	36
INTRODUCTION	37
PASSIVE MICROFLUIDIC DEVICES.....	41
DISCUSSION	67
CONCLUSION.....	71
Chapter 4: Towards centrifugation-free leukapheresis in pediatric patients using high-throughput microfluidic technology	73
OVERVIEW	73
INTRODUCTION	74
METHODS	76
RESULTS	80
DISCUSSION	94
CONCLUSION.....	101
Chapter 5: Final Conclusions	102
CONCLUSIONS.....	102
References.....	105

LIST OF TABLES

Table 1. Detailed cost breakdown of the paper-based SCA screening test kit components	30
Table 2. Overview of the microfluidic approaches discussed in this work and their performance metrics.	70
Table 3. Free hemoglobin (Hb) and potassium (K ⁺) measurements taken before, during, and immediately after the 12 consecutive rounds of recirculation through the device; and measurements taken from a control blood sample left to sit in a tube on the lab bench at room temperature.	94

LIST OF FIGURES

Figure 1. (a) Photograph of the paper-based SCA diagnostic kit with all components necessary to perform the test. (b) Schematic illustration of the steps to perform the test. (c) Representative bloodstains produced by the metabisulfite and hydrosulfite versions of the test for samples with various HbS concentrations.	20
Figure 2. Aggregate confusion matrix for screening of blood samples with characteristic HbS concentrations via visual interpretation of the blood stains produced on paper by the (a) metabisulfite (MS) formulation of the test (555 total scores) and (b) hydrosulfite (HS) formulation of the test (429 total scores).....	26
Figure 3. Representative images of blood stains demonstrating the reagent stability of the metabisulfite (MS) and hydrosulfite (HS) formulations of the paper-based SCA screening test under wet and dry storage conditions.	29
Figure 4. Fundamental principles of size-based separation of cells described in some of the publications reviewed in this work.	42
Figure 5. Principles behind cell separation using combinatorial microfluidic approaches. (a) Size-based particle margination due to triangular channel expansions. (b) Size-based particle diffusion within a co-flow system. (c) Size-based particle separation using controlled incremental filtration.....	63
Figure 6. Design of the microfluidic device for leukodepletion of blood using controlled incremental filtration (CIF). (a) Schematic of blood cells (WBC, RBC, and PLT) cells flowing through the CIF device. (b) Components of the device. (c) An assembled microfluidic device comprised of 48 multiplexed CIF elements.....	82
Figure 7. Performance of the multiplexed CIF device depending on (a) sample HCT, (b) device flow ratio, and (c) sample flow rate.....	85
Figure 8. Removal of WBCs from blood during recirculation. (a) Experimental setup used for the recirculation experiments. (b) Changes in cell concentrations following each round of CIF-based cell separation in the recirculation regime.....	88
Figure 9. Effect of CIF processing on the activation state of WBCs and PLTs. Activation of (a) WBCs (CD11b) remaining in the recirculating blood, (b) WBCs (CD11b) removed with the retentate (waste), and (c) Recirculating PLTs (CD62P). (d) Formation of PLT-WBC aggregates in the recirculating blood..	91

CHAPTER 1: BACKGROUND

This chapter highlights some of the key concepts discussed in this dissertation as well as the aims and goals for this research.

Whole Blood

The circulation of blood throughout the body is paramount in maintaining homeostasis. Circulating blood serves to distribute essential nutrients and oxygen to the organs, transport metabolic waste products for removal, regulate pH and temperature, and deliver different cells throughout the body where they are needed.^{1,2} Whole blood (WB) is complex suspension composed of the following: plasma, platelets (PLT; thrombocytes), red blood cells (RBC; erythrocytes), and white blood cells (WBC; leukocytes). Other rarer cells, have also been detected in the circulation, such as hematopoietic stem cells (e.g., megakaryocytes, erythroblasts)³, fetal cells during pregnancy, and tumor cells in cancer patients.¹

Each component of WB has a different, highly specific, and vital role in maintaining homeostasis. The plasma is the fluid component of blood, containing the cells in addition to proteins, enzymes, hormones, and macro- and micronutrients.⁴ Platelets are small (2-4 μm) anucleate cell fragments of megakaryocytes that play an important role in primary homeostasis to prevent and control bleeding. More recent data also suggest that PLT also function as inflammatory mediators^{5,6} and in wound healing.^{7,8} Erythrocytes are the most abundant cell type, constituting 99% of all the blood cells and representing 40-45% of the total circulating blood volume.⁹ Normal

RBC are approximately 6.2–8.2 μm in diameter with a thickness of 2–2.5 μm ,¹⁰ and form a biconcave disk shape that provides a large surface-to-volume ratio. RBC are highly specialized and well adapted for their primary function of efficiently transporting oxygen on hemoglobin from the lungs to the tissues.¹¹ WBC are normally spherical in shape with their size ranging from 7 to 20 μm in diameter, and these cells are an integral part of the body's immune system. Although WBC only account for approximately 1% of the blood, they play an essential role in wound healing¹²⁻¹⁵ as well as the defense against invading microorganisms. Leukocytes can further be divided into 5 subtypes: neutrophils, lymphocytes, monocytes, basophils, and eosinophils. These highly specialized cells all contribute to different aspects of human immune system. Their total and differential counts in circulation can therefore be an important indicator for several immunological diseases. WBC counts can be used for diagnosis, to monitor disease progression, or to ascertain the efficacy of treatment regimens.^{16,17}

Sickle Cell Anemia & Diagnosis

Hemoglobin (Hb) is the metalloprotein molecule found within human RBC that enables the binding and transport of oxygen from the lungs to tissues and organs throughout the body. Healthy adult Hb is a multi-subunit globular protein made up of two alpha- and two beta-globin chains that contain iron-based heme groups for binding oxygen.¹⁸ Sickle cell disease (SCD) refers to a group of common recessively inherited hemoglobin disorders associated with significant lifelong morbidities and premature mortality. This hemoglobinopathy is caused a single nucleotide mutation (i.e., adenine to thymine; GAG to GTC; glutamic acid to valine) of the β -globin gene which encodes

the beta-globin protein chain subunits that make up hemoglobin molecules.¹⁸ SCD results from the inheritance of this mutated allele coding for the β -globin subunit of hemoglobin along with another mutated allele coding for the same or another aberrant form of hemoglobin ^{18,19}. The mutated β -globin allele results in the production of sickle hemoglobin (HbS), a form of hemoglobin (Hb) that polymerizes when deoxygenated, unlike normal adult hemoglobin (HbA). The polymerization of deoxy-HbS molecules into rigid fibers deforms the red blood cell (RBC) membrane and causes the characteristic ‘sickled’ shape of affected sickle RBCs. Sickle RBCs are markedly less deformable and more fragile than normal, healthy RBCs, which causes them to occlude blood vessels, cause chronic ischemia-reperfusion injury, and lyse frequently, resulting in severe anemia, chronic painful episodes, and predisposition to infection ^{20,21}.

When the allele coding for HbS is inherited heterozygously with the allele coding for HbA (i.e., genotype *HbAS*) it causes what is known as sickle cell trait (SCT) where both forms of Hb are produced and individuals are typically healthy, do not need medical intervention related to HbS, and may have improved resistance to parasites such as *Plasmodium falciparum* ^{20,21}. In Angola, for example, the HbS allele is present in over 20% of the population, with about 98% of those carriers having the allele heterozygously ^{22,23}. However, when the HbS allele is inherited homozygously (i.e., genotype *HbSS*), it causes sickle cell anemia (SCA), a condition in which 40–100% of all Hb produced is HbS and individuals experience some of the most severe symptoms associated with SCD. Homozygous inheritance of the HbS allele and an allele coding for another non-HbS, aberrant form of Hb results in other, less common forms of SCD which have varying degrees of clinical severity ^{24,25}.

SCD affects millions of individuals worldwide, with approximately 300,000 affected births each year and the majority of these births occurring in sub-Saharan Africa, Central America, South America, southern Asia, the Mediterranean basin, and South America.^{19,26} Opportunistic infections associated with SCD make affected children under 5 years of age much higher risk of premature death.²⁷ While the severity of SCD can vary greatly between patients, the frequency and severity of adverse events (e.g., strokes, vaso-occlusive crises) can be reduced if the intraerythrocytic HbS concentration is maintained below 30% with proper treatment.^{21,28} Early detection and accurate and frequent quantification of HbS concentration is crucial for providing life-saving treatment for SCD.^{21,27}

Current diagnosis and monitoring techniques for SCD involve the detection of abnormal hemoglobin in a patient's blood. These established methods include high-performance liquid chromatography (HPLC), hemoglobin electrophoresis (HE), isoelectric focusing (IEF), and hemoglobin solubility assays. HPLC is largely considered to be the 'gold standard' for SCD diagnosis and monitoring HbS concentration. The process utilizes the differences in attraction between and absorbent materials and the various forms of hemoglobin for identification and quantification of the types of hemoglobin (HbA, HbS, fetal Hb, etc.) present in a blood sample²⁹. The different forms of hemoglobin are attracted at different degrees to the porous absorbent material and therefore take different amounts of time to pass through the HPLC column.³⁰ The amount of hemoglobin leaving the column is measured continuously over time, and a quantitative measure of the concentrations of each form of hemoglobin are provided.²⁹

HE is a method that applies the principles of gel electrophoresis which uses the variations in charge between the different forms of hemoglobin to provide a semi-quantitative assessment of the types and relative amounts of hemoglobin present in a blood sample.³¹ Applying an electric current across a two-dimensional porous agarose gel causes hemoglobin to migrate through the gel from the cathode side to the anode side. Different forms of hemoglobin move through the gel at different speeds depending on the specific charge of the hemoglobin molecules. Depending on their speed of travel, the different forms of hemoglobin form separate bands within the gel. Analysis on these bands and their positions within the gel can be used to calculate the percentages of various forms of hemoglobin present in the sample.³¹

Similar to HE, IEF is another form of electrophoresis that uses the variations in isoelectric points between the different forms of hemoglobin to provide a semi-quantitative assessment of the types and relative amounts of hemoglobin present in a blood sample.³² The isoelectric point is the pH at which a particular molecule has no net electric charge. For IEF, an electric current is applied to a porous gel that contains a pH gradient along the same axis as the current. The hemoglobin from the loaded sample migrates through the gel from the cathode side to the anode side, coming to rest at the position where the pH of the gel results in no net charge for the hemoglobin molecule. The positions in the gel at which the different forms of hemoglobin come to rest depends on the specific charge of the hemoglobin molecules. Depending on their isoelectric point, the different forms of hemoglobin form distinct bands within the gel.³³ Analysis on these bands and their positions within the gel can be used to calculate the percentages of various forms of hemoglobin present in the sample.

Solubility-based assays capitalize on the difference in solubility between deoxygenated HbS and other forms of hemoglobin to detect the presence of HbS in a sample. In high osmolarity solutions, HbS polymerizes when deoxygenated while normal adult hemoglobin remains soluble under the same conditions.³⁴ For sickle hemoglobin solubility assays, a sample of whole blood is added to a solubility buffer containing reagents that first lyse the RBC and then deoxygenate the freed hemoglobin. Analysis of the turbidity of the mixture is then done by eye, with a high turbidity indicating the presence of insoluble HbS.³⁵ Unlike HPLC, HE, and IEF, solubility-based assays are not quantitative and are only capable of determining whether any HbS is present. Solubility assays are therefore typically used to screen for SCD, with a positive result indicating the need for further testing using more informative and extensive laboratory-based methods.

Leukemia & Treatment

Leukemia refers to a group of blood cancers that typically begin in the bone marrow and lead to the production of large numbers of abnormal blood cells. These cells, known as blasts, are not fully developed and sometimes dysfunctional when they exit the bone marrow and enter the blood stream.³⁶ Approximately 3000 children are diagnosed with leukemia every year in the United States.³⁷ Pediatric leukemia is the most common malignancy affecting children, accounting for 31% of cancers that occur before 15 years of age and 25% that occur before 20 years of age.³⁸

A high WBC count is characteristic of leukemia that presents in most afflicted patients before treatment. The excessive number of immature WBC can interfere with

the production and level of other cells, causing harmful imbalances in blood cell counts. Due to the lack of healthy and functional blood cells in circulation, symptoms of leukemia can include bruising, fatigue, fever, and an increased risk of opportunistic infections.³⁶ High numbers of leukemic white blood cells, or blasts, cause damage to the bone marrow and can result in a lack of platelet production, which can affect the blood clotting process, and red blood cell production, which can lead to anemia. If leukemic cells spread and cross into the central nervous system, neurological symptoms such as migraines, seizures, or coma can occur as a result of increased brain stem pressure.

In chronic leukemias, WBC counts may become high enough to cause leukostasis, or blood sludging. Leukostasis symptoms occur due to the inadequate delivery of oxygen to tissues and critical-end organs due to the massive plugging of the microvasculature by overabundant WBCs. This can affect retinal vasculature causing vision changes, pulmonary vasculature causing shortness of breath due to decreased efficiency in oxygen exchange, as well as the vasculature in the brain which can lead to neurological deterioration. If left untreated, leukostasis has a high mortality rate.[Rollig, Ehninger 2015 Most forms of leukemia are treated with pharmaceutical intervention, most commonly combining a multi-drug chemotherapy. Some cases are treated with radiation therapy or bone marrow transplants.

Malignant WBC depletion can be indicated to urgently reduce dangerously high WBC counts while chemotherapies or other treatments take into effect. Leukodepletion is indicated to rapidly reduce an excessively elevated WBC count in patients with symptomatic hyperleukocytosis (WBC count >50,000-100,000/ μ L). These cases

typically have pulmonary or neurologic dysfunction[Blum, 2007; Rollig, 2015; Porcu, 2002; Creutzig, 2016; Runco, 2018] caused by leukostasis, and are therefore considered a medical emergency requiring urgent treatment.

For individuals with leukemia, apheresis can be used to rapidly reduce WBC counts to alleviate the symptoms while cytoreductive chemotherapy is taking effect ³⁹⁻⁴². Apheresis is a general term to denote removal of a certain component from WB, such as plasma (plasmapheresis), RBC (erythrocytapheresis), and WBC (leukapheresis).⁴³ Leukapheresis is a medical and laboratory procedure in which WBC are separated from a sample of WB using centrifugation. Blood is continuously removed from a patient by an apheresis machine to separate WBC from the rest of the blood (comprising plasma, PLT, and RBC), which is then returned back to the body.⁴⁴⁻⁴⁶ This procedure is used throughout the practice of medicine for two main applications, leukodepletion and cellular collection.

In addition to its applications for leukemia, the removal of activated immune WBCs from the patient's blood stream also makes leukodepletion an attractive drug-free treatment modality for a number of other emergent indications, such as inflammatory bowel disease, ⁴⁷⁻⁴⁹ steroid-resistant nephrotic syndrome,⁵⁰ and refractory systemic juvenile idiopathic arthritis ⁵¹. Leukapheresis has also been routinely used for the collection of mononuclear cells (MNCs) from peripheral blood of patients to enable a wide range of cellular therapies,⁵²⁻⁵⁸ including hematopoietic stem cell transplantation,⁵⁹⁻⁶¹ and potentially curative gene-based therapies.^{62,63} Cellular collection is also the initial step for an increasing number of highly effective cell-based

treatments for some of the most devastating hematologic and immune system disorders affecting millions of adults and children worldwide.^{40,41,48-50,53-55,59,60}

Leukapheresis procedures use specialized apheresis machines that work to fractionate blood using gentle pressure and return it back to the body at a stable temperature. The most common apheresis method separates cells by density using centrifugation methods. These methods can be divided into two basic categories: Continuous flow centrifugation (CFC) and Intermittent flow centrifugation (IFC).⁶⁴ CFC is the most common form of apheresis which involves the removal of blood from one venipuncture site, spinning and blood fractionation in a chamber, and the return of apheresed blood through a separate venipuncture site simultaneously. The biggest advantage of this method is the low extracorporeal volume of the system, which is most important for elderly and pediatric patients. Extracorporeal volume is calculated using the volume of the apheresis chamber, as well as the hematocrit and total blood volume of the patient. IFC operates in cycles, taking blood from the patient, spinning and processing the sample, and then returning it to the body in a bolus. The use of a single venipuncture site is main advantage of this system. A leukapheresis procedure typically takes between one to three hours depending on the indications for the procedure and the specific apheresis system used.

Microfluidics

A critical first step in many preparative and analytical techniques in medicine and biology is to separate cells or other particles from a solution which may contain

other undesirable or non-target elements.⁶⁵ Separations of such particles are traditionally achieved through batch processing with centrifugation or filtration, which can have larger extracorporeal volume and complex procedures. Lab-on-a-chip devices refer to a class of devices capable of performing chemical or biological laboratory operations on a small scale.⁶⁶ Typically, these devices are designed with flow channels that have at least one dimension in the order of a few to a hundred microns, generally the height dimension. These devices are compact and are often cost effective easy to use, have lesser sample and reagent consumption, and have shorter processing times. Composed of micro- and nano-scale channels patterned in a bulk material (e.g., soft polymer, silicon, plastic, glass), lab-on-a-chip devices are designed to separate particles by their various properties including size, density, charge, and magnetic and dielectric susceptibilities.⁶⁵ These microfluidic platforms offer significant advantages for cell handling as they can manipulate particles, at the micron scale, using unique physical and flow phenomena while maintaining precise control of shear conditions within the microstructures, all with significantly lower extracorporeal volume.

The microfluidic techniques for separating specific particles from a heterogenous mixture can be categorized into two groups: active and passive methods. Active methods rely on external forces such as acoustic force, magnetic force, dielectrophoretic force, or a combination of these to isolate target particles and direct them into specific outlets. Passive techniques utilize the intrinsic properties of a device such as channel geometry, inherent hydrodynamic forces, and/or differences in particle characteristics such as shape, size, and deformability, to achieve efficient separation.^{67,68} Measuring the distribution of particles across the microchannel before exiting the

device or their distribution in specific outlets allows for these active and passive methods to be used for analytical and diagnostic applications. There have also been pioneering developments which enabled the design of microfluidic devices with integrated flow control modules such as small-scale valves, pumps, mixers etc. These additions make these microfluidic platforms compact and inexpensive by eliminating the need for external equipment.⁶⁹

Research Aims

The overall aims of this work include:

Aim 1: To engineer and validate a low-cost and rapid paper-based test capable of screening newborns for sickle cell anemia, specifically targeting limited-resource settings.

Aim 2: To survey the literature to determine the clinical need for alternatives to conventional leukapheresis procedures and to explore existing passive microfluidic techniques for the separation of white blood cells directly from whole blood with the potential to achieve microfluidic leukapheresis with a smaller footprint.

Aim 3: To engineer and validate a small microfluidic device capable of performing leukapheresis at throughputs and efficiencies comparable to conventional apheresis machines and investigating its potential as a viable alternative to leukapheresis for low-weight pediatric patients.

CHAPTER 2: PAPER-BASED MICROFLUIDIC DEVICE FOR NEWBORN SCREENING FOR RAPID DIAGNOSIS OF SICKLE CELL ANEMIA

The following research has previously been published and much of the following text is reprinted from: *MDPI Biosensors* (2017)

OVERVIEW

Sickle cell anemia (SCA) is a genetic blood disorder that is particularly lethal in early childhood. Universal newborn screening programs and subsequent early treatment are known to drastically reduce under-five SCA mortality. However, in resource-limited settings, cost and infrastructure constraints limit the effectiveness of laboratory-based SCA screening programs. To address this limitation our laboratory previously developed a low-cost, equipment-free, point-of-care, paper-based SCA test. Here, we improved the stability and performance of the test by replacing sodium hydrosulfite (HS), a key reducing agent in the hemoglobin solubility buffer which is not stable in aqueous solutions, with sodium metabisulfite (MS). The MS formulation of the test was compared to the HS formulation in a laboratory setting by inexperienced users ($n = 3$), to determine visual limit of detection (LOD), readout time, diagnostic accuracy, intra- and inter-observer agreement, and shelf life. The MS test was found to have a 10% sickle hemoglobin LOD, 21-minute readout time, 97.3% sensitivity and 99.5%

specificity for SCA, almost perfect intra- and inter-observer agreement, at least 24 weeks of shelf stability at room temperature, and could be packaged into a self-contained, distributable test kits comprised of off-the-shelf disposable components and food-grade reagents with a total cost of only \$0.21 (USD).

INTRODUCTION

Sickle cell disease (SCD) refers to a group of common recessively inherited hemoglobin disorders associated with significant lifelong morbidities and premature mortality. Sickle cell anemia (SCA)—the most common form of SCD—is a condition in which 40–100% of all hemoglobin (Hb) produced is mutated sickle hemoglobin (HbS) and individuals experience some of the most severe symptoms associated with SCD. HbS polymerizes when deoxygenated, unlike normal adult hemoglobin (HbA). The polymerization of deoxy-HbS molecules into rigid fibers deforms the red blood cell (RBC) membrane and causes the characteristic ‘sickled’ shape of affected sickle RBCs. Sickled RBCs are less deformable and more fragile causing them to occlude blood vessels, cause chronic ischemia-reperfusion injury, and lyse frequently, resulting in severe anemia, chronic painful episodes, and predisposition to infection ^{20,21}.

The mortality rate for SCA is the highest in the first five years of a child’s life, as young children are prone to acute infections and splenic sequestration crises ⁷⁰. Improvements in survival rates for SCA over the last few decades have been largely due to earlier diagnosis and the initiation of simple, inexpensive prophylaxis, such as penicillin, to combat opportunistic infections. Almost all children born in the United

States, and many other resource-rich countries, are screened for SCA at birth as part of universal newborn screening programs that test for diseases and conditions where early initiation of treatment is crucial for survival and healthy, normal development ⁷¹. However, due to cost and infrastructure limitations, this type of universal screening is oftentimes not feasible in the resource-limited settings where the incidence of HbS is highest, such as in sub-Saharan Africa, where approximately 80% of global individuals with SCA are born ^{19,21,72}. Nearly all children with SCA who are diagnosed soon after birth and promptly given treatment survive into adulthood, while the mortality rates for undiagnosed (and, therefore, untreated) children in sub-Saharan Africa are estimated to be as high as 50–90% by the age of five years ^{19,72}.

The implementation of wide-spread screening and follow-up care for individuals with SCA has been predicted to potentially save the lives of up to 10 million children by 2050 in the countries most affected by the disease (e.g., Nigeria, Angola, Democratic Republic of the Congo, India) ²⁴. Though highly successful, most of the pilot screening programs in these settings have used conventional diagnostic methods such as high-performance liquid chromatography (HPLC) or isoelectric focusing electrophoresis (IEF) to identify SCA, both of which are relatively high-cost, technically complex, and dependent on stable infrastructure ^{30,33}. The requirements and limitations of these conventional diagnostic methods limit screening to those born in major health centers, and prevent life-saving screening efforts from reaching more remote, less well-equipped community health outposts and those born out-of-hospital ^{33,73-75}.

In order to address these limitations, our research group recently developed a simple, equipment- and electricity-free, paper-based test capable of differentiating

normal (*HbAA*), SCT (*HbAS*), and SCA (*HbSS*) blood samples ^{76,77}. The paper-based test was previously shown to be accurate (93% sensitivity, 94% specificity for differentiating SCA), low-cost (\$0.07 in material and reagent costs), robust and easy to use (Angolan health workers were proficient in performing the test after one demonstration), and rapid (less than 30 min from start to readout) ⁷⁸. However, the previously-developed version of the paper-based SCA screening test required the use of a reducing agent—sodium hydrosulfite (HS)—which quickly becomes oxidized in aqueous solutions (especially when exposed to oxygen) ^{77,79}. The relative instability and volatility of HS made shipping and long-term storage of the previous version of the test impractical ^{78,79}. Here we describe how replacing HS with a higher concentration of sodium metabisulfite (MS) addressed the limitations of the previously-developed test without negatively impacting test performance. In this study we found that, compared to the previous test, the novel MS formulation of the paper-based SCA screening test has a superior limit of detection (10% vs. 20% HbS of total Hb content), faster readout time (21 min vs. 30 min), better diagnostic performance (97.3% sensitivity, 99.5% specificity for differentiating SCA), high intra- and inter-observer agreement ($\kappa = 0.93$, $\kappa = 0.87$ respectively), longer shelf stability at room temperature (at least 24 weeks vs. one week for aqueous storage conditions), and could be packaged into a self-contained, distributable test kit with a total cost of only \$0.21 (USD).

METHODS

Blood samples

The study protocol was approved by the University of Houston and Baylor College of Medicine institutional review boards. Venous whole blood samples were obtained with written informed consent in 4 mL Vacutainer tubes (K₂EDTA, BD, Franklin Lakes, NJ, USA) from healthy, normal volunteers and patients of the Texas Children's Hematology Centers (Houston, TX, USA). Blood samples were stored at 4 °C and used within two months following collection. The sickle hemoglobin (HbS) content of blood samples from individuals with sickle cell anemia (SCA) was quantified with high-performance liquid chromatography (HPLC; Primus Ultra Variant, Trinity Biotech, Wicklow, Ireland). Healthy volunteers were assumed to have 0% HbS. Hematocrit (Hct) and hemoglobin concentration (⁸⁰) were measured with an automated hematology analyzer (Medonic, Boule Medical AB, Spånga, Sweden), and ABO-RhD blood type was determined using blood type test kits (EldonCard, Eldon Biologicals, Gentofte, Denmark).

Artificially-reconstituted blood samples with specific Hct (22%—a physiological Hct for SCA) and HbS concentrations (0, 10, 20, 40, and 80% HbS) were made by combining type-matched blood samples from normal (*HbAA*) and SCA (*HbSS*) individuals. Sample Hct was adjusted via centrifugation at 500× *g* for 10 min (Beckman Microfuge 22R, Beckman Coulter, Brea, CA, USA) and reconstitution of red blood cell (RBC) sediment in autologous plasma. The type-matched and Hct-matched *HbAA* and *HbSS* blood samples were then combined at various ratios according to the following equation:

$$\%HbS = \frac{([Hb]_{HbSS})(V_{HbSS})(\%HbS_{HbSS})}{([Hb]_{HbSS})(V_{HbSS}) + ([Hb]_{HbAA})(V_{HbAA})}$$

where V is the volume, subscripted $HbSS$ refers to samples from patients with SCA, and subscripted $HbAA$ refers to samples from healthy, normal volunteers.

For this study, venous blood samples were collected as described above. For the self-contained SCA screening test kit, capillary blood can be collected via finger or heel prick. Capillary and venous blood have both been shown to produce comparable diagnostic results for the assay⁷⁷⁻⁷⁹. Additionally, the HS version of the paper-based SCA screening test has been previously shown to be robust against variations in Hct and associated variations in⁸⁰ within the physiological range^{77,78}. Physiological concentrations of fetal hemoglobin (HbF) amongst infants, adults, and hydroxyurea patients were also shown to not impact test performance^{77,78}.

Blood samples used to perform the study of test kit stability were replaced with new samples—with the same Hcts and HbS concentrations—after 20 days of storage at 4 °C in order to counteract any potential effects due to storage-based RBC and/or Hb deterioration (i.e., storage lesion).

Hemoglobin Solubility Buffers

The hemoglobin solubility buffers compared in this study each consisted of three components: saponin (Sigma-Aldrich, St. Louis, MO, USA), a reducing agent, and a concentrated phosphate buffer⁷⁶⁻⁷⁹. Potassium phosphate buffer at 2.49 M was made by dissolving solid 1.24 M (169 g/L) monobasic and 1.25 M (217 g/L) dibasic potassium phosphate (Sigma-Aldrich, St. Louis, MO, USA) in deionized water. Saponin (4 g/L) was added to irreversibly lyse RBCs by creating holes in the lipid bilayer through

sequestration of cholesterol, thereby releasing hemoglobin into the buffer ⁷⁸. The saponin used in this study was obtained from Quillaja bark (sapogenin content not less than 10%) and contained impurities which made the powder hygroscopic ⁸¹. The reducing agent—either HS (30 g/L; 3% w/v; Sigma-Aldrich, St. Louis, MO, USA) or MS (100, 150 or 200 g/L; 10, 15, 20% w/v; Sigma-Aldrich, St. Louis, MO, USA)—then converts the released Hb into deoxy-Hb, which is either soluble (e.g., deoxy-HbA, deoxy-HbF, deoxy-HbC) or insoluble (deoxy-HbS) in the phosphate buffer ⁷⁶⁻⁷⁹. Additionally, buffer consisting of food-grade MS (Duda Energy LLC, Decatur, AL, USA) and food-grade saponin (Desert King, San Diego, CA, USA) was made using the same concentrations as above.

The stability of the MS and HS solubility buffers was compared under two storage conditions: ‘wet’ and ‘dry’. Dry refers to the saponin and MS or HS being stored in dry powdered form and mixed with concentrated phosphate buffer on the day of the experiment, while wet refers to dry reagents premixed with concentrated phosphate buffer and stored until the day of the experiment. Individual sets of reagents were stored within heat-sealed polyethylene-lined 2 mm thick foil pouches (Xin Jiu Technology, Taoyuan, Taiwan) to prevent exposure of reducing agents and hygroscopic compounds in saponin to oxygen and humidity outside of the packaging. The reagents were stored and tested at room temperature (18–26 °C, 30–50% relative humidity). The buffers were stored between one and 166 days before use. Results from tests performed using stored buffers were compared against those for reagents prepared on the same day of the experiment from dry powdered ingredients stored in their original containers.

Design and Operation of the Paper-Based Test

The design and operation of the paper-based SCA screening test have previously been described in detail ^{76-79,82}. Briefly, 20 μL of whole blood is collected and mixed with Hb solubility buffer by inversion, the blood and buffer mixture is allowed to incubate at room temperature for 10 min, 20 μL of blood is then dropped onto chromatography paper (Whatman Chr 1, Sigma-Aldrich, St. Louis, MO, USA) and allowed to dry (**Figure 1b**). Insoluble deoxy-HbS polymers, if present, become entangled in the paper substrate and form a dark red spot in the center of the stain, while soluble forms of Hb wick laterally through the paper pores and produce a more diffuse pink ring (**Figure 1c**).

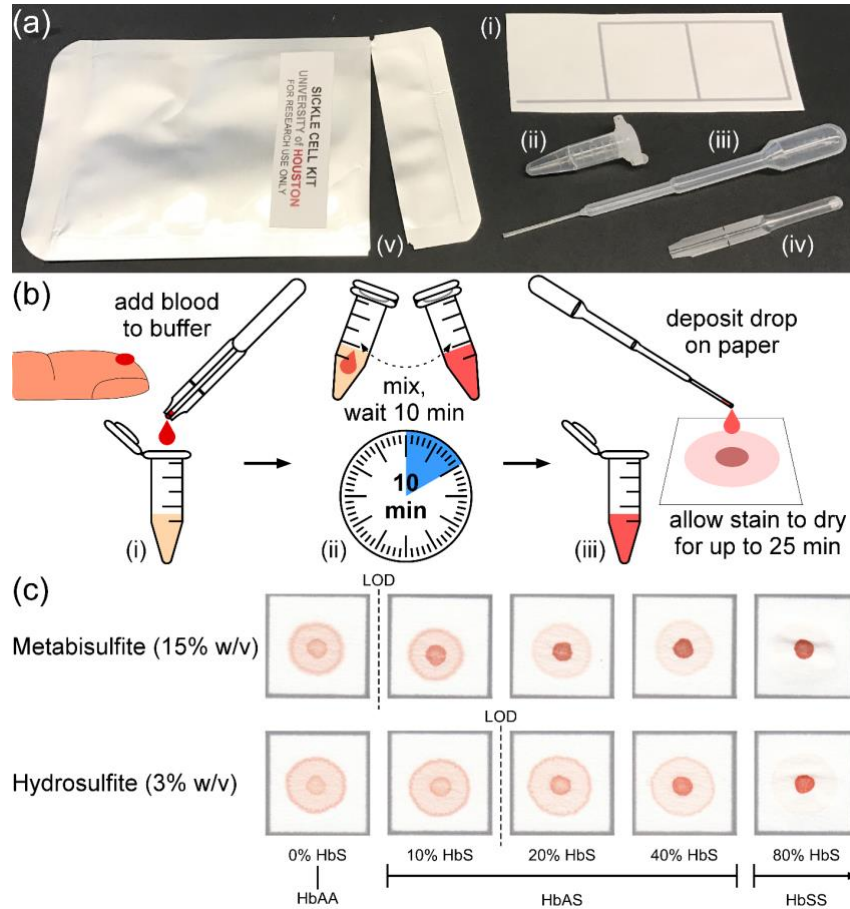


Figure 1. (a) Photograph of the paper-based SCA diagnostic kit with all components necessary to perform the test. (b) Schematic illustration of the steps to perform the test. (c) Representative bloodstains produced by the metabisulfite and hydrosulfite versions of the test for samples with various HbS concentrations.

Figure 1 above shows the overview of the distributable paper-based SCA diagnostic test kit. The detailed descriptions of the subpanels in that figure are as follows: (a) Photograph of the sickle cell kit with all components necessary to perform the test: (i) patterned chromatography paper; (ii) reagent tube containing reagents; (iii) reagent dropper; (iv) blood dropper; and (v) foil pouch. (b) Schematic illustration showing the steps required to perform the paper-based test: (i) $\sim 20 \mu\text{L}$ of whole blood is collected via finger-stick using the blood dropper and deposited in the reagent tube;

(ii) the blood is mixed with a preset volume of buffer (containing either sodium hydrosulfite or sodium metabisulfite) via manual agitation; and (iii) after 10 min, a drop (~20 μ L) of the mixture is deposited on the chromatography paper using the reagent dropper and allowed to dry for up to 25 min before being evaluated visually. (c) Representative bloodstains produced by the metabisulfite (top) and hydrosulfite (bottom) versions of the paper-based test for samples with various sickle hemoglobin (HbS) concentrations. The limit of detection (LOD) for each version is indicated by a dashed line. Typical HbS concentration ranges for adults and children older than six months of age with different genotypes (normal—HbAA; SCT—HbAS; SCA—HbSS) are marked below the stains.

Blood Stain Pattern Interpretation

Blood stain patterns were interpreted visually by eye and/or digitized using a portable scanner (CanoScan LiDE110, Canon USA, Lake Success, NY, USA) and quantified using a custom image analysis algorithm implemented in MATLAB (The MathWorks, Natick, MA, USA). Inexperienced users ($n = 3$) with little to no experience performing and interpreting the paper-based test were provided with a set of representative images of blood stain patterns resulting from both the MS and HS versions of the test performed using normal, SCT, and SCA blood samples (using Hb solubility buffer prepared on the same day of the experiment from dry powdered ingredients stored in their original containers). The previously described ‘S-index’—defined as the quotient of the mean red color intensity of pixels in the center spot area of the blood stain and the mean red color intensity of pixels in the ring area of the blood

stain (red color intensity = $255 - B$, where B is the blue channel of the RGB values for the digitized image)—was used to quantify the differences between blood stain patterns produced by different formulations of the test ⁷⁷.

Test Performance and Statistical Analysis

Test performance metrics were calculated as: Sensitivity = $TP/(TP + FN)$; specificity = $TN/(FP + TN)$; positive predictive value (PPV) = $TP/(TP + FP)$; negative predictive value (NPV) = $TN/(TN + FN)$; and accuracy = $(TP + TN)/(TP + FP + TN + FN)$, where TP = true positive, FP = false positive, TN = true negative, and FN = false negative. Fleiss' kappa statistic was used to assess intra- and inter-operator agreement for visual scoring of blood stains ^{83,84}. Mean, standard deviation, p -values, and confusion matrices were calculated using built-in functions in MATLAB 2014b (The MathWorks, Natick, MA, USA).

RESULTS

We hypothesized that we could improve the stability and performance of our previously-developed paper-based screening test for SCA by replacing a key component of the Hb solubility buffer, sodium hydrosulfite (HS), with sodium metabisulfite (MS), a chemically stable food additive. The concentration of MS used to replace HS was determined by comparing the previously described S-index—defined as the quotient of the red color intensities of the center area (proportional to the amount of HbS) and the ring area (proportional to other forms of Hb) of the blood stain—for buffer formulations

with 10, 15, and 20% MS (w/v) to the S-index for the previously-developed buffer formulation with 3% HS (w/v) for a set of samples with HbS concentrations from 0 to 40% HbS ⁷⁷. 15% MS (w/v) was chosen as the final formulation for the Hb solubility buffer because it produced the greatest difference in the S-Index between 0 and 20% HbS, and the most gradual change in S-Index over the range of 20–40% HbS. The Hb solubility buffer containing 15% MS (w/v) was used to perform all experiments described in this study.

Limit of Detection

The limit of detection (LOD) for this test is defined as the lowest percentage of HbS (out of the total amount of Hb in a sample) that will produce a blood stain on paper which is visually distinguishable from characteristic blood stains for samples without HbS (0%). The previously developed HS test is capable of identifying SCA in adults and children older than six months of age and has a reported LOD of ~15% HbS ⁷⁸. To determine the LOD of the MS version of the test, inexperienced users ($n = 3$) were asked to visually score a set of images of blood stains in paper ($n = 370$) produced by the MS formulation of the test (370 stains \times 3 users = 1110 total scores) as either HbS-negative (HbS = 0%) or HbS-positive (HbS > 0%). The inexperienced users correctly scored 820 of the 888 blood stain images with $\geq 10\%$ HbS (92.3%) as having some HbS and 220 of the 222 blood stain images with $< 10\%$ HbS (99.1%) as having no HbS. These results suggest that, when evaluated visually by an inexperienced user, the LOD of the MS formulation of the paper-based SCA screening test was ~10% HbS. This LOD was

confirmed to produce the greatest AUC (area under the curve) on an ROC (receiver operating characteristic) curve.

Test Readout Time

After the mixture of blood and Hb solubility buffer is deposited on chromatography paper, it takes approximately 25 min for the blood stain to become completely dry. However, accurate visual diagnoses can be made from blood stain patterns before they are completely dry. Inexperienced users ($n = 3$) were asked to visually score blood stains for unknown samples every minute for 25 min as the stains dried following deposition of the mixture onto paper. Samples with 0% HbS (normal) were correctly scored by all three users after 7 min of drying time, samples with HbS levels characteristic of SCT (10–40% HbS) were correctly scored by all users after 11 min, and samples with HbS levels characteristic of SCA (>40% HbS) could be scored correctly after 1 min. These results suggest that the paper-based SCA screening test can be performed and interpreted within 21 min (10 min preparation and incubation + 11 min drying before readout).

Test Performance Metrics

To determine the performance of the MS version of the test, inexperienced users ($n = 3$) were asked to visually score a set of images of blood stains on paper ($n = 185$) produced by the MS version of the test as either normal (*HbAA*; characteristic HbS = 0%), SCT (*HbAS*; characteristic HbS = 10–40%) or SCA (*HbSS*; characteristic HbS > 40%) by comparing them to a set of representative blood stain images from each category. **Figure 2** shows the aggregate confusion matrices of the visual diagnoses made

by the three inexperienced users with both the MS and HS versions of the paper-based test. Using the MS formulation inexperienced users could visually distinguish between blood samples with no HbS and blood samples with $\geq 10\%$ HbS (i.e., *HbAA* vs. *HbAS* and *HbSS*) with 92.8% sensitivity, 100% specificity, 100% positive predictive value (PPV), 77.6% negative predictive value (NPV) and 94.2% overall diagnostic accuracy (**Figure 2a**). Users could also distinguish between blood samples with $\geq 80\%$ HbS (characteristic of SCA) from blood samples with $< 80\%$ HbS (characteristic of normal and SCT) (i.e., *HbSS* vs. *HbAA* and *HbAS*) with 97.3% sensitivity, 99.5% specificity, 98.2% PPV, 99.3% NPV, and 99.1% overall diagnostic accuracy (**Figure 2a**).

When the same three inexperienced users were asked to score blood stains on paper ($n = 143$) produced by the previously-developed HS formulation of the test, they could visually distinguish between blood samples with no HbS and blood samples with $\geq 10\%$ HbS (i.e., *HbAA* vs. *HbAS* and *HbSS*) with 61.2% sensitivity, 100% specificity, 100% PPV, 49.2% NPV, and 71.8% overall diagnostic accuracy (**Figure 2b**). Users could also distinguish between blood samples with $\geq 80\%$ HbS (characteristic of SCA) from blood samples with $< 80\%$ HbS (characteristic of normal and SCT) (i.e., *HbSS* vs. *HbAA* and *HbAS*) with 76.9% sensitivity, 100% specificity, 100% PPV, 95.1% NPV, and 95.8% overall diagnostic accuracy (**Figure 2b**).

		(a) Metabisulfite (MS) Paper-based Test					(b) Hydrosulfite (HS) Paper-based Test		
		AA	AS	SS			AA	AS	SS
Conventional HPLC	AA	111	0	0	Conventional HPLC	AA	117	0	0
	AS	32	299	2		AS	121	113	0
	SS	0	3	108		SS	0	18	60

Figure 2. Aggregate confusion matrix for screening of blood samples with characteristic HbS concentrations via visual interpretation of the blood stains produced on paper by the (a) metabisulfite (MS) formulation of the test (555 total scores) and (b) hydrosulfite (HS) formulation of the test (429 total scores).

Figure 2 above shows the Diagnostic accuracy of the paper-based SCA screening test kit. The detailed descriptions of the subpanels in that figure are as follows:

(a) Aggregate confusion matrix for screening of blood samples ($n = 185$) with characteristic HbS concentrations via visual interpretation (inexperienced users; $n = 3$) of the blood stains produced on paper by the metabisulfite (MS) formulation of the test ($185 \text{ samples} \times 3 \text{ users} = 555 \text{ total scores}$). (b) Aggregate confusion matrix for the screening of blood samples ($n = 143$) with characteristic HbS concentrations via visual interpretation (inexperienced users; $n = 3$) of the blood stains produced on paper by the hydrosulfite (HS) formulation of the test ($143 \text{ samples} \times 3 \text{ users} = 429 \text{ total scores}$). Rows correspond to characteristic genotypes (based on HbS concentration measured using conventional high-performance liquid chromatography—HPLC) and columns

correspond to predicted genotypes (diagnosed by the paper-based test). Shaded cells contain the numbers of correct diagnoses.

Intra- and Inter-Observer Agreement

The Fleiss' kappa statistical measure (κ) for assessing intra-observer agreement of the scoring of blood stains on paper ($n = 370$) produced by the MS version of the test was $\kappa = 0.93 \pm 0.04$ (individual scores: 0.88, 0.93, and 0.97), which suggests that there was almost perfect self-consistency for each of the three inexperienced test users. The Fleiss' kappa statistical measure for assessing inter-observer agreement for the MS version of the test was $\kappa = 0.87$, which suggests that there was almost perfect agreement between the three inexperienced test users. When the same three inexperienced users were asked to score blood stains on paper ($n = 286$) produced by the previously-developed HS formulation of the test, $\kappa = 0.85 \pm 0.09$ (individual scores: 0.72, 0.88, and 0.94) for intra-observer agreement and $\kappa = 0.75$ for inter-observer agreement. These results suggest that there is a very high level of intra- and inter-observer agreement for visual diagnosis of SCT and SCA using the HS version of the test, but that both intra- and inter-observer agreement are better for the MS version of the test.

Test Kit Stability

Figure 3 shows the stability of the reagents comprising the Hb solubility buffer for the MS and HS formulations of the paper-based test when stored under dry (MS powder stored separately from aqueous buffer components) or wet (MS powder mixed with aqueous buffer components before storage) conditions over the course of 24 weeks.

Reagents were considered stable as long as the difference in the S-index—defined as quotient of the red color intensities of the center area and ring area of the blood stain—between samples with 0% HbS and samples with HbS concentrations greater than, or equal, to the LOD of tests performed using fresh reagents (i.e., $\geq 10\%$ HbS for MS and $\geq 20\%$ HbS for HS) remained statistically significant ($p < 0.05$).

The MS formulation maintained its stability over the course of all 24 weeks studied regardless of whether MS was stored under dry or wet conditions. The difference between blood stain patterns for samples with 0% HbS and $\geq 10\%$ HbS was still visually obvious and statistically significant ($p < 0.05$) at the end of the 24-week study period (**Figure 3**). When stored under dry conditions the HS formulation remained 100% stable until day 36 (~5 weeks) of the study period, after which it lost all activity—i.e., the difference in blood stain patterns for samples with 0% HbS and $\geq 20\%$ HbS was not visually obvious or statistically significant ($p > 0.05$). When stored under wet conditions the HS formulation remained 100% stable until day 6 (~1 week) of the study period, after which it lost all activity (**Figure 3**). These results suggest that, regardless of whether MS is stored in dry or wet form, the MS version of the test has a shelf life which is (at the least) ~5 times as long as the shelf life for a dry HS version of the test and ~24 times as long as the shelf life for a wet HS version of the test. Additional testing showed that, when stored under wet conditions, the MS formulation remained 100% stable for (at least) one week when stored at 62 °C (an upper bound on hot temperatures reached in storage in desert climates ⁸⁵).

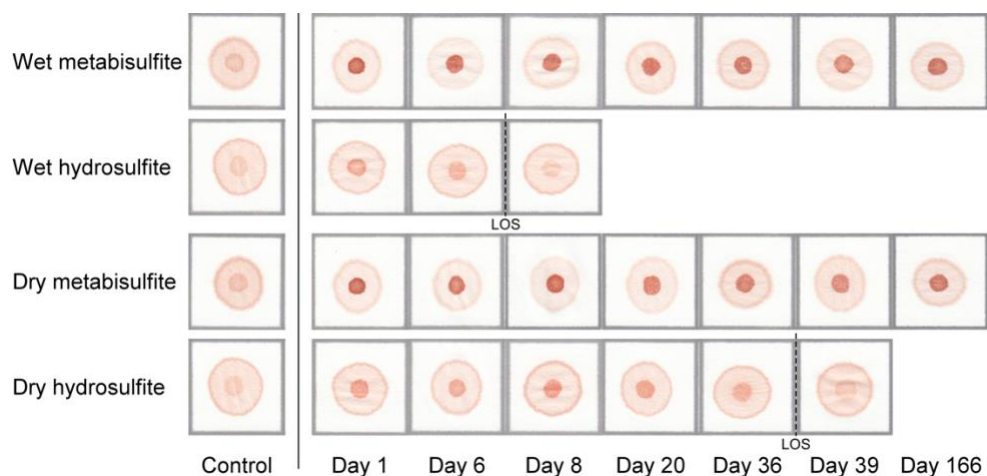


Figure 3. Representative images of blood stains demonstrating the reagent stability of the metabisulfite (MS) and hydrosulfite (HS) formulations of the paper-based SCA screening test under wet and dry storage conditions.

Figure 3 above shows representative images of blood stains demonstrating the reagent stability of the metabisulfite (MS) and hydrosulfite (HS) formulations of the test kit. The detailed descriptions of the sections of that figure are as follows: On the left of the solid line are blood stain images for samples with 0% HbS (control) produced by the MS and HS versions of the test using freshly prepared reagents. On the right of the solid line are blood stain images for samples with 20% HbS (limit of detection of HS version of test) produced by the MS and HS versions of the test using reagents stored under wet (MS powder mixed with aqueous buffer components before storage) or dry (MS powder stored separately from aqueous buffer components) conditions. The limit of stability (LOS)—i.e., the maximum amount of time reagents can be stored before the difference in pattern between samples with 0% HbS and samples with HbS concentrations greater than, or equal to, the limit of detection of tests performed using fresh reagents becomes statistically insignificant—is indicated by a dashed line.

Distributable Test Kit Cost

A self-contained, distributable kit containing all reagents and materials necessary to perform the paper-based SCA screening test as described above was assembled using the following commercially-available, off-the-shelf components: blood dropper (Microsafe 20 μ L, Safe-Tec, Ivyland, PA, USA), reagent tube (0.5 mL microcentrifuge tube, Sigma-Aldrich, St. Louis, MO, USA), reagent dropper (Disposable Graduated Transfer Pipet, VWR, Radnor, PA, USA), chromatography paper (Whatman Chr 1, Sigma-Aldrich, St. Louis, MO, USA), and a foil polyethylene-lined pouch (Xin Jiu Technology, Taoyuan, Taiwan) (**Figure 1a**). The key reagents used in this test kit were food-grade: sodium metabisulfite (Duda Energy, Decatur, AL, USA) and saponin (Desert King, San Diego, CA, USA). **Table 1** shows a cost breakdown for the reagents and materials comprising the self-contained, distributable paper-based SCA screening test kit. The total cost of all materials, reagents and packaging necessary to perform the paper-based SCA screening test using this kit was \$0.21 (USD).

Table 1. Detailed cost breakdown of the paper-based SCA screening test kit components

Test Component	Cost Per Test (USD)
Foil pouch	\$0.02
Reagent dropper	\$0.05
Blood dropper	\$0.08
Chromatography paper	\$0.01
Reagent tube	\$0.03
Food grade reagents	\$0.02
Total	\$0.21

DISCUSSION

Universal screening for SCA using conventional, laboratory-based methods (e.g., IEF, HPLC) is currently unfeasible in many resource-limited settings because of the prohibitively high cost and lack of access to the technical infrastructure required to support such testing. The advent of a simple, stable, equipment-free, visually-interpreted and inexpensive screening test for SCA could greatly improve the survival rate of the hundreds of thousands born with the disease each year, by enabling an earlier initiation of simple and effective prophylactic care. The point-of-care screening technology described in this study has the potential to significantly decrease the cost and technical complexity of implementing universal screening programs in resource-limited regions where SCA has the highest incidence ²⁴.

Recently, multiple research groups have developed screening tests for sickle cell disease intended for use in resource-limited settings ⁸⁶⁻⁸⁹. Some of the most promising emerging technologies include an antibody-based lateral flow assay that can detect HbS, HbA, and HbC and an aqueous multiphase system used to separate dense sickle RBCs from healthy RBC populations with lower density ^{86-88,90}. However, none of the current or developing tests adequately address all of the unique design requirements necessary to create a test which can be distributed, stored, performed, and interpreted in resource-limited settings. For example, antibody-based tests are notoriously prone to stability and reproducibility issues when taken outside the laboratory, since antibodies generally denature above 37 °C (mammalian body temperature) and are rarely specific (nonspecific antibodies may bind unintended antigens to produce a false positive signal) ⁸⁷. However, the antibody-based SCD assay is simple to use, has shown >98%

sensitivity and specificity in a laboratory setting for identifying *HbSS* blood, can accurately determine the presence of HbC (100% sensitivity and specificity) and has the potential to be very effective at identifying other non-HbS hemoglobin variants ^{86,87}. As a result, the antibody-based SCD assay is most appropriate for situations where high genotypic resolution (i.e., the ability to specifically identify different SCD genotypes) is needed, but may be constrained from a cost and long-term stability perspective. The density-based test, on the other hand, is highly sensitive to changes in reagent properties (e.g., change in density due to evaporation) and is not equipment- and electricity-free (i.e., requires a car-battery powered centrifuge) ⁹⁰. The complexity of the density based test, and its sensitivity to comorbidities and other factors that influence RBC density, such as high amounts of HbF in newborns, resulted in lower sensitivity (86%) and specificity (60%) for identifying *HbSS* blood in resource-limited settings in Zambia ⁹⁰. Furthermore, the density-based test has not been able to distinguish *HbAS* from *HbAA* ^{88,90}. As such, none of the technologies currently on the market or in public development fully address the unmet need for a truly simple, stable, and low-cost SCA screening test.

Our research laboratory has previously attempted to meet this need by developing and validating a paper-based SCA screening test capable of sensitive and specific differentiation of SCA from SCT and normal individuals in adults and children older than six months of age ^{76,78}. However, the Hb solubility buffer on which the previously-developed test is based utilized a reducing agent—sodium hydrosulfite (HS)—which is expensive to ship and difficult to store due to its combustibility as a solid (Hazmat Class 4.2—spontaneously combustible) and fast oxidation in aqueous solutions ($t_{1/2} < 1$ day at 25 °C) ⁹¹. Here we presented the development and

characterization of an alternative formulation of the Hb solubility buffer that eliminates the need for HS via substitution of an optimized concentration of sodium metabisulfite (MS)—a common preservative used in the food, textile, and photography industries. MS is approximately half the price of HS when purchased commercially, is not a regulated substance (i.e., does not need to be shipped as hazardous goods), and is stable for up to a year as a solid at room temperature and at least ~6 months in solution with exposure to oxygen⁹¹.

The MS formulation of the paper-based SCA screening test described here successfully addresses many of the technical and logistical problems of the conventional approaches described above as well as the limitations of the previously developed HS formulation. Firstly, the use of MS instead of HS increased the shelf-life of the aqueous Hb solubility buffer by up to ~24× (**Figure 3**), thus allowing for the packaging of a distributable kit containing premade buffer with a reasonably long shelf-life. The MS formulation maintained its stability over the course of a 24-week period regardless of storage under dry or wet conditions—i.e., the difference in the blood stain pattern between samples with 0% HbS and $\geq 10\%$ (the LOD for MS tests performed using fresh reagents) HbS was still visually obvious and statistically significant ($p < 0.05$) at the end of the study period (**Figure 3**). In contrast, the HS formulation only remained stable for ~5 weeks under dry conditions and ~1 week under wet conditions (**Figure 3**). Additional experiments showed that the MS formulation of the test remained stable for at least one week when stored under wet conditions at 62 °C (an upper bound on hot temperatures reached in desert climates on Earth⁸⁵). The improved storage capability

of the MS-based assay will be crucial for the expansion of SCA screening programs in regions without established supply chains and clinical facilities.

Secondly, in addition to improving the stability of the paper-based SCA test, the substitution of MS for HS improved the LOD of the assay by two-fold, allowing for the detection of as little as 10% HbS in a blood sample, compared to 15% HbS with HS. Inexperienced users visually differentiated SCA from normal or SCT samples with 97.3% sensitivity, 99.5% specificity, and almost perfect agreement between scorers (**Figure 2a**). In comparison, when using the HS test, users were only able to visually differentiate SCA with 76.9% sensitivity and 100% specificity (**Figure 2b**). Given the higher concentration of metabisulfite used to achieve blood stain color intensities similar to the HS test, this improvement in LOD could be partially due to the increase in Hb solubility buffer osmolality, which causes more HbS to precipitate out of the solution and form a darker stain center spot on the paper⁷⁷. It has previously been shown that HS deoxygenates HbS rapidly, resulting in the formation of amorphous precipitates of short, randomly oriented Hb fibers, while MS has been shown to deoxygenate Hb more gradually, resulting in the formation of long, organized Hb polymers characteristic of SCA^{92,93}. These comparatively larger deoxy-HbS aggregates formed using MS are more likely to become entangled within the chromatography paper pores—causing a higher fraction of total deoxy-HbS to be retained in the area of the initial drop (center spot)—compared to the smaller, more irregular aggregates formed using HS, which are more likely to be wicked laterally through the paper pores toward the edge of the stain (peripheral ring). Therefore, an alternate explanation for the improvement in LOD could be that the larger fraction of total deoxy-HbS retained in the area of the initial drop, as

a result of using MS compared to HS, produces center spots which are both darker (higher absolute amount of deoxy-HbS in the center spot) and more well-defined (lower fraction of deoxy-HbS in peripheral ring) ⁹⁴. This improvement in signal detection is an important development for screening young children, who produce less HbS (due to increased HbF (fetal Hb) production) than is observed in typical adult Hb profiles.

Additionally, the MS formulation of the test can be performed and interpreted more rapidly than the HS formulation. Inexperienced users made accurate visual diagnoses from blood stain patterns within 11 min of deposition onto chromatography paper (i.e., before the blood stains on the paper were fully dry) which corresponds to 21 min from the start of the test. This is an improvement over the reported readout time of 30 min for the HS test. The more rapid availability of test results could permit immediate clinical intervention at the point-of-care and could potentially enable counseling of families with SCA newborns before discharge. The ability to deliver results during the first visit to a health clinic is vital because in regions which lack established communication infrastructure, re-contact and follow-up rates for affected newborns have been reported to be as low as 50% ²².

Finally, using MS allowed for the design of a self-contained, low-cost test kit comprised of easily accessible, food-grade reagents (not an option for HS) and off-the-shelf disposable plastic components with a total cost of \$0.21 (USD) (**Table 1**). The test kit consists of a blood dropper, reagent dropper, reagent tube, food grade reagents, chromatography paper and a foil pouch (**Figure 1a**), with >66% of the total cost being accounted for by the disposable plastic droppers. Switching from HS to MS also decreased the amortized cost of the test significantly (primarily due to shipping

restrictions on HS). The transportation, storage, and material cost savings of this MS-based test, as well as the wide availability of food-grade MS, make the SCA screening test a tangible reality in even the most resource-limited settings.

The MS formulation of the paper-based test described in this study has two important limitations. First, when visually interpreted, the test cannot differentiate between SCA and other heterozygous forms of SCD (e.g., HbSC). This is because the blood stain pattern produced in paper is determined by the concentration of HbS in the blood sample being tested and is unaffected by the relative proportions of other soluble forms of Hb making up the rest of the sample. As such, the paper-based test would have the highest clinical utility in regions with low SCD genotypic variation (e.g., Angola where the majority of SCD cases are SCA ²²) and lowest utility in regions where other forms of SCD are present (e.g., Burkina Faso and Central West Africa where HbSC is prevalent ⁹⁵). Importantly however, we have previously shown that automated image analysis of scanned blood stain patterns can be used to differentiate *HbAS* from *HbSC* (sensitivity of 100%, specificity of 59%) despite human scorers being unable to differentiate the patterns by eye ⁷⁸. Second, while the LOD of the MS formulation of the test has been improved to 10% HbS, this LOD may still be insufficient for detecting SCT or SCA in newborns less than six months of age. This is because at birth the cord blood of SCT newborns contains $9.5 \pm 4.2\%$ HbA and $6.5 \pm 2.8\%$ HbS, and the blood of newborns with SCA contains $10.2 \pm 3.9\%$ HbS, meaning that newborns with HbS concentrations near the low end of this physiological range may produce false negative results ^{96,97}. To address this limitation we have previously developed and validated a separate HS-based test which employs a disposable filter to further improve the LOD

of the test, however, this version of the test is currently incapable of differentiating SCT from SCA ⁷⁹.

In summary, we have improved and characterized the performance of our previously developed paper-based test for rapid, low-cost, and equipment-free diagnosis of SCA in resource-limited settings. We have demonstrated that the test, compared to the previous version, had a superior limit of detection, faster readout time, better diagnostic performance, longer shelf stability at room temperature, and could be packaged into a self-contained, distributable test kit with a total cost of only \$0.21 (USD). A point-of-care test with these qualities represents a significant step towards enabling population-wide screening in resource-limited settings, which, in combination with prompt initiation of prophylactic treatment, could have a transformative impact on the health and well-being of the hundreds of thousands of individuals with SCA born in developing countries each year.

CHAPTER 3: RECENT ADVANCES TOWARDS PASSIVE MICROFLUIDIC TECHNOLOGIES FOR HIGH THROUGHPUT LEUKAPHERESIS OF WHOLE BLOOD

OVERVIEW

Blood is a complex biological fluid comprised of various cellular components that perform distinct roles in maintaining homeostasis and each have important diagnostic and therapeutic uses. Efficient, accurate, and high throughput fractionation of blood into its individual cellular components thus has many applications in clinical diagnosis, medicine, and biological research. Leukapheresis is a complex extracorporeal procedure during which patient's blood is passed through an apheresis machine to separate white blood cells from red blood cells and platelets, which are then returned back to the patient. Leukapheresis is a life-saving medical procedure most frequently used for leukodepletion and cellular collection. Although it is well tolerated by adults and older children, leukapheresis poses significant risk to neonates and low-weight infants because of the large extracorporeal volume of the centrifugation-based apheresis machines.

Recent advances in microfluidics have enabled the realization of smaller scale devices offering cell separation capabilities at high throughputs. New microfluidic based technologies that can provide efficient blood cell separation have emerged that may have potential to address this clinical need for more accessible leukapheresis

procedures. This paper provides an extensive review of passive microfluidic devices, published in the last decade, that can isolate WBC directly from whole blood. We discuss the basic theories behind and working principles of these devices as well as the experimental parameters and results regarding their cell separation performances. We classify these techniques as either (i) physical filtration, (ii) filtration through hydrodynamic effects, or (iii) combinatorial approaches to filtration. We compare their microfluidic approaches, present metrics of efficiency, and discuss their potential for future use as high throughput microfluidic leukapheresis platforms.

INTRODUCTION

Leukapheresis is a complex medical procedure during which blood is continuously removed from the body by an apheresis machine to separate (via centrifugation) white blood cells (WBCs) from the rest of the blood, which is then returned back to the patient.⁴⁴⁻⁴⁶ This procedure is used throughout the practice of medicine for two main applications, leukodepletion and cellular collection.

Leukodepletion is indicated to urgently reduce a dangerously elevated WBC counts in patients with symptomatic hyperleukocytosis (WBC count $>100,000/\mu\text{L}$, with pulmonary or neurologic dysfunction), a common symptom of leukemia.³⁹⁻⁴² Leukapheresis procedures can rapidly lower WBC counts to quickly alleviate symptoms, while cytoreductive chemotherapy is taking effect.³⁹⁻⁴² If left untreated, symptomatic hyperleukocytosis has a high mortality rate, mostly from neurological and pulmonary complications.³⁹ The removal of activated immune WBC from the patient's

blood stream also makes leukodepletion an attractive drug-free treatment modality for a number of other emergent indications, such as inflammatory bowel disease,⁴⁷⁻⁴⁹ steroid-resistant nephrotic syndrome,⁵⁰ and refractory systemic juvenile idiopathic arthritis.⁵¹

Cellular collection is the initial step for an increasing number of highly effective cell-based treatments for some of the most devastating hematologic and immune system disorders affecting millions of adults and children worldwide.^{40,41,48-50,53-55,59,60} Granulocytes collected via leukapheresis can be used to help stave off infections in neutropenic patients.^{98,99} Various types of mononuclear white blood cells (MNCs) are isolated from peripheral blood via leukapheresis to enable established cell-based treatments and a wide range of novel cellular therapies for treating disease.⁵² For example, CD34+ cells are harvested as a popular source of grafts for hematopoietic stem cell transplantation,⁵⁹⁻⁶¹ and also serve as the initial cellular material for novel potentially curative gene-based therapies for sickle cell disease and β -thalassemia.^{62,63} CD14+ monocytes are isolated to generate patient-derived, tumor antigen-loaded dendritic cells to treat various malignancies, including medulloblastoma.⁵³ CD3+ lymphocytes can be extracted from the blood to manufacture a rapidly expanding number of chimeric antigen receptor (CAR) T-cell therapies for treating hematologic malignancies, and other types of cancer.^{54,55} CD26+ lymphocytes can be collected and engineered to attack tumors that may evade T-cell recognition.⁵⁶

Whereas both leukodepletion and cellular collection procedures can provide potentially life-saving treatments for millions of patients, conventional leukapheresis may not be widely accessible or available to many due to the complexity and

prohibitively large size of apheresis machines¹⁰⁰. Currently, leukapheresis is most often performed using centrifugation-based apheresis machines that require technical expertise and training, as well as reliable infrastructural support for device maintenance and access to replacement supplies.^{80,101} These constraints make it challenging to provide therapeutic leukapheresis procedures for patient in parts of the world where adequate funding and infrastructure are lacking and basic services, such as a dependable power supply, are not available.¹⁰¹

Conventional leukapheresis is also largely unavailable to neonates and low-weight infants because of the substantial technical challenges and serious risks associated with performing apheresis in these patients using adult-size machines.^{100,102-105} Centrifugation-based apheresis machines have a substantial extracorporeal volume (ECV), typically ranging from 150 to 250 mL,⁵² whereas, for comparison, the total blood volume (TBV) of a 4 kg neonate is only ~400 mL, and just ~800 mL for a 10 kg infant.^{106,107} The ECV of these machines represents a particularly large fraction of their TBV, and these vulnerable patients consequently experience a significantly higher incidence of hypotension, symptomatic hypocalcemia, allergic reactions, catheter-related thrombosis, infections, severe anemia and even death.^{42,103-105} There is currently no practical alternative to adult-size apheresis machines for performing leukapheresis in neonates and low-weight infants (<10kg), and these patients often receive sub-optimal or risky treatments.

In the past decade, new microfluidic based technologies that can provide efficient blood cell separation have emerged that may have potential to address this clinical need for more accessible leukapheresis procedures. These novel attempts aim

to undertake the limitations of bulky and complex instrumentation that require technical expertise as well as high sample processing costs. Microfluidic platforms offer significant advantages for WBC handling as they are able to manipulate particles using unique physical and flow phenomena at the micron scale while simultaneously maintaining precise control of shear conditions within the microstructures.¹⁰⁸ The ideal microfluidic leukapheresis platform would allow for high throughput and efficient separation of WBC from WB and provides a system that does not require pre-preparation of the blood sample. The system should also not clog over time or activate or damage the cells as they are being processed. *Sethu et al.* presented a technique for WBC depletion from WB using a continuous flow microfluidic diffusive filter and their group was one of the first to propose the use of microfluidic devices for high throughput leukapheresis.² Since then, many developments have been made towards the next generation of microfluidic devices for the isolation of WBC.

In this work, we review passive microfluidic devices that can separate WBC directly from whole blood, focusing on the technological developments made in the last decade. The technologies reviewed here are categorized as: (i) physical or (ii) migration-based filtration techniques. We compare their passive microfluidic approaches and present common metrics including cell separation efficiency and sample throughput. Finally, we also discuss their potential for future use as high throughput microfluidic leukapheresis platforms.

PASSIVE MICROFLUIDIC DEVICES

The microfluidic techniques for isolating specific cells from a heterogeneous mixture of WB can be categorized into two groups: active and passive separation methods. Active techniques rely on external forces such as magnetic force, acoustic force, dielectrophoretic force, or a combination of these to separate the target particles and direct them into specific outlets. Passive methods exploit properties intrinsic to the device such as channel geometry, inherent hydrodynamic forces, and/or differences in cell characteristics such as shape, size, and deformability.^{67,68} Generally, active separation methods allow for more precise particle manipulation and greater control over cell positioning within a flow, as compared to passive approaches, leading to higher separation efficiencies and purities.^{108,109} While high selectivity is especially beneficial for sorting rare blood cells, there are several disadvantages to using active fractionation techniques.⁶⁷ Such microfluidic devices often require complex experimental setup thus reducing their practicality, especially at the point-of-care.^{108,109} Furthermore, there is potential for unexpected physiological effects on the cells due to external forces, making the separated components unsuitable for downstream applications.¹¹⁰ Active devices also typically require extensive sample preparation such as RBC lysis to reduce the large amounts of RBC which can interfere with the efficient trapping of WBC or other rare cells.⁶⁷ Passive separation devices do not require cell-labelling or complex apparatuses and are relatively easy to fabricate and integrate with downstream processing of samples.^{67,111} These factors, in addition to not requiring a power source, make passive fractionation devices a viable alternative to conventional centrifugation-based methods

for cell separation. In this work we therefore focus on passive microfluidic techniques designed to extract and separate WBC from whole blood.

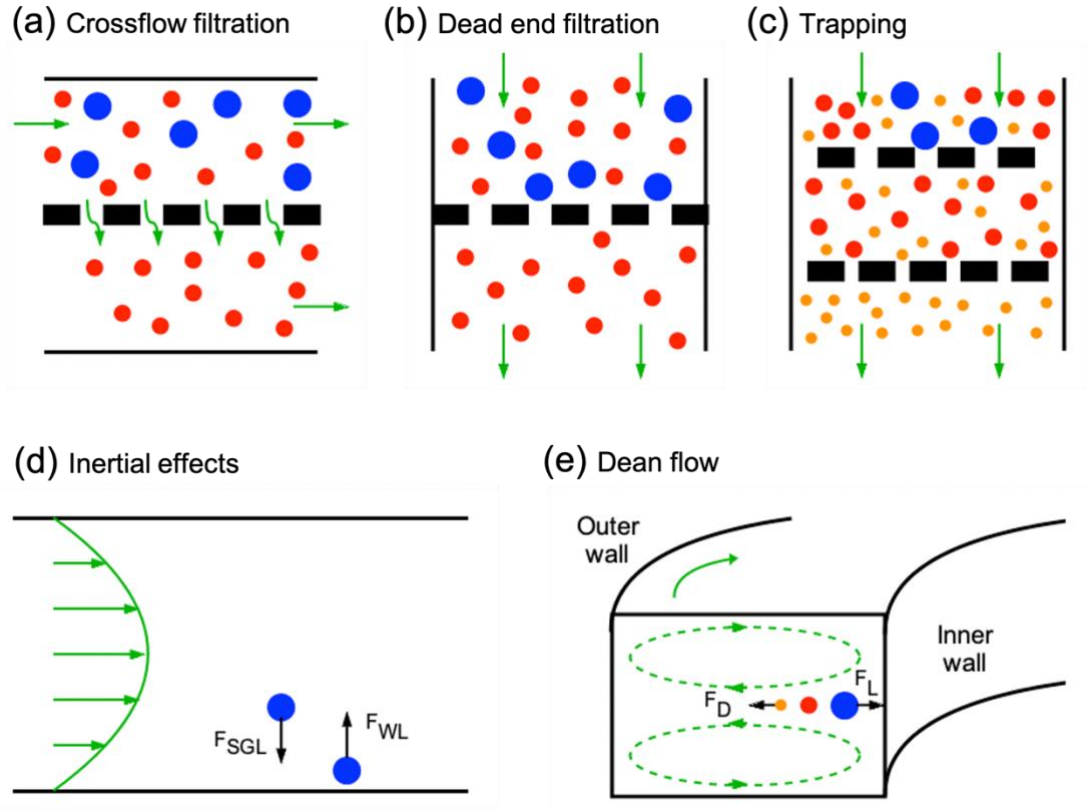


Figure 4. Fundamental principles of size-based separation of cells described in some of the publications reviewed in this work.

Figure 4 above illustrates the fundamental principles of size-based separation of cells utilized in the some of the microfluidic devices presented in this review. The detailed descriptions of the subpanels in that figure are as follows: (a) Crossflow filtration through a porous membrane, (b) dead end filtration through a porous membrane, and (c) trapping with microstructures. (d) Effect of inertial forces on

particles in a straight channel. (e) Effect of Dean flow on particles in a curved channel. Fluid flow is denoted by green arrows. Particle size is denoted by different colored circles (blue>red>orange). Force phenomena and direction are denoted by black arrows (F_{SGL} = shear gradient-induced lift force, F_{WL} = wall-induced lift force, F_D = Dean force, F_L = net inertial lift force).

1. Physical Filtration

Physical filtration is a common method utilized in microfluidics which involves the use of microstructures such as pores and pillars to physically sort particles within a stream. Microfluidic devices can be designed with structures that either selectively divert them based on their characteristics or trap target cells. As blood cells vary in size and deformability, physical filtration techniques can be utilized to separate WBC from other cells within the blood.

Porous Membranes

Microfiltration is one of the most common blood fractionation techniques, in which structures such as porous membranes and pillars are utilized to conduct sized-based separation of blood cells. Generally, the mechanisms of microfiltration can be categorized as crossflow filtration or dead-end filtration. In crossflow filtration, the fluid to be filtered flows parallel to the porous membrane surface as the retentate is removed from the same side, and the permeate is transferred to the other side of the membrane (**Figure 4a**). In dead-end filtration, the fluid flow is fed perpendicular to the filter

element and the retentate particles are collected on the membrane surface (**Figure 4b**). Dead-end filtration is often used at laboratory scale due to the high product recovery, simple operation, and relatively low cost of separation.¹¹² However, the main disadvantage of dead-end filtration is the extensive membrane fouling. Crossflow filtration is much less sensitive to clogging and fouling due to the sweeping effect of the fluid flowing tangentially to the filtration membrane.¹¹³

Wei et al. used a hybrid of crossflow and dead-end filtration to achieve high-efficiency cell separation from murine blood supplemented with human acute lymphoblastic leukemia cells (Reh cells).¹¹⁴ The microfluidic device consisted of two filtration assemblies that consist of a porous PDMS membrane sandwiched between two chambers with rounded cross-sections. The membranes in the two assemblies had different pore sizes so as to enable filtration of particles with disparate dimensions. In the first assembly, the input blood sample flowed from the bottom chamber to the top chamber through the portion of the membrane with the larger pores, thus removing the largest particles (WBC) from the stream. Afterwards, the fluid flowed from top into bottom chamber through the section on the membrane with the smaller pores, enabling the separation of intermediate (RBC) and small-sized particles (PLT) from one another. To minimize membrane clogging, the device underwent flushing after every separation and collection cycle. Utilizing a membrane with a pore-size of 6.4 μm , the device separated the cells into two groups: one with diameter lower than 6.4 μm , and one with diameter greater than 6.4 μm . Although operating at a low throughput of 2-3 $\mu\text{L}/\text{min}$ and processing blood samples diluted by a factor of 40 in phosphate-buffered saline (PBS), the device demonstrated considerable fractionation efficiency. RBC were

sorted with a separation efficiency of 99.9%, while WBC had a separation efficiency of 99.7%. Furthermore, cell viability was preserved as demonstrated by the fluorescent imaging of the collected samples using CellTracker Orange CMTMR.

Hosokawa et al. used dead-end filtration to trap leukocytes in a microcavity array made of nickel, with the average top surface pore diameter of $3.0 \pm 0.1 \mu\text{m}$.¹¹⁵ The use of nickel ensures uniformity and helps prevent unexpected blocking by blood cells. This mechanism separates leukocytes from diluted whole blood (1:200) with an efficiency of >90% and does not significantly impact cell viability, which is maintained at approximately $97.4 \pm 1.7\%$, as measured by evaluating membrane integrity. Clogging is prevented by keeping the top surface diameter of the microcavities at $3 \mu\text{m}$, allowing the device to trap leukocytes while other blood components pass through. However, even though the presence of a negative pressure pump enhances the flow rate, as compared to *Wei et al.*, the focus of this research to recover leukocytes from minimal amounts ($\sim 1 \mu\text{L}$) of whole blood.¹¹⁴ Processing larger amounts of sample could result in blockage, leading to device malfunction.

Such issues are minimized in the continuous-flow device presented by *Li et al.*, which relies on the principle of crossflow filtration.¹¹⁶ The PDMS device consisted of top and bottom microfluidic channels and a PDMS microfiltration membrane (PMM) sandwiched in between. A sheath flow injected downstream of the blood sample flow pushed the sample flow downward into the bottom channel. Blood cells smaller than the membrane pore size pass across the PMM and exit through the bottom outlet, whereas cells larger than the pores stay in the top channel and are carried away by the tangential flow to the top outlet. The channel is laid out in a serpentine design to increase

the total channel length and, subsequently, the cell sorting efficiency. With unprocessed whole blood, WBC samples collected at the outlet had a $93.5 \pm 0.5\%$ purity, with approximately $27.4 \pm 4.9\%$ of WBC from the input sample being recovered and a throughput of $16.7 \mu\text{L}/\text{min}$. This crossflow mechanism had minimal effect on cell viability. In addition to unprocessed whole blood (porcine), the study also tested the PMM device using WBC-depleted blood samples spiked with THP-1 cells. The THP-1 cells maintained 98% viability after processing through the microfluidic device. Although crossflow filtration inherently reduces the likelihood of clogging, the high porosity (as high as 30%) and a large surface area (as large as $3 \text{ cm} \times 3 \text{ cm}$) of this device also help in preventing clogging of PMM. Experimentation with microbeads revealed that the chip could operate for 30 minutes before signs of clogging started to become noticeable under brightfield microscopy.

Cheng et al. proposed a microfiltration chip that worked with a crossflow filtration mode in combination with a dead-end filtration mode and reported WBC recovery rate as high 72.1%, from undiluted whole blood, after 5 passes through the device.⁶⁸ As with *Li et al.*, the filtration region is composed of two fluidic chambers separated by a microporous membrane.¹¹⁶ In this case however, the embedded membrane was composed of polycarbonate and designed with 3 mm pores. Smaller cells, such as RBC and PLT, pass through the membrane and flow into the waste outlet while the larger WBC remain in the bottom chamber and accumulate in the tail of the snake-shaped channel, where the WBC outlet is located. One unique feature of this microdevice is the integration of rotatory micropumps, which not only help drive the fluid flow, but can also be reversed to force the fluid flow backward to flush out the

cells trapped within micropores, thus reducing the likelihood of clogging. Although the purity of its WBC output sample is quite low at 15.1%, the device still manages a ~232-fold enrichment of WBC and can remove up to 99.7% RBC after 5 cycles of filtration in an 8-minute period. While this device reported a relatively high throughput, the flow rate is limited to 37.5 $\mu\text{L}/\text{min}$ as more WBC were shown to leak through the microporous membrane with faster flow. This is likely due to the increase in the pressure drop between the two sides of the membrane at higher flow rates, resulting in more WBC deformation and allowing them to squeeze through the pores and through to the other side.

Trapping Microstructures

Microfluidic trapping mechanisms involve capturing the target cells, while allowing the rest of the cells in the fluid to pass through (**Figure 4c**). Cellular trapping has inherent clogging issues that can be addressed through innovative design features or mechanisms to counter the effects of obstruction within the device. The entrapment of leukocytes from whole blood can be achieved through a variety of structural entities ranging from pillars to microcavities. For instance, while *Hosokawa et al.* reported on a device, discussed the previous section, that is characterized as a porous membrane, it is also described to have a trapping mechanism that captures WBC within its microcavities. *Alvankarian et al.* presented a U-shaped array of pillars that was used to trap and isolate WBC from whole blood.¹¹⁰ The pillar arrays are arranged in parallel within a rectangular chamber with inlet and outlet ports for blood flow and collection.

Fabricated out of polyurethane methacrylate, these arrays consist of square pillars to ensure a constant gap of $\sim 5.5 \mu\text{m}$, which allows most RBC and other small cells to flow through but traps WBC. The removal efficiency of RBC from the input blood samples ranged from $\sim 84\%$ to $\sim 89\%$ with flow rates between 15-50 $\mu\text{L}/\text{min}$. However, the average WBC separation was only around 18% at 50 $\mu\text{L}/\text{min}$ and 25% at 15 $\mu\text{L}/\text{min}$. Increasing the flow rate led to greater fluid pressures, which caused more WBC to escape out from the array of pillars. The device was also reported to have clogging-related complications as the use of undiluted whole blood sample led to rapid obstruction of the microstructures, thus severely affecting cell separation efficiencies.

Kuan et al. also employed a trapping mechanism to isolate WBC from the rest of the cellular components found in whole blood.⁶⁷ The device consisted of a blood sample and buffer inlets, a bifurcation region with specific zones for the separation of plasma and RBC, a main channel made up of pillars for WBC entrapment, and an outlet for waste. The bifurcation region contains six bead-packed side channels for plasma extraction, four-necked side channels for RBC collection, and one main channel that leads into WBC-trapping zone. To ensure RBC/WBC separation, the device design employs bifurcation law and crossflow filtration. For efficient cell separation, the flow pattern is established close to the side of the channel that contains the plasma zone and the RBC zone. This is achieved using the flow of buffer, which pushes the whole blood flow to the side wall. The plasma zone channels, packed with 10- μm polystyrene beads, only allow plasma to pass through. The rest of the cells continue on and the RBC then squeeze into the RBC zone due to the 2- μm necked nature of those side-channels. Finally, the remaining cells, mostly leukocytes, travel across the boundary of the flow

patterns of whole blood and buffer and enter the WBC region. The WBC-trapping region is composed of rows of hydrodynamic-based trapping units, each consisting of one triangular pillar and two rectangular pillars with a gap of 2.5 μm . A 30- μm gap at the end of each row allows for efficient use of all trapping units as cells are directed to flow to the next row in instances where all trapping units of one row are filled. This reduces the effect of clogging on WBC separation performance. Additionally, five rectangular pillars are placed at the entrance of WBC zone that prevent any aggregated cell clusters from entering the region and obstructing the flow. The device is able to isolate ~ 1800 WBC in 20 minutes from 6 μL input sample of whole blood. Furthermore, the extracted plasma demonstrates low hemolysis and a minimum plasma dilution factor of 0.76-fold.

2. Hydrodynamic Effects

Some microfluidic devices rely on the properties of the fluid, the channel geometry, and the size-based effect on cells for the purpose of blood fractionation. Cell separation via migration involves the movement of cells until they reach their equilibrium positions within the fluid streams. These positions are determined by cell size, microchannel dimensions, and the physical characteristics of the fluid. While many techniques have been developed to achieve migration-based separation of blood cells, here we focus on inertial effects, geometric and structural effects.

Inertial Effects

Particles in a fluid flowing through a microchannel experience inertial lift forces and viscous drag. The latter primarily originates from the viscous nature of the fluid and is responsible for moving particles along the flow, while the former causes cell migration across the channel cross-section.¹¹⁷ Inertial lift forces involve a combination of shear-induced lift force resulting due to the parabolic velocity flow profile and the wall-induced lift force due to the particles traveling close to channel walls.¹¹⁸ The wall-induced lift forces push particles away from the walls, while the shear-gradient lift forces push them towards the periphery. The interplay between these two inertial forces results in the lateral migration of particles to stable equilibrium positions around the boundary of a microchannel (**Figure 4d**).¹¹⁹ These equilibrium positions are dependent on particle size, fluid shear rate, and geometry of the channel cross-section. For example, in a straight microchannel with a square cross-section, particles focus at 4 equilibrium positions near channel corners when Reynolds number is high, but 8 equilibrium positions when Reynolds number is low. On the other hand, a rectangular cross-section microchannel with a high aspect ratio will have an asymmetric shear rate that leads to a greater tendency of particles to align along the longer dimension.¹¹⁷

In addition to inertial lift forces, microfluidic devices can rely on secondary flows to further enhance and control the particle migration. These flows are induced by curvatures in the microchannels; fluid passing through a curved channel experiences a radially outward centrifugal acceleration, which results in the formation of two vortices in the upper and lower halves of the channel cross-section (**Figure 4e**).¹¹⁸ These vortices are known as Dean vortices or Dean flow, and are responsible for exerting a Dean drag force on the particles in the fluid, leading to streamlining of the equilibrium positions

established due to inertial forces. A particle's position in the cross-section of the microchannel is dependent on the ratio of F_L (Net Inertial Lift) to F_D (Dean Force), and $F_L/F_D \propto d^3$, where d is the diameter of particle. Therefore, smaller particles become more entrained in the Dean flow while larger particles stick closer to the inertial equilibrium positions. In a rectangular microchannel with low-aspect ratio ($W \gg H$), as shown in **Figure 4e**, this phenomenon leads to large cells moving closer to the inner wall, and small cells being farther away.^{120,121}

Several groups have developed migration-based microfluidic devices that combine inertial effects, with secondary flows to achieve blood cell separation. For instance, *Wu et al.* utilized a spiral microchannel with a trapezoidal cross-section to focus large blood cells close to the inner wall, while shifting smaller cells more towards the outer wall.¹²² In addition to the inertial effects faced by the particles, the curvature of the microchannel contributes to the position of blood cells by exerting viscous drag of secondary flow on the cells. Fluid passing through a spiral channel undergoes centrifugal acceleration, which generates a secondary flow made up of counter-rotating vortices across the cross-section known as Dean vortices. The combination of inertial effects and dean vortices allows for precise manipulation of the locations of cells in the microchannels. A common challenge with the use of spiral channels for blood fractionation is low separation resolution and the challenge of manipulating vast numbers of RBC without a negative impact on WBC separation efficiency.¹²² The large number of RBC elongate the stream-width due to cell-cell interactions, which causes issues with cell focusing. To address this problem, *Wu et al.* designed a trapezoidal microchannel with the outer wall being the longer side, thus creating an altered velocity

field and resulting in the formation of Dean vortex cores leaning towards the outer wall, where the small cells were focused. For the purposes of WBC isolation from whole blood, the trapezoidal cross-section helped to improve the separation resolution, and focused WBC close to the inner wall, while RBC formed a band closer to the outer wall. These design modifications allowed the microdevice to process relatively large volumes at a high throughput. The device is able to separate polymorphonuclear leukocytes (PMN) and mononuclear leukocytes (MNL) from dilute blood (1-2% Hct) with an efficiency upwards of 80%, while removing RBC with an efficiency >86%, leading to WBC being enriched to more than 90% of the cell population. The clogging risk for this device was minimized due to the large dimensions of the microchannel and cell activation (specifically, PMN activation) is found to be negligible.

In a similar vein, *Nivedita et al.* developed a spiral microchannel to fractionate blood. This device has an inlet at the center of the spiral and four separate outlets at the end of the spiral channel for collection of RBC, WBC, PLT and plasma.¹²³ WBC, being the larger cells, focused closer to the inner channel wall and eluted in the first outlet. The second and third outlets contained mostly RBC with a few PLT and the fourth outlet collected only PLT and plasma. Although the cross-section is rectangular, the channel's broadness is increased to allow for the creation of distinct streams of blood cells. This allows for a high-throughput fractionation (1.8 mL/min) of whole blood diluted to ~0.1% Hct, with WBC separation efficiency of ~95% and RBC separation efficiency of ~94%. Cell viability is maintained, and although the paper does not investigate clogging, it can be assumed that given the large dimensions, the risk of clogging will be low with when processing dilute blood.

Wu et al. also present a microfluidic device that used a combination of inertial focusing and secondary flow.¹⁰⁹ However, the source of the secondary flow is not due to the curvature or spiral pattern of the device. Instead, square microstructures are designed within a straight channel to induce the secondary flow. Each channel consists of three distinct parts: a straight, rectangular channel with low-aspect-ratio (section i), a rectangular channel with equidistant square microstructures (section ii), and a trifurcating outlet (section iii). Similar to the aforementioned inertial devices, the position of particle/cell in the fluid is determined by the interplay of inertial lift force and microstructure induced secondary flow. Therefore, when passing through sections (i) and (ii), large particles align themselves in the center of the channel while small particles are focused along the side walls. WBC are therefore expected to flow in the middle of the channel and be collected in the center trifurcated outlet, while RBC are diverted to the outlets to either side. This design provided a WBC efficiency of 89.7% and a purity of 91.0%. RBC separation efficiency and purity were 99.8% and 99.6%, respectively. Furthermore, clogging was prevented through the placement of 30- μm gaps between each of the square microstructures. A straight channel design was selected to maximize the capacity for parallelization, which helps increase the overall throughput. By multiplexing the device into 72 radially arranged channels, the study theorizes an expected throughput of 10.8 mL/min when processing dilute blood (0.25% Hct). This high throughput would also allow for processing of large blood volumes, which is important for therapeutic leukapheresis. While this device has favorable characteristics for leukapheresis, its effect on cell activation and viability is undetermined.

Mutlu et al. takes on a different approach from the inertial microfluidic devices discussed previously. Instead of separating cells after their inertial equilibrium has been achieved (i.e., when they have assumed their positions in the microchannel), this device carries out a non-equilibrium separation using an array of microfluidic islands, and is called a NISA (Non-equilibrium Inertial Separation Array).¹²⁴ The ‘islands’ in the NISA device are long, rectangular pillars that cause a wall-induced inertial lift force on cells. As previously discussed, cell size is a factor in the inertial lift force, which is responsible for determining the cell’s equilibrium position. Different sized cells, therefore, have different migration paths. During this movement, a portion of the flow is siphoned off from the regions near the walls, before the cells reach their equilibrium position. Smaller cells (RBC and PLT) are siphoned off with the flow at each island while larger WBC migrate away from the channel walls due to the wall lift force, therefore avoiding siphoning and continue to move through the device. An advantage of this non-equilibrium separation system is its ability to function efficiently using of shorter microstructures (island walls) compared to the longer feature dimensions required for equilibrium separation. This design enables a compact array structure and maximizes scalability over a small area. *Mutlu et al.* were able to parallelize 104 NISA devices on a 12 cm disk, which allowed the processing of 400 mL of WB in 3 hours. A microfluidic concentrator¹²⁵ was added downstream of the fully parallelized NISA for volume reduction of the output product. The continuous siphoning of the device design also minimizes WBC loss and RBC carryover. WBC are reported to separate at an efficiency of ~97% with high purity, while RBC are removed with >99.9% efficiency. Notably, this device requires minimal dilution of the input whole blood sample (1:1).

Furthermore, hemolysis analysis showed that RBC suffered negligible damage. Minimal clogging was ensured by maintaining a large channel width. The device was shown capable of processing large volumes of blood for up to 3 hours without any blockage.

Zhang et al. took another unique approach towards inertial separation of WBC from whole blood. While the device relies on the interplay between inertial forces and secondary flow (Dean vortices) as some of the previous devices discussed in this work, but the channel design is different. This device implements a series of U-turns within the microfluidic channel, resulting in a serpentine path that introduces a secondary flow drag force.¹²⁶ A trifurcation outlet at the end of the serpentine channel that directs the cells to their respective outlets. Through parallelization of 8 serpentine channels, the device is able to achieve a throughput of 4.8 mL/min with dilute WB (1:20 in PBS). The device yielded an average WBC enrichment ratio of 10, with the purity of ~48%. While the purity is relatively low, the high throughput allows large sample processing of blood. Furthermore, due to the channel width of 200 μm and lack of any structural obstructions, there were minimal clogging issues associated with the device. The shear rate was also assumed low enough to not cause any functionality or viability issues with WBC, when compared to existing literature.^{127,128}

Recently, *Jeon et al.* developed a microfluidic platform composed of two spiral channels with different dimensions called the multi-dimensional double spiral (MDDS) device.¹²⁹ This novel inertial microfluidic device was designed for fully automated leukocyte separation as an alternative to centrifugation. The MDDS platform performs blood sample focusing and separation without sheath flow, which improves the cell

separation efficiency. The two spiral channels are connected sequentially, with the first channel conducting sample focusing, due to its smaller dimensions and rectangular cross section, and the second channel contributing to blood cell separation, due to its larger dimensions and trapezoidal cross section. Smaller particles migrate to the outer wall of the trapezoidal cross-section due to strong dean vortices at the outer half of the channel. The device also incorporates a check-valve-based recirculation platform that redirects the WBC-rich output back into circulation, for further purification and concentration. A double quad-version of the MDDS device (8 single devices multiplexed) was developed to increase the throughput from 2.3 mL/min, using a single-quad version, to 18.4 mL/min. From a sample of whole blood (diluted 1:500 in PBS) the double-quad device recovered 80% of the WBC with >40% purity and removing >99.9% of RBC. This amounted to a ~6-fold concentration of the WBC when compared to the input sample. These results were achieved with no significant ex vivo cell activation and under a high throughput, which is made possible through parallelization and scaling up. However, more parallelization leads to greater dead volume, which limits the number of recirculation possible, thus minimizing the separation efficiency of the device. The authors note however, that while multiplexing more devices reduces operation time, the resulting increase in dead volume of the system can decrease the cell separation performance and limit the number of recirculation runs. While more recirculation steps produce samples with higher purity and concentration, more cells are lost throughout the process.

Structural Effects

The migration and trajectory of cells can be induced by the distinct structural or geometric features of a microfluidic device. For instance, *Kim et al.* utilized an array of slanted ridges to direct WBC migration in a process known as deterministic migration. Deterministic migration is a migration phenomenon of WBC induced by ridge patterns that generate transverse flows composed primarily of two oppositely flowing currents.¹²⁷ The flow direction along the ridge patterns is parallel to the patterns, while the flow direction is reversed under the patterns. WBC are assumed to be located under the ridges as a result of blood cell interactions and therefore, their migration position can be determined by the direction of transverse flows under the ridge patterns. The transverse flow generated by the ridges is the main driver of the WBC migration and the cells are able to reach their positions even at high flow rates. RBC flow along the ridge pattern and prevent WBC from entering onto the ridges, through vertical displacement, therefore keeping them in their migration positions. When comparing to conventional margination processes,¹³⁰⁻¹³³ deterministic migration is much less sensitive to changes in flow rate, Hct and the aspect ratio of the channel.

In their study, *Kim et al.* developed a device designed with discontinuous slant array (DSA) ridges to induce deterministic migration of WBC.¹²⁷ To ensure efficient cell separation without clogging, channel height was set to be, at minimum, larger than WBC. Four DSA channels were integrated within a multistage device and were each connected through bifurcating regions. Through deterministic migration, a focused stream of WBC was generated along the side wall within each DSA microchannel. At each bifurcation, an RBC stream passed to the RBC reservoir, while the focused WBC

stream passed into another DSA microchannel. Following flow through the 4 channels, the enriched WBC sample was collected in the WBC reservoir. The separation process produced an enriched population of WBC, up to ~50-fold, with 80% WBC recovery. Flow cytometry analysis indicated that the viability of sorted WBC reached up to ~99.8% indicating that their cell separation system is gentle and noninvasive to the WBC. Notably, their platform demonstrated separation of WBC from undiluted whole blood (Hct 40%). While their optimal flow rate was reported as 150 $\mu\text{L}/\text{min}$, the authors project that future parallelization of the device will be straightforward the throughput can be scaled up for larger scale blood processing.

While many migration-based separation methods rely solely on cell size, *Guo et al.* also takes into consideration cell deformability in a device that implements a microfluidic ratchet mechanism.¹³⁴ The underlying principle of this mechanism involves selectively transporting cells using a ratcheting effect. This method involves a matrix of funnel-shaped micropillars designed with progressively smaller pore sizes from the bottom row to the top row. A sample of unprocessed whole blood is introduced at the bottom corner of the device. The blood cells then flow along a diagonal path and are separated into specific outlets based on the interplay of vertical oscillatory flow, horizontal cross flow, and pore size. Cells continue to flow through the device until they are constricted by a gap that prevents them from moving upward. Smaller and more deformable RBC are pushed upward through the pillar-gaps during the forward flow but are prevented from returning during the reverse flow. RBC can therefore be found in the uppermost outlets of the sorting region. Larger and less deformable WBC, trapped by the constrictions, do not move upward through the rows and are forced out into the

lower outlets by the horizontal flow. With this approach, the device yielded a WBC separation efficiency >98% from whole blood, with a purity of 100% (no RBC contamination), at a sample throughput of 5 μ L/hour. The also author's claim that as the cell deformation induced by the micropillars is less than what WBC naturally experience within the body's microcapillaries, the microfluidic ratchet mechanism does not adversely affect cell viability. While device clogging is alleviated partly by the secondary tangential flow, the oscillating flow gets rid of any non-specific adherent cells with each reverse flow. This enables a clog-free, and nearly perpetual, cell separation process from high-density whole blood samples. While the device possesses a lot of favorable characteristics, the current low flow rate limits its use for high throughput leukapheresis applications. Device parallelization is mentioned as an option to increase device throughput however, an attempt was not presented in this work.

Yamada et al. also present a microfluidic platform that utilizes distinct geometric features to enable continuous size-based separation of WBC from dilute blood (1:20).¹³⁵ The device consists of a lattice-shaped network made up of "main channels" and "separation channels" that cross perpendicularly and are slanted against the macroscopic flow direction, with a fixed angle ranging from 15-45°. The density of the separation channels is 30-100 times greater than that of the main channels produces an asymmetrical flow distribution at each intersection of the channels. Particles smaller than a critical value flow along the streamline and enter the separation channels. Larger particles do not enter these channels and just flow along the main channels until they reach a specific outlet, primarily depending on their size. This separation mechanism yielded WBC separation from RBC with ~40% efficiency, and a purity of up to ~95%.

Furthermore, the lattice design mitigated clogging issues as bypass flows are generated when several points become obstructed. This study reported no signs of microchannel clogging after 30 minutes of operation. A parallelized version of the device with 8 lattice units was shown to operate at 400 $\mu\text{L} / \text{min}$ with no degradation of particle sorting precision, demonstrating the possibility for further parallelization and operation at higher throughputs. The effect of varied mechanical stresses, experienced by cells while flowing through various points of intersection, on cell activation and viability still need assessed.

Deterministic lateral displacement (DLD) is a hydrodynamic, microfluidic technology, first developed in 2004 by *Huang et al.* to separate particles on based on their size in continuous flow process with a resolution of down to 10 nm.¹³⁶ DLD utilizes an array of pillars to conduct size-based particle separation.¹³⁷ The microarray is tilted so as to generate a fluid bifurcation and distinct streamlines between the gaps; therefore, the flow of particles is determined by the combination of fluidic forces and the effect of pillar obstacles.¹³⁸ Particles whose radii are smaller than the width of the first streamline will follow it and travel along the flowlines, whereas particles with radii larger than the streamline width will bump into the pillars and displace laterally to the next streamline (**Figure 1f**).¹³⁶ This cutoff width is known as the DLD critical diameter and is dependent on various design factors such as the downstream and lateral pillar gap, pillar diameter, and the row shift fraction.¹³⁸

Civin et al. utilized this phenomenon to fractionate leukocytes from whole blood for high-quality. The microchip consisted of three zones of increasingly smaller posts and gaps, which led to progressively smaller critical diameter cutoffs (zone 1: $\sim 8 \mu\text{m}$,

zone 2: $\sim 5.5 \mu\text{m}$, zone 3: $\sim 4\mu\text{m}$).¹³⁹ The channel consisted of two micropost arrays mirrored against each other, with a central bypass channel containing the buffer stream. The arrays bump the larger cells, WBC, into the central stream that culminates in the product outlet, while the smaller cells, RBC and PLT, continue following in the initial fluid direction toward the downstream waste outlets. The microchip was able to process 200 μL of 1:1 diluted whole blood (incubated with Tritest agent for flow cytometry purposes) in approximately 20 minutes. On average, using an optimized buffer system, the device was able to remove $\sim 99.9\%$ RBCs, with a WBC recovery of 88%. The microchip decreased the RBC:WBC ratio from 800:1 in the input sample to 0.19:1 in the output sample, resulting in an enrichment of $\sim 4200\times$. Furthermore, the device did not exhibit any clogging issues and conducted the fractionation with high product viability.

Campos-González et al. also utilized a DLD chip to conduct cell separation with the final goal of isolating CAR T-cells, a subset of WBC used to manufacture immunotherapies.¹⁴⁰ Their device was able to achieve an average WBC recovery of $>90\%$, with the RBC and PLT depletion of $>96\%$ and $>75\%$ respectively. Although this microchip had a relatively high throughput of 1.167 mL/min, the input sample processed was residual leukocytes from plateletpheresis product, diluted 1:4, and not whole blood. While these samples had near-regular RBC counts, ~ 10 -fold higher PLT counts, 10–20-fold higher lymphocytes and monocytes, and almost no granulocytes, it is important to note that this work was not done with whole blood. Despite that, we chose to include this work in our review as the higher lymphocyte and monocyte counts of the input samples could be argued to resemble a blood sample from a patient with lymphocytic

or monocytic leukemia, for which leukapheresis is sometimes indicated. While their current work reported on results using a parallelized 24-lane microchip, they envisioned that, when scaled-up, their closed-format, and automatable DLD platform could enable a fully automated closed system, in which an apheresis sample could be prepared and fully processed within 2–3 hours of collection.

3. Combinatorial Microfluidic Approaches

Some microfluidic devices employ a combination of mechanisms and geometric techniques to achieve cell separation, instead of relying on one particular method. Some of the devices discussed in previous sections exhibit this phenomenon. For instance, *Guo et al.* presented a device that employed microstructures in combination with cross flow and oscillatory flow to fractionate different types of blood cells.¹³⁴ Similarly, *Kuan et al.* used crossflow filtration and bifurcation law along with trapping pillars to obtain plasma, RBC, and WBC separately.⁶⁷

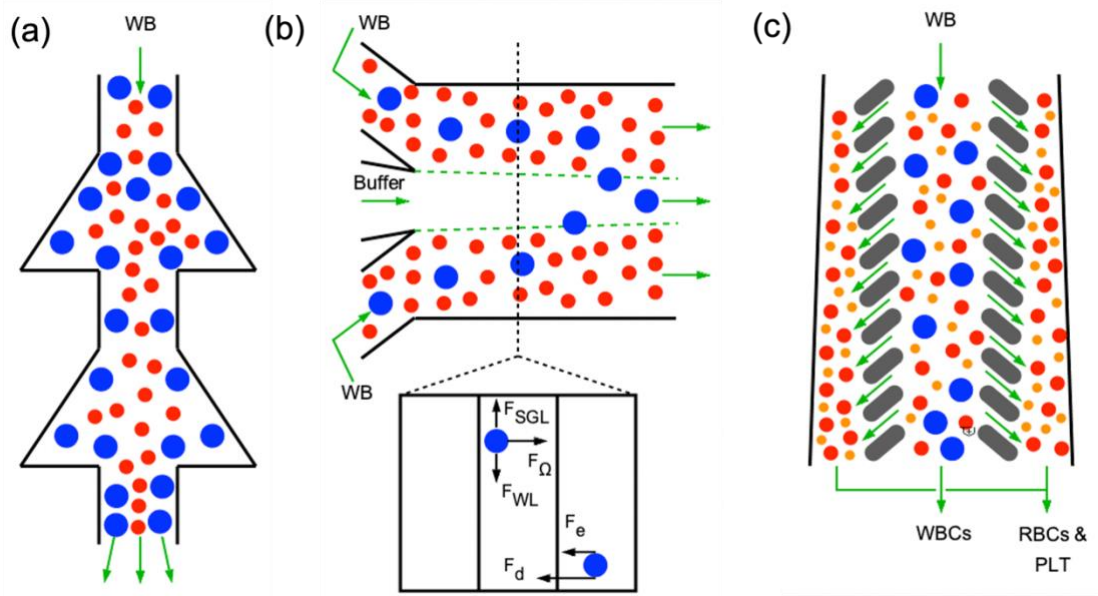


Figure 5. Principles behind cell separation using combinatorial microfluidic approaches. **(a)** Size-based particle margination due to triangular channel expansions. **(b)** Size-based particle diffusion within a co-flow system. **(c)** Size-based particle separation using controlled incremental filtration.

Figure 5 above illustrates the fundamental principles of size-based separation of cells utilized in the some of the microfluidic devices that employ combinatorial approaches presented in this review. The detailed descriptions of the subpanels in that figure are as follows: (a) Principle behind size-based particle margination due to triangular channel expansions (adapted from *Jain et al. 2011*). (b) Principle behind size-based particle diffusing in a co-flow system (adapted from *Zhou et al. 2019*). (c) Principle behind size-based particle separation using controlled incremental filtration (adapted from *Lezzar et al. 2021*). Whole blood flow is denoted by green arrows. Particle size is denoted by different colored circles (blue>red>orange). Force phenomena and direction are denoted by black arrows (F_{SGL} = shear gradient-induced

lift force, F_{Ω} = rotation-induced force, F_{WL} = wall-induced lift force, F_e = possible elastic force, F_d = shear-induced diffusion).

Jain et al. induced cell margination utilizing a combination of hydrodynamic principles and dependence on structural changes within microchannels to develop a biomimetic, cell extraction device to isolate nucleated cells (NC), including WBC, from whole blood.¹⁴¹ The device uses repeated expansion and contraction of its triangular geometry to mimic postcapillary venules and to enhance cell margination and extraction (**Figure 5a**). The design incorporates a straight microchannel interrupted by triangular ‘expansions’ at regular intervals. Within these triangular expansions, there is a decrease in shear stress, which activates homotypic adhesion of cells, resulting in the exclusion of nucleated cells from the bulk flow. The RBC, therefore, aggregate loosely around the axis of the flow, while most of the NC marginate to the wall, residing in a plasma-rich layer. Two extraction channels leading off of the side walls then collect the NC. The device operated on unprocessed whole blood with an NC extraction efficiency of $\sim 94 \pm 4.5\%$, purity of 5%, and enrichment in concentration of 45.75 ± 2.5 -fold. The functioned at a relatively low flow rate of $\sim 0.3 \mu\text{L}/\text{min}$, but it is suggested that the throughput can be easily scaled up. However, investigation of cell activation and channel clogging need to be conducted to identify the suitability of this device for leukapheresis.

Zhou et al. another unique approach to enrich WBC from undiluted WB by combining inertial migration with shear-induced diffusion through the parallel flow of Newtonian and non-Newtonian fluids. This is achieved by utilizing a co-flow microfluidic system in which two streams of whole blood flank a central stream of saline buffer within a rectangular microchannel.¹⁴² As a result of shear-induced diffusion

(SID), the cells are theorized to undergo size-dependent lateral migration towards the center of the channel and get focused within the buffer stream (**Figure 5b**). The larger-sized cells migrate faster towards the channel center than smaller cells such as RBC, resulting in their enrichment in the central outlet. Simultaneously, inertial forces in the buffer flow help guide the particle/cell migration within the central stream, with certain lift forces also possibly affecting particle movement across the fluid interface. For instance, a follow-up study proposed that a shear-induced lift force, counteracting SID, may contribute to governing the dynamics of migration across the fluid interface. By running the blood sample (spiked with microparticles) and buffer at 112.5 $\mu\text{L}/\text{min}$ each, the results showed an RBC removal efficiency of 97.6% for samples diluted 2-fold (22.5% Hct) with saline, and 64.8% for the undiluted sample (45% Hct). In a follow up study, the group attempted to isolate WBC by utilizing the same co-flow system with two streams of undiluted whole blood flanking a central stream of phosphate buffer.¹⁴³ While this mechanism enabled WBC separation at 133 $\mu\text{L}/\text{min}$ for WB and 267 $\mu\text{L}/\text{min}$ for the buffer, the performance in terms of WBC enrichment ($\sim 2.6\times$) and purity was lower than some of the existing methods that processed highly dilute blood samples. Furthermore, no studies have been conducted to investigate cell activation or viability.

Gifford et al. introduced a new technology that relies on the combination of unique structural features and crossflow filtration to perform high throughput cell separation¹⁴⁴. Known as ‘controlled incremental filtration’ (CIF), the technology is a modification of the traditional crossflow filtration approach. The microchannel is divided into three sub-channels by two rows of equally spaced pillars. These include a central channel with a constant width and two side channels on either side whose width

increases at a constant rate. Unlike a conventional crossflow approach, the filtration of cells is not dependent on the size of gaps between the pillars but rather on the rate of increase of the side channels. This rate of increase determines the critical diameter or size cutoff for separation. Cells larger than the critical diameter stay in the central channel, while those lower than the critical diameter flow to the side channels (**Figure 5c**). Because the separation relies on the rate of change of the geometric structure of the channel, the device can perform cell fractionation even at higher gap sizes ($>15\ \mu\text{m}$). This enables the fabrication of deep, high-aspect-ratio devices that can process large amounts of fluid at once, especially when the channels are parallelized.

For instance, our lab has developed a microfluidic device containing 48 CIF-based channels to perform high-throughput blood cell separation and to enable centrifugation-free leukapheresis.¹⁴⁵ The multiplexed device was capable of processing whole blood (diluted 1:4 with saline) at 10 mL/min with 84% total WBC removal, ~89% separation of RBC and PLT ($<12\%$ overall loss), and void volume of just 0.4 mL. While we reported the optimal blood fractionation at 10 mL/min and with a 10% sample HCT, the device still performed with results on par with conventional centrifugation-based apheresis methods at flow rates up to 30 mL/min and with samples with up to 30% HCT. When tested in a recirculation circuit, to mimic conventional leukapheresis, the device operated without clogging or decline in separation performance and was able to lower WBC counts exponentially, with minimal activation of WBC and PLT and no measurable damage to RBCs over the duration of the 3.5-hour recirculation procedure. Our results suggest that with further development, CIF-based devices may be able to

remove WBC from whole blood with both volumetric throughput and separation efficiency sufficiently high to ultimately enable centrifugation-free leukapheresis.

DISCUSSION

While there has been significant progress in microfluidic technologies for blood fractionation in the last decade, their implementation in clinical practice is still limited. There are several fundamental drawbacks that prevent the implementation of microfluidic platforms in clinical settings. Some of them are common to all of the microfluidic devices and some are specific to particular methods. Here we have described the main challenges and how to potentially overcome them. One of the key differences between conventional leukapheresis and microfluidic devices is the continuous nature of clinical leukapheresis, when processed blood is returned back to the patient. Currently, no microfluidic methods have shown the possibility to be performed in such a way in vivo. The necessity to return the blood to the patient without an excessive amount of diluent limits the scope of input sample dilution, which is an essential principle of some microfluidic methods.

Sample dilution is most critical for microfluidic devices with both straight and spiral channels as well as platforms exploiting inertial flow, Dean flow and DLD principles for cell separation. It has been shown in *Wu et al.*¹²² and *Nivedita et al.*¹²³ that cells begin to migrate under the influence of the inertial forces only after a certain dilution and flow rate is achieved. This limitation is very hard to overcome as the necessity of certain Reynolds numbers must be met in order to trigger the particle

migration effect.¹⁴⁶ An additional hurdle is that the dilution should be high enough to make the effect of bumping between cells negligible. Both obstacles make it so that large dilutions of the input sample are required to achieve efficient cell separation. While deterministic lateral displacement methods have been shown to operate with smaller sample dilutions,^{139,140} the blood sample concentration still has an influence on DLD performance due to the particle–particle interaction effect. Higher blood concentrations result in cell collisions with a non-deterministic nature, with undiluted blood samples having a high enough concentration to disrupt the streamline of the surrounding fluid and changing the critical diameter cutoff and efficiency of cell separation.¹³⁸

Another challenge for clinical implementation of these microfluidic devices is the requirement of a high-enough throughput to perform the procedure within a reasonable amount of time. This means that to filter the typical patient’s blood, the device must be capable of processing ~5L of whole blood within a couple of hours. This problem is most challenging for traditionally low-throughput methods, such as particle trapping and porous membrane filtration, as well as devices with separation based on specific microstructures or geometry. The trapping and filtration approaches that we reviewed here did not exceed a 200 $\mu\text{L}/\text{min}$ flow rate, because they all require the physical holding of blood cells within their microstructures. Thus, to catch a typical half a billion cells during leukapheresis, such a device should have hundreds of millions of microstructures. This poses a big challenge in manufacturing and operation.^{147,148} Finally, cell activation and device clogging additional factors that may limit the widespread implementation of these microdevices in clinical settings. Any clinical

procedure must be safe for the patient and should not activate the body's natural coagulation processes.

One of the possible solutions to overcome these challenges is to utilize a combination of different microfluidic methods together within a single device. Using the combination of techniques that allow for high-throughputs and low sample dilution seem to be most promising. For example, *Jain et al.* and *Lezzar et al.* achieved >80% WBC separation with undiluted blood and 1:4 input sample dilution, respectively. *Jain et al.* utilized an approach combining hydrodynamic principles and unique structural changes within microchannels, while *Lezzar et al.* used a combination of unique structural features and crossflow filtration.^{141,145} Both of these combinatorial techniques allowing for high WBC separation with low input sample dilution (in comparison to the other techniques discussed).

Another promising solution is to multiplex individual microfluidic devices within a larger platform, thus multiplying the throughput while preserving advantages of low-throughput methods. Using a higher flow rate to achieve faster separation can also improve the throughput, however, with risk of streamline disruption at a higher Reynolds number regime as well as device delamination issue. To avoid this, stacking or parallelization of devices along with the utilization of higher flow rates have been reported. This idea has been represented in *Lezzar et al.*,¹⁴⁵ with 48 CIF-based devices parallelized and blood processed at 10 mL/min, and in *Mutlu et al.*,¹⁴⁹ with 104 NISA devices parallelized and a processing rate of 6 mL/min, with cell separation efficiencies (>80% WBC) and procedure times (~3 hours) comparable to conventional centrifugation-based leukapheresis.

Table 2. Overview of the microfluidic approaches discussed in this work and their performance metrics.

	Author	Fundamental Principle	Notable Modification(s)	Input sample dilution	Flow rate	Target output(s)	WBC Separation performance
Porous Membranes	Wei et al. ¹²⁴	Crossflow & dead end filtration hybrid	Porous membrane made without plasma oxidation & with smaller pores	1:40	2-3.33 $\mu\text{L}/\text{min}$	WBC, RBC, PLT	99.7% ($d > 6.4\mu\text{m}$)
	Hasokawa et al. ¹²⁵	Dead end filtration	Size of microcavities controlled by application of pressure	1:200	200 $\mu\text{L}/\text{min}$	WBC	>90%
	Li et al. ¹²⁶	Crossflow filtration	Combines crossflow filtration scheme with a high porosity PDMS microfiltration membrane	none	1 mL/hr	WBC	27.4 \pm 4.9%
Trapping Microstructures	Cheng et al. ⁶⁸	Crossflow & dead end filtration	Integrates a bidirectional micropump to flush micropores to avoid membrane clogging.	none	37.5 $\mu\text{L}/\text{min}$	WBC	72.10%
	Alankarian et al. ¹²⁰	Pillar-based filtration	U-shaped array of pillars	none	15-50 $\mu\text{L}/\text{min}$	WBC	~18%-25%
	Kuan et al. ⁶⁷	hydrodynamic-based trapping units; bifurcation law and crossflow filtration	Bifurcation regions leading to filtration zones with pillars or beads	none	0.3 $\mu\text{L}/\text{min}$	WBC, RBC, Plasma	1200-1800 trapped WBC
Physical Filtration	Wu et al. ¹²²	Inertial forces within spiral microchannel	Trapezoidal channel cross-section	(1-2% Hct)	0.8 mL/min	WBC (PMN, MNL)	>80%
	Nivedita et al. ¹²³	Inertial forces within spiral microchannel	Optimized spiral devices with reduced size (10x)	1:500 (0.1% Hct)	1.8 mL/min	WBC, RBC	~95%
	Wu et al. ¹⁰⁹	Inertial lift force & microstructure-induced localized secondary flow	Induce secondary flows modify the original cell focusing profiles in straight rectangle channels	1:400 (0.25% Hct)	150 $\mu\text{L}/\text{min}$	WBC, RBC	89.7%
	Mutlu et al. ¹⁴⁹	Inertial forces; Non-equilibrium inertial separation array	Non-equilibrium separation allows shorter wall lengths which reduces the pressure requirement & allows for a compact structure	1:1	6 mL/min	WBC	~96%
	Zhang et al. ¹²⁶	Inertial forces within serpentine microchannels	Symmetric serpentine channels provide differential inertial focusing along the lateral direction	1:20	4.8 mL/min	WBC	>90% (10X enrichment)
	Jeon et al. ¹²⁹	Inertial forces within spiral microchannel	Two spiral channels with different dimensions, check-valve-based recirculation	1:500	18.4 mL/min	WBC	~80%
	Kim et al. ¹²⁷	Deterministic migration	Slanted ridges	none	~143 $\mu\text{L}/\text{min}$	WBC	80%
	Guo et al. ¹³⁴	Microfluidic ratchets; matrix of micrometer-scale tapered constrictions	Oscillatory flow creates ratcheting transport depending on particle size/deformability & prevents clogging	none	~0.083 $\mu\text{L}/\text{min}$	WBC	>98%
	Yamada et al. ¹³⁵	Lattice-shaped sieve; channel density & slant angle affect sorting behaviors	Sorting size cutoff controllable by altering lattice geometry (e.g. densities of perpendicularly crossing channels)	1:20	400 $\mu\text{L}/\text{min}$	WBC (MNC)	~40%
	Civin et al. ¹²⁹	Deterministic lateral displacement	Commercially produced, inexpensive, plastic microchip	1:1	10 $\mu\text{L}/\text{min}$	WBC	88%
Structural Effects	Campos-Gonzalez et al. ¹⁴⁰	Deterministic lateral displacement	First instance using microfluidic device to separate & purify LRS samples	LRS sample 1:4	1.17 mL/min	WBC (CAR T-cells)	>90%
	Jain et al. ¹⁴¹	Margination	Expansion of triangular segments of the microchannel enhance cell margination	none	18 $\mu\text{L}/\text{hr}$	WBC (nucleated cells)	94 \pm 4.5%
	Zhou et al. ¹⁴³	Shear-induced diffusion	Co-flow system	None	133 $\mu\text{L}/\text{min}$	WBC	2.6X enrichment
	Lezzer et al. ¹⁵⁰	Controlled incremental filtration	Capable of efficient cell separation in a closed-loop recirculation regime	1:4 (10% Hct)	10 mL/min	WBC, RBC, PLT	>80%
Combinatorial Microfluidic Approaches							

In **Table 2** we have compiled the microfluidic approaches discussed in this work and their performance metrics, including flow rate, sample dilution and cell separation efficiencies. Despite the challenges described, microfluidic devices potentially have several advantages over conventional centrifugation-based leukapheresis. Smaller dead volume can be critical for the patient with a low circulating blood volume, such as neonates and low-weight infants, and can drastically reduce medical complications among them. Microfluidic devices can also be gentler on the cells in terms of lower PLTs activation and have fewer complications for the patient overall. Microdevices also have a clinical impact as an easier-to-use approach that can be applied at the point-of-care and in regions with limited resources and cannot afford to maintain standard leukapheresis equipment. Through this work we see significant potential in microfluidic technologies as an inexpensive, easy to use and applicable approach for microfluidic leukapheresis.

CONCLUSION

Efficient blood fractionation into its specific components is a major step for blood analysis, clinical diagnosis, and biological research. High throughput separation and extraction of WBC from whole blood is critical in many areas of medicine. Leukapheresis is a centrifugation-based medical and laboratory procedure used to isolate a patient's WBC from whole blood while returning the rest of blood components back to the body. This procedure is used throughout the practice of medicine for two main applications, leukodepletion and cellular collection to provide potentially life-

saving treatments for millions of patients. However, conventional leukapheresis may not be widely accessible or available to many due to their complexity and prohibitively large size, making it challenging to provide therapeutic leukapheresis procedures for patients in resource-limited settings and at-risk neonates and low-weight infants. Recent developments microfluidic-based devices have the potential to provide efficient blood cell separation in order to address this clinical need for more accessible leukapheresis procedures.

Unlike apheresis machines, microfluidic systems are more easily produced single-use devices, can be relatively simple to set up and operate without necessitating specialized equipment, attendant training, large storage space or maintenance. These features could allow for more wider spread implementation of microfluidic leukapheresis platforms in clinical or in limited resource settings. In this work, we have reviewed passive microfluidic technologies that can separate WBC directly from whole blood, focusing on the technological developments made in the last decade. While *Lezzar et al.* and *Mutlu et al.* have shown WBC from whole blood with smaller blood dilution factors and sample higher throughputs, when compared to many other microfluidic cell separation platforms, these systems need further development and improvements to become applicable in clinical settings. Despite that however, this work has demonstrated that there is movement in the field towards microfluidic platforms that can achieve efficient, accurate, and high-throughput separation of WBC from whole blood in order to provide viable alternatives to centrifugation-based leukapheresis.

CHAPTER 4: TOWARDS CENTRIFUGATION-FREE LEUKAPHERESIS IN PEDIATRIC PATIENTS USING HIGH- THROUGHPUT MICROFLUIDIC TECHNOLOGY

OVERVIEW

Leukapheresis, extracorporeal separation of white blood cells (WBCs) from red blood cells (RBCs) and platelets (PLTs) which are then returned to the patient, is a life-saving procedure frequently used for leukodepletion and cellular collection. Well tolerated by adults and older children, leukapheresis poses significant risk to neonates and low-weight infants because of the large extracorporeal volume (ECV) of the centrifugation-based leukapheresis machines. Here we describe a microfluidic device with a low void volume capable of removing WBCs from blood with separation efficiency on par with conventional leukapheresis when operating in a closed-loop recirculation regime. The device was designed using principles of controlled incremental filtration (CIF) and fabricated via soft lithography from polydimethylsiloxane. The separation performance of the device and its effect on blood cell properties were tested in both flow-through and recirculation regimes using blood from healthy donors. The CIF device (with a void volume of just 0.4 mL) was capable of processing whole blood (diluted to 10% hematocrit) at 10 mL/min with >80% WBC removal and only ~10% loss of RBCs and PLTs. In the recirculation regime, the device reduced the WBC count exponentially with minimal activation of WBC and PLTs and no measurable damage to RBCs over the entire duration of a 3-hour simulated

leukapheresis procedure. The results of this proof-of-concept study suggest that, with further development, CIF-based devices may be able to remove WBCs from whole blood with volumetric throughput and separation efficiency sufficiently high to ultimately enable centrifugation-free, low-ECV leukapheresis for the most vulnerable pediatric patients.

INTRODUCTION

Leukapheresis is a complex medical procedure during which patient's blood is passed through an apheresis machine to separate white blood cells (WBCs) from red blood cells (RBCs) and platelets (PLTs), which are then returned back to the patient.⁴⁴⁻
⁴⁶ A typical leukapheresis procedure reduces the peripheral WBC count by 20-60% (with a 10-15% loss of RBCs and PLTs), while processing 1-4 total blood volumes (TBV) of patient's blood at a flow rate of 10-50 mL/min.¹⁵¹⁻¹⁵³ Leukapheresis enables two potentially life-saving applications: leukodepletion and WBC collection. Leukodepletion can be used to reduce a dangerously high WBC count in patients with leukemia,^{39,154} or to remove activated WBCs as a drug-free treatment for inflammatory bowel disease¹⁵⁵⁻¹⁵⁷ and other conditions.^{158,159} Collection of WBCs via leukapheresis is the initial step in manufacturing a wide range of cellular therapies,¹⁶⁰ including granulocyte infusion,^{161,162} adoptive immunotherapies,^{56,163-165} hematopoietic stem cell transplantation,^{153,166,167} and novel gene-based treatments.^{168,169}

Although generally well-tolerated by adults and older children, performing leukapheresis for neonates and low-weight infants is technically challenging and

clinically risky. Currently, leukapheresis is performed using centrifugation-based apheresis machines, which have a substantial extracorporeal volume (ECV) typically ranging 150-250 mL,¹⁶⁰ whereas TBV of a 10 kg infant is only ~750 mL.^{106,170} Because the ECV represents such a large fraction of their TBV, pediatric patients experience a significantly higher incidence of serious complications associated with the leukapheresis procedure, including hypotension, symptomatic hypocalcemia, allergic reactions, catheter-related thrombosis, infections, severe anemia and even death.^{42,102,171-174}

There have been multiple attempts to miniaturize leukapheresis using various microfluidic cell separation techniques. The earliest work utilized a continuous-flow diffusive filter to remove WBCs from a sample of blood with high efficiency (>97%), albeit with a significant RBC loss (~50%) and at a flow rate of only 5 $\mu\text{L}/\text{min}$.¹⁷⁵ Although the throughput of microfluidic devices designed for separating WBCs from blood has significantly improved over the years,^{109,126,129,149,176} none so far have been able to match the performance required by a typical leukapheresis procedure.¹⁵¹⁻¹⁵³

Here we describe the development and initial validation of a new approach for performing leukapheresis based on ‘controlled incremental filtration’ (CIF), a high-throughput microfluidic technology for separating cells by size.¹⁷⁷⁻¹⁸⁰ We fabricated a multiplexed device comprising 48 CIF elements arranged in parallel, capable of processing whole blood (diluted to 10% hematocrit) at 10 mL/min with >80% WBC removal, <15% loss of RBCs and PLTs, and void volume of just 0.4 mL. When tested in the recirculation regime, the device operated without clogging or any decline in separation performance and was able to reduce WBC count exponentially, with minimal

activation of WBCs and PLTs and no measurable damage to RBCs over the entire duration of 3.5-hour recirculation procedure. These results suggest that with further development, CIF-based devices may be able to remove WBCs from whole blood with both volumetric throughput and separation efficiency sufficiently high to ultimately enable centrifugation-free, low-ECV leukapheresis in the pediatric setting.

METHODS

Blood samples

Units of whole blood (WB) were purchased from the Gulf Coast Regional Blood Center (Houston, TX). Sample of fresh WB were obtained by venipuncture from healthy, consenting volunteers (anticoagulant: acid citric dextrose, solution A; Vacutainer, BD Biosciences, Franklin Lakes, NJ). Samples were used immediately or stored in a blood bank refrigerator (4°C, iB111, Helmer Scientific, Noblesville, IN) until use, and diluted with isotonic saline (0.9% w/v NaCl, RICCA Chemical Company, Arlington, TX) to achieve the desired hematocrit (HCT). The experimental protocol was approved by the University of Houston Institutional Review Board.

Device fabrication

The design and fabrication of devices based on controlled incremental filtration (CIF) technology has been previously described in detail.¹⁷⁷⁻¹⁸⁰ Briefly, the CIF device design, generated using a custom code in MATLAB (The MathWorks Inc, Natick, MA),

was transferred into a ~140 μ m-thick layer of photoresist (SU-8 3050; Kayaku Advanced Materials Inc, Westborough, MA) on a 4" silicon wafer (University Wafer, South Boston, MA) using soft lithography. The master wafer was replicated in poly(dimethylsiloxane) (PDMS; Sylgard 184, Dow Corning Corp, Midland, MI), and the PDMS replica (device layer) was sealed against a PDMS-coated Petri dish (flat substrate) using oxygen plasma (PDC-001, Harrick Plasma, Ithaca, NY). The inlet and outlet ports in the device layer were created using biopsy punches (Acuderm Inc, Fort Lauderdale, FL) of appropriate size to match tubing connections (1.02- and 0.58-mm inner diameters; Scientific Commodities, Havasu City, AZ). An additional PDMS layer containing a system of large channels for collecting the filtrate and retentate outputs from the individual CIF elements of a multiplexed device was bonded on top of the device layer. After bonding, each assembled CIF device was treated with 1% (w/v) aqueous solution of mPEG-silane (MW 5000, Laysan Bio Inc, Arab, AL) for 25 min at 70°C. Finally, the device was flushed with GASP buffer (9 mM Na₂HPO₄, 1.3 mM NaH₂PO₄, 140 mM NaCl, 5.5 mM glucose, 1% w/v bovine serum albumin, 290 mmol/kg, pH 7.4) and stored in a refrigerator at 4°C until use.

Recirculation setup

The recirculation setup consisted of a blood bag (500 mL; Fenwal 4R1590, GenesisBPS, Ramsey, NJ) which was connected to the multiplexed CIF device and other components of the circuit by plastic tubing (Scientific Commodities) linked through appropriately sized Luer-lock connectors (Qosina, Ronkonkoma, NY). The

tubing conveying the blood sample from the bottom of the blood bag to the CIF device was connected to a syringe pump (Genie Touch, Kent Scientific, Torrington, CT) and the inlet of the CIF device via two 3-way stopcocks (Qosina). One stopcock was used for sampling the blood coming from the bag, and the other stopcock was used for connecting the syringe pump with either the outlet of the bag (to withdraw blood from the bag) or the inlet of the device (to infuse blood through the device). The mode of pump operation (infuse / withdraw) and the position of the stopcock were set manually during the experiment. The blood bag was mixed by hand between each recirculation round.

Measurements of separation performance and cell properties

Complete blood counts with a 5-part differential were measured using a hematology analyzer (XS-1000i, Sysmex America, Inc., Mundelein, IL). WBC, RBC and PLT counts were used to calculate the percent removal for each cell type as follows: $\% \text{ removal} = C_r / (C_r + C_f \times FR) \times 100$, where C_r is the cell count in the retentate (central channel output of all CIF elements), C_f is the cell count in the filtrate (side channel output of all CIF elements), and FR is the flow ratio of the device (defined as the ratio of the cumulative volume of the filtrate output to that of the retentate output of the device).¹⁸⁰

Imaging flow cytometry (FC, Amnis Imagestream^X Mk II, Luminex Corporation, Austin, TX) was used to measure PLT and WBC surface antigen activation markers, and the prevalence of PLT-WBC aggregates, using the following antibody

cocktails (all from BD Biosciences, San Jose, CA). PLT activation: CD41a/APC (20 μ L; BD 559777), CD62P/PE (20 μ L; BD 555524), Dulbecco's phosphate buffered saline without calcium or magnesium (DPBS-/-; 10 μ L). Thrombin receptor agonist peptide 6 (TRAP; 70 μ M; Sigma) was used as the positive control for PLT activation. WBC activation: CD45/APC (5 μ L; BD 561864), CD62L/FITC (20 μ L; BD 555543), CD11b/PE (20 μ L; BD 555388), and DPBS-/- (25 μ L). Phorbol myristate acetate (PMA; 0.5 μ g/mL; Sigma) was used as the positive control for WBC activation. PLT-WBC aggregates (PLA): CD45/APC (5 μ L), CD41a/FITC (20 μ L; BD 555466), and DPBS-/- (45 μ L). TRAP (70 μ M) was used as the positive control for PLA formation. To perform the FC measurements, 30 μ L of the blood sample were added to each antibody cocktail, gently mixed, and left to incubate in the dark for 15 min at room temperature (RT). After antibody labeling, RBCs were lysed using 1X BD FACS lysing solution for 15 min at RT. After lysis, samples were centrifuged at 900 \times g for 5 min to remove the supernatant, pelleted cells were resuspended in 100 μ L of 1% paraformaldehyde, and then stored at 4°C until FC measurements were performed (within 24 hours).

The level of free hemoglobin (Hb) in the supernatant was measured using the modified cyanmethemoglobin method following the manufacturer's instructions (Drabkin's reagent; D5941, Sigma). Briefly, a blood sample was centrifuged at 1000 \times g for 5 min to pellet the RBCs, then 40 μ L of the supernatant was added to 160 μ L of Drabkin's reagent, and incubated for 20 min. The absorbance was measured at 540 nm using a plate reader (SpectraMax M5, Molecular Devices, Sunnyvale, CA). Concentration of Hb was calculated using a calibration curve constructed with a human

Hb standard (Pointe Scientific Inc, Canton MI). The level of potassium (K^+) was measured using a handheld blood analyzer (i-STAT, Abbott Laboratories, Abbott Park, IL) using CHEM8+ cartridges, as previously described.¹⁸¹

Statistical analysis

All values were expressed as mean \pm standard deviation or mean \pm standard deviation (minimum – maximum). Statistical significance (defined as $p < 0.05$) of the observed differences was determined using either the paired two-sided t-test (cell count data), one-way ANOVA for (Hb measurements) or either 2-way repeated measures ANOVA or a mixed-effects model (restricted maximum likelihood) matched for both time and activation state with Sidak's multiple comparisons test (FC measurements).

RESULTS

Figure 6 illustrates the design of the multiplexed CIF device. A typical CIF design consist of three collinear flow channels separated by a series of 'pill'-shaped posts ($\sim 35\mu\text{m} \times 70\mu\text{m}$), which define the filtration gaps ($\sim 20\mu\text{m}$) connecting the central and the side channels fluidically (**Figure 6a**).^{177,178} As the blood sample flows through the central channel, a vanishingly small fraction of that flow is syphoned off into the side channels through every filtration gap. The width of the side channels gradually increases along the length of the device to accommodate the influx of the filtrate. When designing the device, the rate of this increase is calculated to precisely control the

fraction of flow extracted through each filtration gap. It is the magnitude of this flow fraction (not the width of the filtration gaps) that determines the size cutoff for the particles that are too large to be pulled into the side channels along with the syphoned fluid (critical diameter of the device).¹⁷⁷ Because the extracted flow fraction per gap is very small, each CIF element contains thousands of filtration gaps along the length of the device to reach the desired flow ratio, a quotient of the filtrate (combined output of the side channels) and retentate (output of the central channel) produced by the device.

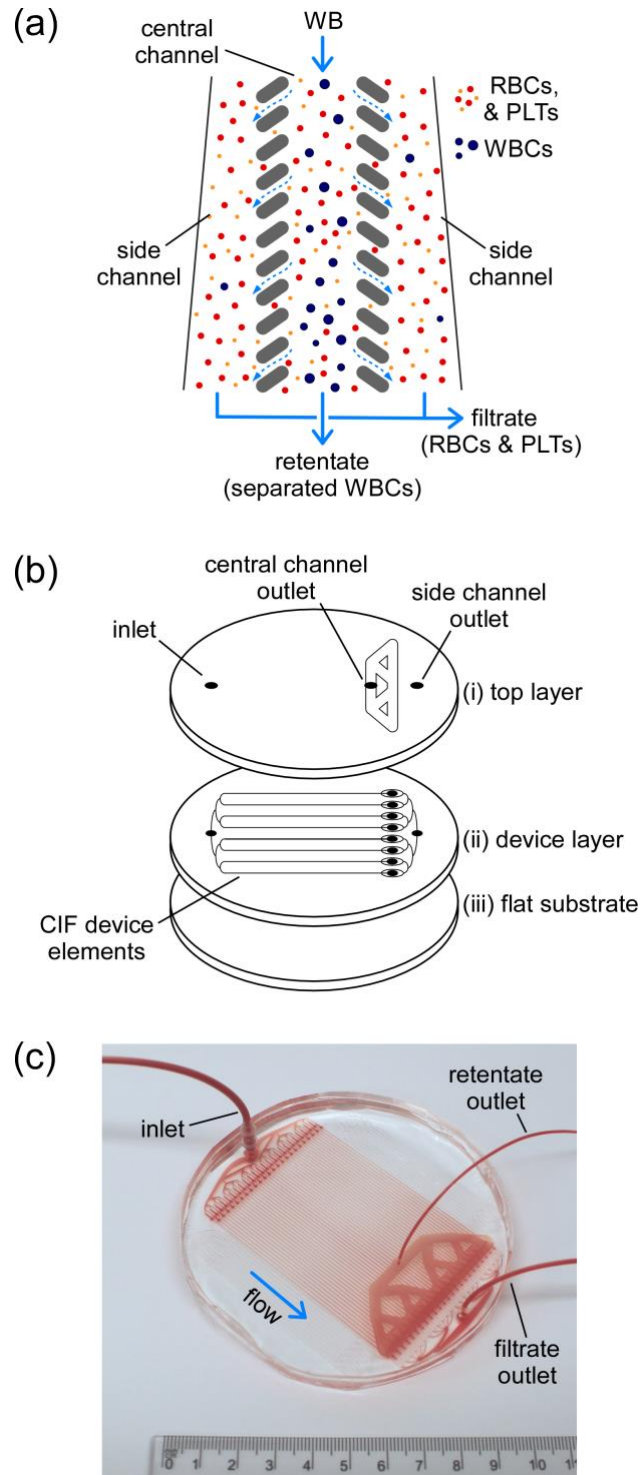


Figure 6. Design of the microfluidic device for leukodepletion of blood using controlled incremental filtration (CIF). (a) Schematic of blood cells (WBC, RBC, and PLT) cells flowing through the CIF device. (b) Components of the device. (c) An assembled microfluidic device comprised of 48 multiplexed CIF elements.

The multiplexed CIF device comprised an array of 48 individual CIF elements arranged in parallel. Each device consisted of three layers of PDMS stacked on top one another (**Figure 6b**). The device layer containing the array of CIF elements was sealed against a flat substrate to complete the channels. A series of thru holes in the device layer provided fluidic access to the common inlet and the outlets of each CIF element of the device. The outputs of all CIF elements were collected through a network of large channels in the separate top layer. As a result, a fully assembled multiplexed CIF device had one inlet through which blood sample was distributed to each CIF element of the device, and two outlets for collecting the outputs of the center channels (retentate) and side channels (filtrate) of all CIF elements (**Figure 6c**).

More detailed descriptions of the subpanels in **Figure 6** are as follows: (a) As WB flows through the central channel of the CIF device, most WBCs remain in the central channel. Smaller RBCs and PLTs are carried by the fluid into the two side channels, distributing between the central and the side channels according to the flow ratio. (b) The components of the device: (i) a ‘top layer’ containing a system of larger channels for collecting the central channel output from each CIF element of the device, (ii) a ‘device layer’ consisting of many individual CIF elements multiplexed in parallel, and (iii) a flat substrate for sealing the channels of the device. (c) An assembled microfluidic device comprised of 48 multiplexed CIF elements.

Figure 7 illustrates the performance characteristics of the multiplexed CIF device. To test the effect of sample HCT on the separation performance of the device, WB samples were diluted with normal saline down to $5.27 \pm 0.24\%$, $9.93 \pm 0.05\%$, $14.80 \pm 0.22\%$, $19.87 \pm 0.25\%$ and $29.30 \pm 0.50\%$ HCT, and passed through the device

at a flow rate of 10 mL/min (**Figure 7a**). The efficiency of WBC removal was the highest ($88.4 \pm 1.3\%$) for the sample with ~10% HCT, and then decreased precipitously as the HCT of the sample increased. The percent removal (loss) of smaller blood cells increased modestly with increasing HCT (from $10.6 \pm 0.9\%$ for RBCs and $9.1 \pm 0.5\%$ for PLTs at 5% HCT to $14.8 \pm 0.1\%$ for RBCs and $14.1 \pm 0.5\%$ for PLTs at 30% HCT). Overall, the level of RBC and PLT removal was consistent with cells smaller than the critical diameter of the device distributing between the filtrate and retentate according to the device flow ratio (**Figure 7a**, dashed line). For example, in our experiments with ~10% HCT samples the device operated at a flow ratio of 8.25 ± 0.23 for which we would expect 10.8% of the smaller cells to remain in the retentate, while the actual losses were $11.39 \pm 0.96\%$ for RBCs and $11.34 \pm 0.97\%$ for PLTs.

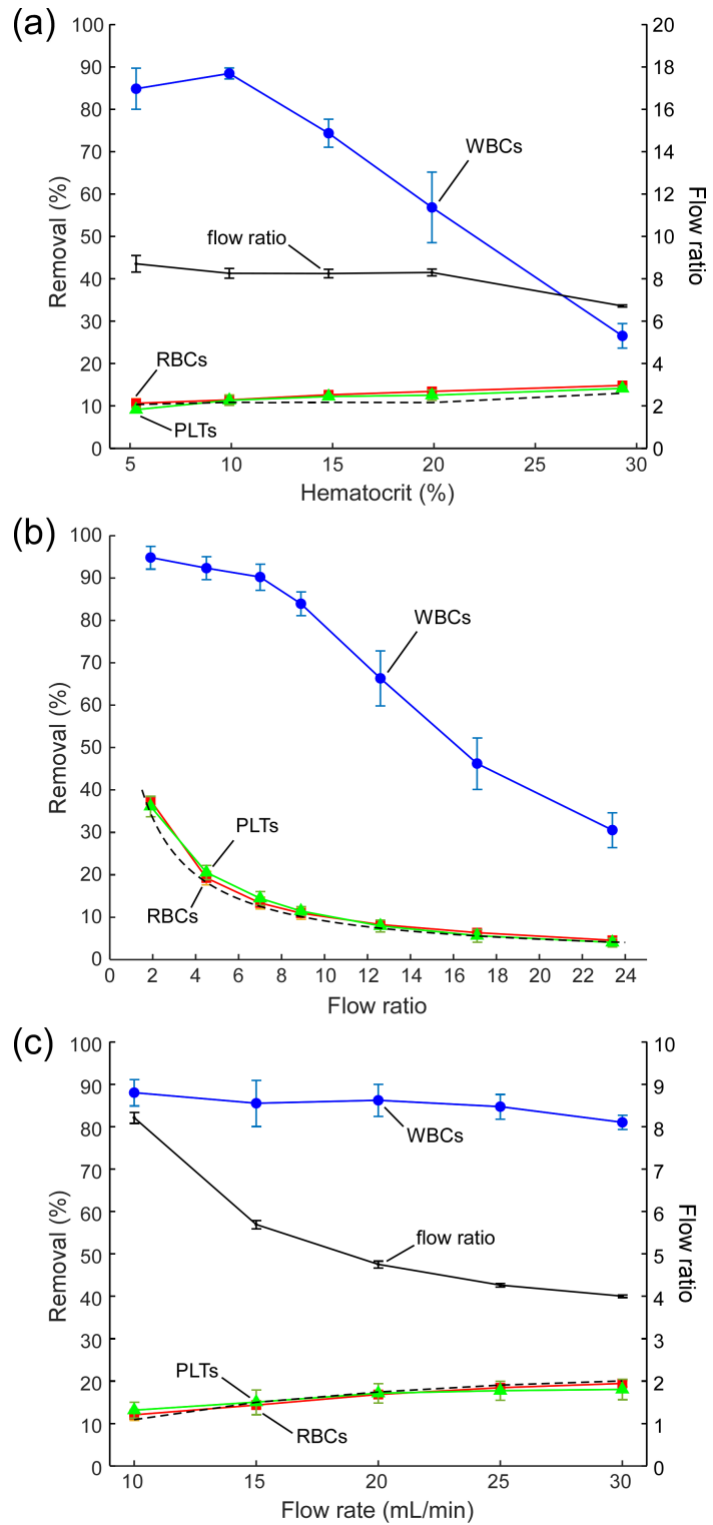


Figure 7. Performance of the multiplexed CIF device depending on (a) sample HCT, (b) device flow ratio, and (c) sample flow rate.

To determine how the separation performance of the multiplexed CIF device depended on its flow ratio, we passed samples of WB diluted to 10% HCT through the device at 10 mL/min and measured the output volumes and cell counts (**Figure 7b**). To control the flow ratio of the device *in situ*, we changed the pressure difference between the retentate and filtrate outlets by varying the relative height of the reservoirs collecting the output streams. This simple manipulation allowed us to control the flow ratio of the device within a relatively wide range (from 1.9 ± 0.1 to 23.4 ± 4.5). Lower flow ratios were associated with higher values of WBC removal, which remained consistently above 80% for all flow ratios up to ~ 9 . Further increase of the flow ratio resulted in a significant decline of WBC removal, decreasing from $84 \pm 3\%$ for the flow ratio of 8.9 ± 1.5 down to only $30 \pm 4\%$ for the flow ratio of 23.4 ± 4.5 (highest value tested). The removal (loss) of RBCs and PLTs followed the expected reciprocal dependence on flow ratio (**Figure 7b**, dashed line), decreasing rapidly from $37.5 \pm 0.8\%$ for RBCs and $36.1 \pm 2.4\%$ for PLTs at the flow ratio of 1.9 ± 0.1 to $10.9 \pm 1.5\%$ for RBCs and $11.4 \pm 1.3\%$ for PLTs at the flow ratio of 8.9 ± 1.5 , and further down to $4.5 \pm 0.6\%$ for RBCs and $4.0 \pm 1.1\%$ for PLTs at the flow ratio of 23.4 ± 4.5 (**Figure 7b**).

We further evaluated the separation efficiency of the multiplexed CIF device at flow rates ranging from 10 to 30 mL/min (**Figure 7c**). At higher flow rates the device features began to visibly deform, and the flow ratio declined significantly from 8.21 ± 0.13 at 10 mL/min down to 4.00 ± 0.03 at 30 mL/min. The percent WBC removal declined gradually with increasing flow rate from $88.0 \pm 2.5\%$ at 10 mL/min to $81.0 \pm 1.4\%$ at 30 mL/min (**Figure 7c**). The RBC and PLT loss increased from $12.0 \pm 1.1\%$ for RBCs and $13.1 \pm 1.5\%$ for PLTs at 10 mL/min to $19.4 \pm 0.6\%$ for RBCs and $18.0 \pm$

2.0% for PLTs at 30 mL/min, following the trend expected based on the device flow ratio (**Figure 7c**, dashed line).

More detailed descriptions of the subpanels in **Figure 7** are as follows: The dependence of cell removal on (a) sample HCT (10 mL/min flow rate, $n = 3$), (b) device flow ratio (10% HCT, 10 mL/min flow rate, $n = 5$), and (c) flow rate (10% HCT, $n = 3$). In panels (a) and (c), the device flow ratio was set at 8.70 ± 0.39 and 8.21 ± 0.13 respectively, and then allowed to change depending on the parameters of the experiment. Dashed lines indicate expected percent removal for cells that distribute between retentate and filtrate according to the flow ratio measured in each experiment. Values shown are mean \pm standard deviation.

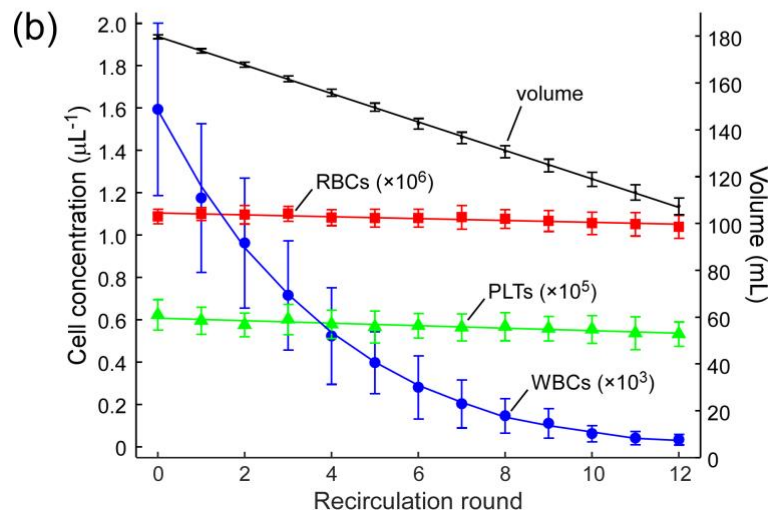
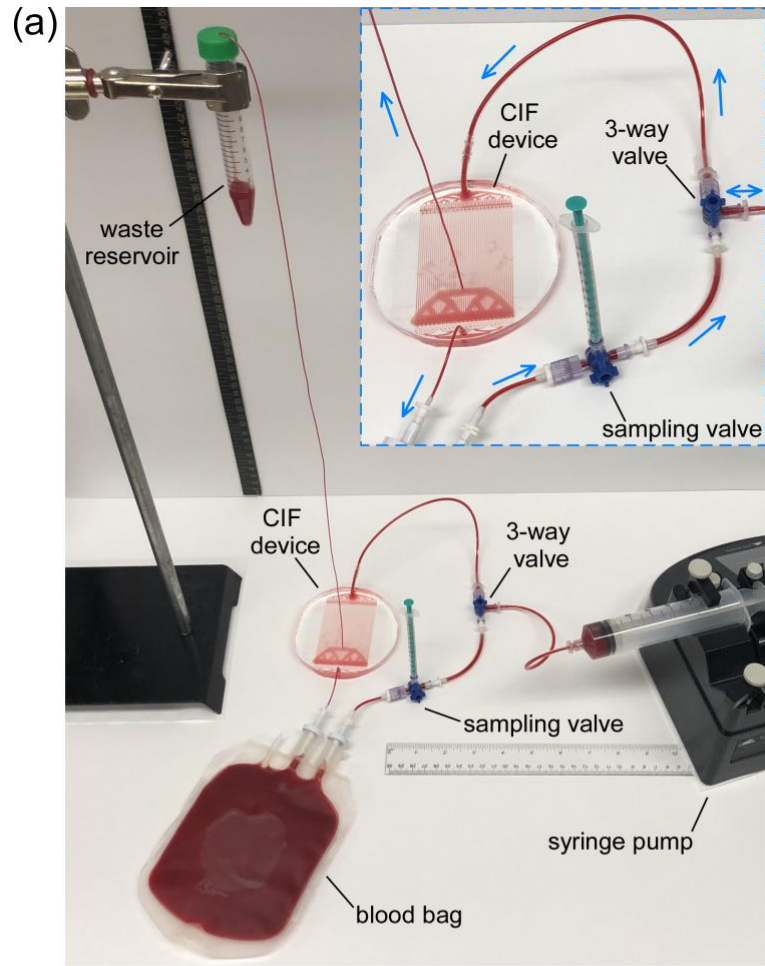


Figure 8. Removal of WBCs from blood during recirculation. (a) Experimental setup used for the recirculation experiments. (b) Changes in cell concentrations following each round of CIF-based cell separation in the recirculation regime.

Figure 8 shows the experimental setup in which we tested the ability of the multiplexed CIF device to remove WBCs from blood in the recirculation regime. In our setup, a blood bag filled with 179.7 ± 0.8 mL of WB diluted to 10% HCT was used to emulate the TBV of a subject. During each recirculation round, 56.5 ± 0.8 mL of the blood sample was withdrawn from the bag and then passed through the CIF device at a flow rate of 10 mL/min (controlled by the syringe pump). The retentate output (5.6 ± 0.5 mL per round) was collected into a conical tube, which was elevated 55 cm above the CIF device to produce the flow ratio of 8.8 ± 0.3 (**Figure 8a**). The filtrate output was fed back into the blood bag via a length of tubing inserted through the sampling port of the bag. This withdraw-infuse cycle was repeated 12 times over ~3 hours. The blood bag was mixed during each recirculation round to ensure uniform distribution of cells throughout the bag. Following the completion of each round, a 0.2 mL sample was taken from the bag (via the sampling valve) and from the retentate output (separated WBCs) for measurements. The volumes of the retentate and of each sample collected for measurements were recorded after each recirculation round to calculate the change in volume of the blood bag during the experiment.

As expected, the concentration of WBCs in the blood bag declined exponentially throughout the recirculation experiment (**Figure 8b**). After only 3 recirculation rounds (~170 mL processed volume), WBC concentration decreased by 55%, from $1.59 \pm 0.41 \times 10^3/\mu\text{L}$ in the initial sample down to $0.72 \pm 0.26 \times 10^3/\mu\text{L}$. At round 6 (~340 mL processed volume), WBC concentration decreased further down to $0.28 \pm 0.15 \times 10^3/\mu\text{L}$ (82% decrease from the initial level). By the end of the recirculation experiment (round 12, ~680 mL processed volume), WBCs in the bag were virtually depleted (~98%

decrease from the initial level). A simple model that assumes 56.5 mL of the current volume in the bag is passing through the device at each round and the separation efficiency of the device remains constant provided the best fit (in the root-mean-square error sense) to the data for WBC removal of 81% (**Figure 8b**). In contrast, the concentration of RBCs and PLTs decreased linearly over the entire duration of the recirculation experiment: by ~4.5% for RBCs (from $1.09 \pm 0.03 \times 10^6/\mu\text{L}$ to $1.04 \pm 0.05 \times 10^6/\mu\text{L}$; $y = -0.0044x + 1.1037$, $R^2 = 0.8218$), and by ~14.5% for PLTs (from $0.62 \pm 0.07 \times 10^5/\mu\text{L}$ to $0.53 \pm 0.06 \times 10^5/\mu\text{L}$; $y = -0.0059x + 0.6072$, $R^2 = 0.8485$). The volume also decreased linearly ($y = -0.0608x + 1.7975$, $R^2 = 0.9997$) by ~40% overall, at a rate consistent with the volume of retentate extracted and samples withdrawn during the experiment.

More detailed descriptions of the subpanels in **Figure 8** are as follows: (a) The experimental setup used for the recirculation experiments. The blood bag was filled with 179.7 ± 0.8 mL of WB diluted to 10% HCT with normal saline. The waste reservoir collecting the retentate (separated WBCs) was placed 55 cm above the device; the resulting device flow ratio was 8.8 ± 0.3 . At each recirculation round, 56.5 ± 0.8 mL of the sample was withdrawn from the bag and then infused through the CIF device at a flow rate of 10 mL/min, while producing 5.6 ± 0.5 mL of retentate (waste). A 1-mL syringe was used to sample the blood coming from the bag. Arrows indicate the direction of flow of blood in the circuit. (b) The changes in cell concentrations following each round of CIF-based cell separation in the recirculation regime. Values shown are mean \pm standard deviation ($n = 9$, using blood from 6 unique subjects). Solid lines are linear fits for volume ($y = -0.0608x + 1.7975$, $R^2 = 0.9997$), RBCs ($y = -0.0044x$

+ 1.1037, $R^2 = 0.8218$) and PLTs ($y = -0.0059x + 0.6072$, $R^2 = 0.8485$), and a model fit for WBCs (with 81% WBC removal minimizing the root-mean-square error).

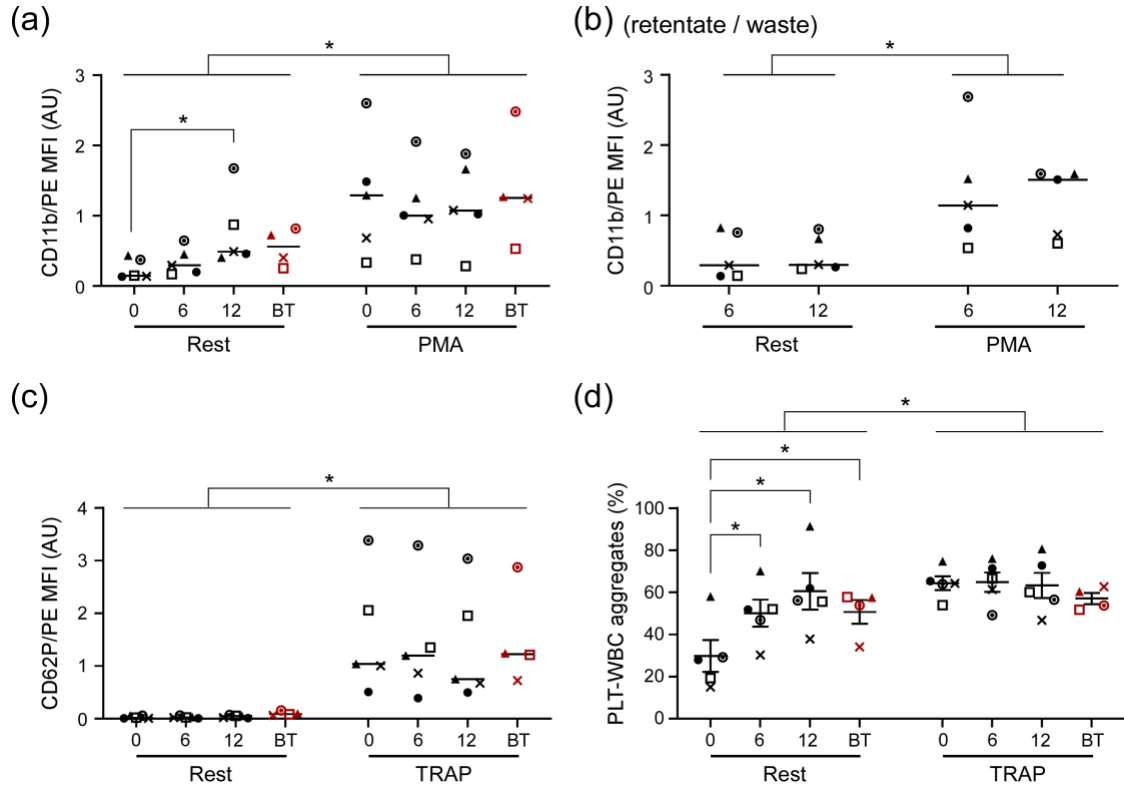


Figure 9. Effect of CIF processing on the activation state of WBCs and PLTs. Activation of (a) WBCs (CD11b) remaining in the recirculating blood, (b) WBCs (CD11b) removed with the retentate (waste), and (c) Recirculating PLTs (CD62P). (d) Formation of PLT-WBC aggregates in the recirculating blood.

Figure 9 describes the effect of CIF processing in the recirculation regime on cell properties. Activation of WBCs (CD11b) and PLTs (CD62P), and PLT-WBC aggregate formation were measured via imaging flow cytometry (FC) for samples collected from the bag before (round 0), during (round 6), and immediately after (round

12) the recirculation experiments. Activation of separated WBCs (retentate output) was measured during (round 6) and after (round 12) of the experiment. Additionally, in four out of five recirculation experiments, a sample of the subjects' blood was set aside on the benchtop (BT) for the duration of the experiment to control for possible auto-activation of WBCs and PLTs from simply being stored at room temperature for a prolonged period of time. All samples were tested at rest (as collected) and after incubation with either PMA (for WBCs, **Figure 9a-b**) or TRAP (for PLTs and PLT-WBC aggregates, **Figure 9c-d**) to evaluate how CIF recirculation affected the ability of WBCs and PLTs to become activated in response to relevant stimuli.

There was a significant increase in activation of the recirculated WBCs between round 0 and round 12 ($p < 0.05$), but the difference between round 12 and BT control was not significant (**Figure 9a**). WBCs were still able to undergo significant further activation in response to PMA, regardless of when they were sampled during the recirculation experiment (**Figure 9a**). Removed WBCs (in the retentate) had similar levels of activation after rounds 6 and 12 and were also able to undergo significant activation following exposure to PMA (**Figure 9b**). Surprisingly, activation of PLTs in the recirculating blood did not increase significantly over the entire duration of the experiment, and in the end was not different from PLT activation in the BT control (**Figure 9c**). Importantly, PLTs retained their ability to become significantly activated in response to TRAP stimulation (**Figure 9c**). The number of PLT-WBC aggregates in the recirculating blood increased steadily and significantly over time (**Figure 9d**). However, there was no significant difference between the level of PLT-WBC aggregates in recirculating blood sampled after round 12 and in BT control. Furthermore, the

number of PLT-WBC aggregates was able to increase upon stimulation with TRAP in all samples (**Figure 9d**).

More detailed descriptions of the subpanels in **Figure 9** are as follows: Effect of CIF processing in the recirculation regime on the activation state of WBCs and PLTs. (a) Activation of WBCs (CD11b) remaining in the recirculating blood. (b) Activation of WBCs (CD11b) removed with the retentate (waste). (c) Activation of recirculating PLTs (CD62P). (c) Formation of PLT-WBC aggregates in the recirculating blood. Measurements were performed via flow cytometry for samples collected before (round 0), during (round 6), and after (round 12) the recirculation experiment, both at rest and after additional activation with PMA (panels a & b) or TRAP (panels c & d). BT (red symbols) represent blood samples set aside for the duration of each recirculation experiment to assess the effect of time alone on cell activation. Statistical significance is denoted by * for $p < 0.05$. Each symbol represents a different recirculation experiment ($n = 5$, using blood from 4 unique subjects).

Finally, to determine if CIF processing damaged RBCs during the recirculation experiments, free hemoglobin (Hb) and potassium levels were measured before, during (round 6), and immediately after the 12 consecutive rounds of recirculation through the device. We did not observe any significant changes in free Hb levels throughout the procedure, and potassium levels remained below the detectable level (< 0.2 mM) in all samples (**Table 3**).

Table 3. Free hemoglobin (Hb) and potassium (K⁺) measurements taken before, during, and immediately after the 12 consecutive rounds of recirculation through the device; and measurements taken from a control blood sample left to sit in a tube on the lab bench at room temperature.

	Recirculation Trial	1	2	3	4	5
BEFORE (Round 0)	Free Hb (g/dL)	0.2253 ± 0.003	0.2866 ± 0.0001	0.3419 ± 0.002	0.3170 ± 0.001	0.3550 ± 0.001
	K ⁺ (mmol/L)	< 2.0	< 2.0	< 2.0	< 2.0	< 2.0
DURING (Round 6)	Free Hb (g/dL)	0.2272 ± 0.001	0.2881 ± 0.003	0.3445 ± 0.001	0.3147 ± 0.002	0.3572 ± 0.004
	K ⁺ (mmol/L)	< 2.0	< 2.0	< 2.0	< 2.0	< 2.0
AFTER (Round 12)	Free Hb (g/dL)	0.2315 ± 0.009	0.2870 ± 0.0004	0.3445 ± 0.002	0.3163 ± 0.005	0.3599 ± 0.005
	K ⁺ (mmol/L)	< 2.0	< 2.0	< 2.0	< 2.0	< 2.0
BENCH CONTROL (After Round 12)	Free Hb (g/dL)	n/a	0.2894 ± 0.001	0.3462 ± 0.003	0.3140 ± 0.001	0.3586 ± 0.001
	K ⁺ (mmol/L)	n/a	< 2.0	< 2.0	< 2.0	< 2.0

A more detailed description of **Table 3** is as follows: Free Hb and K⁺ measurements (mean of triplicate) taken before, during, and immediately after the 12 consecutive rounds of recirculation through the device (n = 5, using blood from 4 unique subjects); and measurements taken from a control blood sample left to sit in a tube on the lab bench at room temperature (n = 4 using blood from 4 unique subjects). Values shown are mean ± standard deviation.

DISCUSSION

The goal of leukapheresis is to remove as many WBCs as possible in the shortest amount of time without losing too many RBCs and PLTs. Currently, a leukapheresis procedure involves recirculating a large volume of blood (equivalent to 1-4 of patient's

TBV) through a centrifugation-based apheresis machine with a significant void volume (150-250 mL) over a prolonged period of time (3-4 hours). A result of this process is a 20-60% reduction in the peripheral WBC count of the patient, with a 10-15% loss of RBCs and PLTs.^{151-153,182} The multiplexed CIF device described in this study was able to consistently remove >80% of the WBCs passing through the device, reducing WBC count in the recirculating blood by ~55% after only 3 recirculation rounds, which is equivalent to processing approximately one TBV in our experimental setup. CIF-based leukapheresis with such a level of WBC separation efficiency could significantly reduce the volume of blood required for clinically relevant leukodepletion and/or cellular collection. The CIF device was able to operate in the recirculation regime for >3 hours without losing separation efficiency or causing any significant damage to recirculating blood cells. Importantly, the void volume of the multiplexed CIF device (~0.4 mL) was substantially less than that of a conventional centrifugation-based apheresis machine. Leukapheresis with such an ultra-low ECV could eliminate the need for priming the circuit with allogeneic blood products, minimize fluctuations in patient's hemodynamic parameters and thus significantly reduce the risk of complications for low-weight neonates and infants undergoing the procedure.

The separation performance of the CIF device was maximized at 10% HCT and declined precipitously for blood samples with higher HCTs. Pediatric cancer patients undergoing leukapheresis for leukodepletion or cellular collection are often anemic, with a HCT of 20-25%.^{150,183} For samples with a HCT of ~20%, the current CIF device was able to remove $57 \pm 7\%$ of the WBCs initially present in the blood passing through the device. Such a level of separation performance in our setup would reduce WBC

count in the recirculating blood by ~40% after 3 recirculation rounds (equivalent to processing one TBV), which may already be sufficient in some special cases, particularly if the loss of RBCs and PLTs is kept acceptably low. Alternatively, current CIF device could be used at its maximal performance (>80% WBC removal) if the blood is diluted down to 10% HCT with sterile saline prior to entering the device and then concentrated back to its native HCT before reinfusion to the patient. Hemoconcentration can be accomplished using one of the commercially available ultrafiltration devices which are used routinely as part of the extracorporeal circuit during pediatric cardiopulmonary bypass procedures to remove and discard excess fluid.¹⁸⁴⁻¹⁸⁷ Nevertheless, increasing the HCT at which the CIF device can operate with its maximum separation efficiency to the 25-35% range will be an important design challenge for our future work.

The flow ratio of the CIF device determines the volume of retentate removed with the separated WBCs, and hence the number of RBCs and PLTs lost during the separation process. Each CIF device is designed to operate optimally with a particular flow ratio, which is calculated assuming same pressure in both outlets of the device. By creating a difference in pressure between the outlets we can control the flow ratio of the device in real time, albeit at the expense of some drop in separation performance. In this study we adjusted the pressure difference by changing the height at which the waste reservoir was located relative to the device. This simple manipulation allowed us to adjust the flow ratio within a wide range (~10-fold), although as expected the efficiency of WBC removal declined precipitously for flow ratios above 9. Importantly, the loss of RBCs and PLTs closely followed the expected reciprocal dependence on the flow

ratio, declining from $37.5 \pm 0.8\%$ for RBCs and $36.1 \pm 2.4\%$ for PLTs at the flow ratio of 2 (33% expected loss) down to $4.5 \pm 0.5\%$ for RBCs and $4.0 \pm 1.0\%$ for PLTs at the flow ratio of 23 (4% expected loss). The ability to modify CIF device performance within such a range in real time (by adjusting the device flow ratio) could be useful for matching key parameters of the leukapheresis procedure to the unique needs of individual patients. In the recirculation experiments, current CIF device operated at a flow ratio of 8.8 ± 0.3 , which corresponds to a 10-11% loss of RBCs and PLTs passing through the device. Improvements in the CIF design to maximize the flow ratio at which the device can operate optimally would further reduce the RBC and PLT loss without compromising the efficiency of WBC removal.

In a CIF device, cells that are smaller than the critical diameter experience no separation (i.e. distribute according to the flow ratio) and therefore their concentration should remain the same in both filtrate and retentate. We observed, however, that the concentrations of RBCs and PLTs in recirculating blood (filtrate) declined slightly over time during the recirculation experiments. For RBCs, we did not observe any significant increase in free Hb or potassium to indicate hemolysis, and therefore the only likely explanation for the decline of RBC concentration in the filtrate is that some RBCs were separated and retained in the retentate. Indeed, the RBC concentration in the retentate (waste) was consistently higher than in the filtrate (recirculating blood), on average by about $0.1 \times 10^6 / \mu\text{L}$. For PLTs, a possible explanation for the decline of PLT concentration is that a majority of PLTs that become activated promptly bind to the available WBCs and were thus excluded from the count. Indeed, the number of PLT-WBC aggregates steadily increased during each recirculation experiment, while overall

PLT activation remained unchanged and at a relatively low level. From the clinical perspective, minimizing the loss of RBCs and PLTs during the leukapheresis procedure is important for reducing the risks associated with transfusion of allogeneic blood products.

The multiplexed CIF device was able to operate at flow rates ranging 10-30 mL/min, which is on par with the flow rates typically used by the conventional centrifugation-based apheresis machines (10-50 mL/min¹⁵¹⁻¹⁵³). However, the flow ratio of the device decreased significantly at flow rates higher than 10 mL/min, which was likely due to deformation (bulging) of the device channels made of PDMS elastomer at high driving pressures that we previously observed for similar devices.¹⁸⁰ As expected, lower flow ratio increased the loss of RBCs and PLTs, and the deformation of device structures also resulted in a reduction of WBC removal efficiency. To minimize device deformations and enable maximal separation performance at flow rates higher than 10 mL/min future designs of the CIF device must ultimately be manufactured from thermoplastic.^{149,188} It is also noteworthy that the flow rate at which the CIF device operated in the recirculation experiments (10 mL/min) was significantly higher than that reported for other microfluidic devices designed to separate WBCs from diluted whole blood and other concentrated suspensions (most of which operate at 10s-100s of $\mu\text{L}/\text{min}$).^{68,108,109,116,127,189}

Exposure to high shear forces during centrifugation can cause mechanical damage to cell membranes, induce excessive cell activation, and trigger hemostatic responses, contributing to the host of adverse outcomes associated with leukapheresis in neonates and infants.^{42,102,171,181,190} We found that PLT activation in the recirculating

blood was low and (even after 12 rounds of recirculation) on par with BT control. Given high sensitivity of PLTs to shear and our previously published findings with similar CIF devices^{178,179} we expected to observe at least some increase in PLT activation. Low PLT activation could potentially be caused by PLT refractoriness, which was not the case because recirculating PLTs were able to activate significantly upon exposure to TRAP (positive control). One possible explanation is that the formation of PLT-WBC aggregates consumed most activated PLTs. Indeed, the number of PLT-WBC aggregates increased steadily during each recirculation experiment. However, the number of aggregates in the recirculating blood after 12 rounds of recirculation was the same as in the BT control, suggesting that the increase was likely due to time of processing, and the contribution from our CIF device and the recirculation setup was relatively minor. WBCs in recirculating blood become progressively more activated, but at the end of recirculation experiment (after round 12) they were no more activated than BT control. Separated WBCs were about as activated as WBCs remaining in the recirculating blood, and there was no significant difference in activation between cells extracted at round 6 and 12. Both recirculating and separated WBCs were able to become significantly more activated after incubation to PMA (positive control), which suggests that the cells were not made refractory by the processing. This finding agrees well with our previous work in which lymphocytes enriched using a similar device were able to become activated and expanded in culture at rates significantly higher than cells processed via centrifugation.¹⁸⁰ Finally, we found no evidence of RBC damage in our experiments while employing the same assays we used previously to document the negative effects of centrifugation-based washing on stored RBCs.^{181,191} Taken together,

our data strongly suggest that the CIF device operating in the closed-loop recirculation regime did not significantly activate or damage the blood cells.

Our study has several limitations. We established recirculation in our experimental system using the ‘withdraw-infuse’ approach (implemented with a syringe pump), which most closely resembles operation of apheresis machines with discontinuous blood withdrawal typically employed for leukapheresis procedures with larger extracorporeal volume and longer duration.¹⁵² Our setup may also provide a potentially useful alternative to the manual exchange transfusion sometimes performed for low-weight infants when conventional apheresis is considered too risky.^{42,182} Nevertheless, operating the CIF device in the continuous flow regime must be an important goal for further research. In this initial proof-of-concept study we processed blood samples from healthy donors rather than leukemia patients. Although there is a significant variability among patients, leukemic blast cells are typically 10-20 μm in diameter,¹⁹² and therefore we expect them to be retained in the retentate of the device alongside normal WBCs. Finally, in this paper we only tested the ability of the CIF device to separate all WBCs indiscriminately. Although these separated WBCs (with additional enrichment) could already be used for cellular therapy applications, further device development is needed to enable selective isolation of specific WBC subtypes (e.g., lymphocytes, haemopoietic stem cells).

CONCLUSION

In summary, this paper describes a significant progress towards enabling centrifugation-free leukapheresis in pediatric patients using a novel high-throughput microfluidic platform. Our microfluidic device, based on CIF technology, is capable of processing whole blood (diluted to 10% HCT) at 10 mL/min with >80% WBC removal, only ~10% loss of RBCs and PLTs, and void volume of just 0.4 mL. When tested in the recirculation regime, the device operated without clogging or any decline in separation performance and was able to deplete the WBC count exponentially, with minimal activation of WBC and PLTs and no measurable damage to RBCs over the entire duration of a 3-hour simulated leukapheresis procedure. These results suggest that, with further development, CIF-based devices may be able to remove WBCs from whole blood with both volumetric throughput and separation efficiency sufficiently high to ultimately enable centrifugation-free, low-ECV leukapheresis for neonates and low-weight infants.

CHAPTER 5: FINAL CONCLUSIONS

CONCLUSIONS

Whole blood is a complex biological fluid made up of mainly of plasma, platelets, red blood cells, and white blood cells. Each of these hematological components perform distinct and fundamental functions to maintain homeostasis and thus contain a myriad of information about the functioning of the human body and have important diagnostic and therapeutic uses. The ability to handle blood samples efficiently separate and sort cells into distinct populations has been of a great interest to clinicians and researchers. While conventional methods of processing blood have been successful in generating relatively pure cell fractions, they are often labor intensive, time consuming, and require complex machinery and technical expertise to operate and maintain. These drawbacks particularly inhibit the implementation of established fractionation techniques in limited resource settings. Conventional blood separation techniques, such as centrifugation-based apheresis, are performed with bulky machinery with large extracorporeal volumes making potentially life-saving treatments inaccessible to some high-risk pediatric patients with low blood volumes.

In the past decade, many novel microfluidic technologies have emerged to address this clinical need. Microfluidics is an attractive solution for this application as it provides numerous advantages over conventional methods. Microfluidic platforms manipulate particles using unique flow and physical phenomena at the micron scale while simultaneously maintaining precise control of fluid behavior and shear conditions

within the microchannels, all with significantly lower extracorporeal volumes. Microfluidic systems are also more easily produced single-use devices, can be relatively simple to set up and operate without necessitating specialized equipment, attendant training, large storage space or maintenance. In combination, these features could allow for more widespread implementation of microfluidic-based cell sorting platforms in limited resource settings and increase quality of care for populations of underserved pediatric patients. This dissertation covers two instances of blood related disease, sickle cell anemia and leukemia, and reports on the development of novel microfluidic technologies for their diagnosis and treatment in pediatric populations.

In Chapter 2, we reported on the development and validation of a paper-based microfluidic device designed to enable universal newborn screening and low-cost, rapid, and equipment-free diagnosis of sickle cell anemia in resource-limited settings. A point-of-care diagnostic device with these qualities represents a significant step towards enabling population-wide screening in resource-limited settings. If adopted, this technology could have a transformative effect on the quality of care and clinical outcomes for hundreds of thousands of individuals with SCA born in developing nations each year.

In Chapter 3, this dissertation provides a review of the literature in regards to novel passive microfluidic devices reported to have successful and efficient separation of WBC directly from whole blood. In reviewing 20 unique microfluidic devices, developed in the last decade, we determined that there is a there is movement in the field towards microfluidic platforms that can achieve efficient, accurate, and high-throughput

separation of WBC from whole blood in order to provide viable alternatives to centrifugation-based leukapheresis with a smaller footprint.

In Chapter 4, we describe the development and optimization of a small microfluidic device, a low void volume, capable of high throughput and efficient separation of WBC from whole blood recirculating through a closed-loop circuit, at throughputs and efficiencies comparable to conventional apheresis machines. We also show no device clogging, minimal activation of WBC and PLT, and no measurable damage to RBCs over a 3-hour procedure. Our results suggest that, with further development, this device may be able to remove WBC from whole blood with both volumetric throughput and separation efficiency sufficiently high to ultimately enable centrifugation-free, low-ECV leukapheresis for neonates and low-weight infants. This microfluidic leukapheresis system This device could provide a viable treatment alternative for underserved pediatric patients with leukemia, for which leukapheresis is indicated.

If adopted, these novel microfluidic technologies, for diagnosing sickle cell anemia and treatment of leukemia, could significantly improve the quality and accessibility of clinical care for millions of individuals worldwide, regardless of socioeconomic status or patient size.

REFERENCES

- 1 Hou, H. W., Bhagat, A. A. S., Lee, W. C., Huang, S., Han, J. & Lim, C. T. Microfluidic devices for blood fractionation. *Micromachines* **2**, 319-343 (2011).
- 2 Sethu, P., Sin, A. & Toner, M. Microfluidic diffusive filter for apheresis (leukapheresis). *Lab on a Chip* **6**, 83-89 (2006).
- 3 Schreier, S. & Triampo, W. The Blood Circulating Rare Cell Population. What is it and What is it Good For? *Cells* **9**, 790 (2020).
- 4 Fung, Y. & Skalak, R. Biomechanics: mechanical properties of living tissues. (1981).
- 5 Lam, F. W., Burns, A. R., Smith, C. W. & Rumbaut, R. E. Platelets enhance neutrophil transendothelial migration via P-selectin glycoprotein ligand-1. *American Journal of Physiology-Heart and Circulatory Physiology* **300**, H468-H475 (2011).
- 6 Lam, F. W., Vijayan, K. V. & Rumbaut, R. E. Platelets and their interactions with other immune cells. *Comprehensive Physiology* **5**, 1265 (2015).
- 7 Lam, F. W., Phillips, J., Landry, P., Magadi, S., Smith, C. W., Rumbaut, R. E. & Burns, A. R. Platelet recruitment promotes keratocyte repopulation following corneal epithelial abrasion in the mouse. *Plos one* **10**, e0118950 (2015).
- 8 Golebiewska, E. M. & Poole, A. W. Platelet secretion: From haemostasis to wound healing and beyond. *Blood reviews* **29**, 153-162 (2015).
- 9 Tripathi, S., Kumar, Y. B., Agrawal, A., Prabhakar, A. & Joshi, S. S. Microdevice for plasma separation from whole human blood using bio-physical and geometrical effects. *Scientific reports* **6**, 1-15 (2016).

- 10 Turgeon, M. L. *Clinical hematology: theory and procedures*. (Lippincott Williams & Wilkins, 2005).
- 11 Pittman, R. N. in *Regulation of Tissue Oxygenation* (Morgan & Claypool Life Sciences, 2011).
- 12 Li, Z., Burns, A. R., Rumbaut, R. E. & Smith, C. W. $\gamma\delta$ T cells are necessary for platelet and neutrophil accumulation in limbal vessels and efficient epithelial repair after corneal abrasion. *The American journal of pathology* **171**, 838-845 (2007).
- 13 Li, Z., Burns, A. R. & Smith, C. W. Two waves of neutrophil emigration in response to corneal epithelial abrasion: distinct adhesion molecule requirements. *Investigative ophthalmology & visual science* **47**, 1947-1955 (2006).
- 14 Liu, Q., Smith, C. W., Zhang, W., Burns, A. R. & Li, Z. NK cells modulate the inflammatory response to corneal epithelial abrasion and thereby support wound healing. *The American journal of pathology* **181**, 452-462 (2012).
- 15 Wang, J., Jiao, H., Stewart, T. L., Lyons, M. V., Shankowsky, H. A., Scott, P. G. & Tredget, E. E. Accelerated wound healing in leukocyte-specific, protein 1-deficient mouse is associated with increased infiltration of leukocytes and fibrocytes. *Journal of leukocyte biology* **82**, 1554-1563 (2007).
- 16 Sell, S., Max, E. E. & Berkower, I. *Immunology, immunopathology and immunity*. (ASM press Washington, DC, 2001).
- 17 McConnell, T. H. *The nature of disease : pathology for the health professions*. (Lippincott Williams & Wilkins, 2007).

- 18 Stuart, M. J. & Nagel, R. L. Sickle-cell disease. *The Lancet* **364**, 1343-1360, doi:10.1016/s0140-6736(04)17192-4 (2004).
- 19 Modell, B. & Darlison, M. Global epidemiology of haemoglobin disorders and derived service indicators. *Bull World Health Organ* **86**, 480-487 (2008).
- 20 Powars, D. R., Chan, L. S., Hiti, A., Ramicone, E. & Johnson, C. Outcome of sickle cell anemia: a 4-decade observational study of 1056 patients. *Medicine (Baltimore)* **84**, 363-376 (2005).
- 21 Rees, D. C., Williams, T. N. & Gladwin, M. T. Sickle-cell disease. *The Lancet* **376**, 2018-2031 (2010).
- 22 McGann, P. T., Ferris, M. G., Ramamurthy, U., Santos, B., de Oliveira, V., Bernardino, L. & Ware, R. E. A prospective newborn screening and treatment program for sickle cell anemia in Luanda, Angola. *Am J Hematol* **88**, 984-989, doi:10.1002/ajh.23578 (2013).
- 23 Ware, R. E. Is sickle cell anemia a neglected tropical disease? *PLoS Negl Trop Dis* **7**, e2120, doi:10.1371/journal.pntd.0002120 (2013).
- 24 Piel, F. B., Hay, S. I., Gupta, S., Weatherall, D. J. & Williams, T. N. Global burden of sickle cell anaemia in children under five, 2010-2050: modelling based on demographics, excess mortality, and interventions. *PLoS Med* **10**, e1001484, doi:10.1371/journal.pmed.1001484 (2013).
- 25 Weatherall, D. J. The inherited diseases of hemoglobin are an emerging global health burden. *Blood* **115**, 4331-4336, doi:10.1182/blood-2010-01-251348 (2010).

- 26 Frenette, P. S. & Atweh, G. F. Sickle cell disease: old discoveries, new concepts, and future promise. *The Journal of clinical investigation* **117**, 850-858 (2007).
- 27 McGann, P. T., Ferris, M. G., Ramamurthy, U., Santos, B., de Oliveira, V., Bernardino, L. & Ware, R. E. A prospective newborn screening and treatment program for sickle cell anemia in Luanda, Angola. *American Journal of Hematology* **88**, 984-989, doi:10.1002/ajh.23578 (2013).
- 28 Rees, D. C., Olujuhungebe, A. D., Parker, N. E., Stephens, A. D., Telfer, P., Wright, J. & Party, B. C. f. S. i. H. G. H. T. F. b. t. S. C. W. Guidelines for the management of the acute painful crisis in sickle cell disease. *British journal of haematology* **120**, 744-752 (2003).
- 29 Kutlar, A., Kutlar, F., Wilson, J. B., Headlee, M. G. & Huisman, T. H. Quantitation of hemoglobin components by high-performance cation-exchange liquid chromatography: its use in diagnosis and in the assessment of cellular distribution of hemoglobin variants. *American journal of hematology* **17**, 39-53 (1984).
- 30 Head, C. E., Conroy, M., Jarvis, M., Phelan, L. & Bain, B. J. Some observations on the measurement of haemoglobin A2 and S percentages by high performance liquid chromatography in the presence and absence of alpha thalassaemia. *J Clin Pathol* **57**, 276-280 (2004).
- 31 Clarke, G. M. & Higgins, T. N. Laboratory investigation of hemoglobinopathies and thalassemias: review and update. *Clinical chemistry* **46**, 1284-1290 (2000).
- 32 Rodriguez-Diaz, R., Wehr, T. & Zhu, M. Capillary isoelectric focusing. *Electrophoresis* **18**, 2134-2144 (1997).

- 33 Jenkins, M. A. & Ratnaike, S. Capillary isoelectric focusing of haemoglobin variants in the clinical laboratory. *Clin Chim Acta* **289**, 121-132, doi:S0009898199001679 [pii] (1999).
- 34 Schmidt, R. M. & Wilson, S. M. Standardization in detection of abnormal hemoglobins: Solubility tests for hemoglobin S. *JAMA* **225**, 1225-1230 (1973).
- 35 Chen, K., Ballas, S. K., Hantgan, R. R. & Kim-Shapiro, D. B. Aggregation of normal and sickle hemoglobin in high concentration phosphate buffer. *Biophysical Journal* **87**, 4113-4121 (2004).
- 36 in *National Cancer Institute, Maryland, USA* (2013).
- 37 Madhusoodhan, P. P., Carroll, W. L. & Bhatla, T. Progress and prospects in pediatric leukemia. *Current problems in pediatric and adolescent health care* **46**, 229-241 (2016).
- 38 Maloney, K. W., Giller, R. & Hunger, S. P. Recent advances in the understanding and treatment of pediatric leukemias. *Advances in pediatrics* **59**, 329-358 (2012).
- 39 Röllig, C. & Ehniger, G. How I treat hyperleukocytosis in acute myeloid leukemia. *Blood* **125**, 3246-3252 (2015).
- 40 Porcu, P., Farag, S., Marcucci, G., Cataland, S. R., Kennedy, M. S. & Bissell, M. Leukocytoreduction for acute leukemia. *Therapeutic apheresis* **6**, 15-23 (2002).
- 41 Creutzig, U., Rössig, C., Dworzak, M., Stary, J., von Stackelberg, A., Wössmann, W., Zimmermann, M. & Reinhardt, D. Exchange transfusion and

- leukapheresis in pediatric patients with AML with high risk of early death by bleeding and leukostasis. *Pediatric blood & cancer* **63**, 640-645 (2016).
- 42 Runco, D. V., Josephson, C. D., Raikar, S. S., Goldsmith, K. C., Lew, G., Pauly, M. & Fasano, R. M. Hyperleukocytosis in infant acute leukemia: a role for manual exchange transfusion for leukoreduction. *Transfusion* **58**, 1149-1156, doi:10.1111/trf.14512 (2018).
- 43 Padmanabhan, A., Connelly-Smith, L., Aqui, N., Balogun, R. A., Klingel, R., Meyer, E., Pham, H. P., Schneiderman, J., Witt, V. & Wu, Y. Guidelines on the use of therapeutic apheresis in clinical practice—evidence-based approach from the Writing Committee of the American Society for Apheresis: the eighth special issue. *Journal of clinical apheresis* **34**, 171-354 (2019).
- 44 Brecher, M. L. & Roberts, J. in *Pediatric Critical Care* 1173-1184 (Elsevier, 2006).
- 45 Faderl, S. & Kantarjian, H. M. in *Hematology: Basic principles and practice* Ch. 59, 924-943 (Elsevier Inc., 2018).
- 46 Staley, E. M., Schwartz, J. & Pham, H. P. in *Transfusion Medicine and Hemostasis* 483-486 (Elsevier, 2019).
- 47 Sigurbjörnsson, F. T. & Bjarnason, I. Leukocytapheresis for the treatment of IBD. *Nature Clinical Practice Gastroenterology & Hepatology* **5**, 509-516 (2008).
- 48 Hanai, H., Takeda, Y., Eberhardson, M., Gruber, R., Saniabadi, A., Winqvist, O. & Lofberg, R. The mode of actions of the Adacolumn therapeutic

- leucocytapheresis in patients with inflammatory bowel disease: a concise review. *Clinical & Experimental Immunology* **163**, 50-58 (2011).
- 49 Saniabadi, A. R., Tanaka, T., Yamamoto, T., Kruis, W. & Sacco, R. Granulomonocytapheresis as a cell-dependent treatment option for patients with inflammatory bowel disease: Concepts and clinical features for better therapeutic outcomes. *Journal of clinical apheresis* **34**, 51-60 (2019).
- 50 Takakura, M., Shimizu, M., Mizuta, M., Inoue, N., Tasaki, Y., Ohta, K., Furuichi, K., Wada, T. & Yachie, A. Successful treatment of rituximab-and steroid-resistant nephrotic syndrome with leukocytapheresis. *Journal of clinical apheresis* **33**, 409-411 (2018).
- 51 Miyazono, A., Abe, J., Ogura, M., Sato, M., Fujimaru, T., Kamei, K. & Ito, S. Successful remission induced by plasma exchange combined with leukocytapheresis against refractory systemic juvenile idiopathic arthritis. *European journal of pediatrics* **173**, 1557-1560 (2014).
- 52 Padmanabhan, A. Cellular collection by apheresis. *Transfusion* **58**, 598-604 (2018).
- 53 Nair, S. K., Driscoll, T., Boczkowski, D., Schmittling, R., Reynolds, R., Johnson, L. A., Grant, G., Fuchs, H., Bigner, D. D. & Sampson, J. H. Ex vivo generation of dendritic cells from cryopreserved, post-induction chemotherapy, mobilized leukapheresis from pediatric patients with medulloblastoma. *Journal of neuro-oncology* **125**, 65-74 (2015).
- 54 Maude, S. L., Laetsch, T. W., Buechner, J., Rives, S., Boyer, M., Bittencourt, H., Bader, P., Verneris, M. R., Stefanski, H. E. & Myers, G. D. Tisagenlecleucel

- in children and young adults with B-cell lymphoblastic leukemia. *New England Journal of Medicine* **378**, 439-448 (2018).
- 55 Ceppi, F., Rivers, J., Annesley, C., Pinto, N., Park, J. R., Lindgren, C., Mgebroff, S., Linn, N., Delaney, M. & Gardner, R. A. Lymphocyte apheresis for chimeric antigen receptor T-cell manufacturing in children and young adults with leukemia and neuroblastoma. *Transfusion* **58**, 1414-1420 (2018).
- 56 Cerwenka, A. & Lanier, L. L. Natural killers join the fight against cancer. *Science* **359**, 1460-1461 (2018).
- 57 Nikolajeva, O., Mijovic, A., Hess, D., Tatam, E., Amrolia, P., Chiesa, R., Rao, K., Silva, J. & Veys, P. Single-donor granulocyte transfusions for improving the outcome of high-risk pediatric patients with known bacterial and fungal infections undergoing stem cell transplantation: a 10-year single-center experience. *Bone marrow transplantation* **50**, 846-849 (2015).
- 58 Price, T. H., Boeckh, M., Harrison, R. W., McCullough, J., Ness, P. M., Strauss, R. G., Nichols, W. G., Hamza, T. H., Cushing, M. M. & King, K. E. Efficacy of transfusion with granulocytes from G-CSF/dexamethasone-treated donors in neutropenic patients with infection. *Blood* **126**, 2153-2161 (2015).
- 59 Díaz, M. A., Garcia-Sanchez, F., Lillo, R., Vicent, M. G., Vicario, J. L. & Madero, L. Large-volume leukapheresis in pediatric patients: pre-apheresis peripheral blood CD34+ cell count predicts progenitor cell yield. *Haematologica* **84**, 32-35 (1999).
- 60 Cecyn, K. Z., Seber, A., Ginani, V. C., Gonçalves, A. V., Caram, E. M., Oguro, T., Oliveira, O. M. W., Carvalho, M. M. & Bordin, J. O. Large-volume

- leukapheresis for peripheral blood progenitor cell collection in low body weight pediatric patients: a single center experience. *Transfusion and apheresis science* **32**, 269-274 (2005).
- 61 Karow, A., Wilhelm, A., Ammann, R. A., Baerlocher, G. M., Pabst, T., Taleghani, B. M., Roessler, J. & Leibundgut, K. Peripheral blood progenitor cell collection in pediatric patients optimized by high pre-apheresis count of circulating CD34+ cells and high blood flow. *Bone marrow transplantation* **54**, 885-893 (2019).
- 62 Ribeil, J.-A., Hacein-Bey-Abina, S., Payen, E., Magnani, A., Semeraro, M., Magrin, E., Caccavelli, L., Neven, B., Bourget, P. & El Nemer, W. Gene therapy in a patient with sickle cell disease. *New England Journal of Medicine* **376**, 848-855 (2017).
- 63 Thompson, A. A., Walters, M. C., Kwiatkowski, J., Rasko, J. E., Ribeil, J.-A., Hongeng, S., Magrin, E., Schiller, G. J., Payen, E. & Semeraro, M. Gene therapy in patients with transfusion-dependent β -thalassemia. *New England Journal of Medicine* **378**, 1479-1493 (2018).
- 64 Lisenko, K., Pavel, P., Bruckner, T., Puthenparambil, J., Hundemer, M., Schmitt, A., Witzens-Harig, M., Ho, A. D. & Wuchter, P. Comparison between intermittent and continuous spectra optia leukapheresis systems for autologous peripheral blood stem cell collection. *Journal of clinical apheresis* **32**, 27-34 (2017).
- 65 Pamme, N. Continuous flow separations in microfluidic devices. *Lab on a Chip* **7**, 1644-1659 (2007).

- 66 Daw, R. & Finkelstein, J. Insight: Lab on a chip. *Nature* **442**, 367-418 (2006).
- 67 Kuan, D.-H., Wu, C.-C., Su, W.-Y. & Huang, N.-T. A microfluidic device for simultaneous extraction of plasma, red blood cells, and on-chip white blood cell trapping. *Scientific reports* **8**, 1-9 (2018).
- 68 Cheng, Y., Ye, X., Ma, Z., Xie, S. & Wang, W. High-throughput and clogging-free microfluidic filtration platform for on-chip cell separation from undiluted whole blood. *Biomicrofluidics* **10**, 014118, doi:10.1063/1.4941985 (2016).
- 69 Thorsen, T., Maerkl, S. J. & Quake, S. R. Microfluidic large-scale integration. *Science* **298**, 580-584 (2002).
- 70 Vichinsky, E., Hurst, D., Earles, A., Kleman, K. & Lubin, B. Newborn screening for sickle cell disease: effect on mortality. *Pediatrics* **81**, 749-755 (1988).
- 71 Platt, O. S., Brambilla, D. J., Rosse, W. F., Milner, P. F., Castro, O., Steinberg, M. H. & Klug, P. P. Mortality in sickle cell disease. Life expectancy and risk factors for early death. *The New England journal of medicine* **330**, 1639-1644, doi:10.1056/NEJM199406093302303 (1994).
- 72 Makani, J., Cox, S. E., Soka, D., Komba, A. N., Oruo, J., Mwamtemi, H., Magesa, P., Rwezaula, S., Meda, E., Mgaya, J., Lowe, B., Muturi, D., Roberts, D. J., Williams, T. N., Pallangyo, K., Kitundu, J., Fegan, G., Kirkham, F. J., Marsh, K. & Newton, C. R. Mortality in sickle cell anemia in Africa: a prospective cohort study in Tanzania. *PloS one* **6**, e14699, doi:10.1371/journal.pone.0014699 (2011).

- 73 Cronin, E. K., Normand, C., Henthorn, J. S., Hickman, M. & Davies, S. C. Costing model for neonatal screening and diagnosis of haemoglobinopathies. *Arch Dis Child Fetal Neonatal Ed* **79**, F161-167 (1998).
- 74 Diallo, D. & Tchernia, G. Sick cell disease in Africa. *Current opinion in hematology* **9**, 111-116 (2002).
- 75 Montagu, D., Yamey, G., Visconti, A., Harding, A. & Yoong, J. Where do poor women in developing countries give birth? A multi-country analysis of demographic and health survey data. *PLoS One* **6**, e17155, doi:10.1371/journal.pone.0017155 (2011).
- 76 Yang, X., Kanter, J., Piety, N. Z., Benton, M. S., Vignes, S. M. & Shevkoplyas, S. S. A simple, rapid, low-cost diagnostic test for sickle cell disease. *Lab Chip* **13**, 1464-1467, doi:10.1039/c3lc41302k (2013).
- 77 Piety, N. Z., Yang, X., Lezzar, D., George, A. & Shevkoplyas, S. S. A rapid paper-based test for quantifying sickle hemoglobin in blood samples from patients with sickle cell disease. *Am J Hematol* **90**, 478-482, doi:10.1002/ajh.23980 (2015).
- 78 Piety, N. Z., Yang, X., Kanter, J., Vignes, S. M., George, A. & Shevkoplyas, S. S. Validation of a Low-Cost Paper-Based Screening Test for Sickle Cell Anemia. *PLoS One* **11**, e0144901, doi:10.1371/journal.pone.0144901 (2016).
- 79 Piety, N. Z., George, A., Serrano, S., Lanzi, M. R., Patel, P. R., Noli, M. P., Kahan, S., Nirenberg, D., Camanda, J. F., Airewele, G. & Shevkoplyas, S. S. A Paper-Based Test for Screening Newborns for Sickle Cell Disease. *Sci Rep* **7**, 45488, doi:10.1038/srep45488 (2017).

- 80 Eichbaum, Q., Smid, W. M., Crookes, R., Naim, N., Mendrone Jr, A., Marques Jr, J. F. C. & Marques, M. B. Apheresis in developing countries around the World. *Journal of clinical apheresis* **30**, 238-246 (2015).
- 81 *Safety Data Sheet: Saponin, from Quillaja Bark (Cas No.: 8047-15-2)*, <<http://www.sigmaaldrich.com/catalog/product/sigma/s2149?lang=en®ion=US>> (2017).
- 82 Shevkoplyas, S. S., Yang, Xiaoxi, Washko, Julie Kanter, Piety, Nathaniel Zane. Paper Based Diagnostic Test. United States patent WO2013071301 (2013).
- 83 Fleiss, J. L. Measuring nominal scale agreement among many raters. *Psychological bulletin* **76**, 378 (1971).
- 84 Roila, F., Lupattelli, M., Sassi, M., Basurto, C., Bracarda, S., Picciafuoco, M., Boschetti, E., Milella, G., Ballatori, E., Tonato, M. & Del Favero, A. Intra and interobserver variability in cancer patients' performance status assessed according to Karnofsky and ECOG scales. *Annals of Oncology* **2**, 437-439 (1991).
- 85 El Fadli, K. I., Cerveny, R. S., Burt, C. C., Eden, P., Parker, D., Brunet, M., Peterson, T. C., Mordacchini, G., Pelino, V., Bessemoulin, P., Stella, J. L., Driouech, F., Wahab, M. M. A. & Pace, M. B. World Meteorological Organization Assessment of the Purported World Record 58°C Temperature Extreme at El Azizia, Libya (13 September 1922). *Bulletin of the American Meteorological Society* **94**, 199-204, doi:10.1175/bams-d-12-00093.1 (2013).

- 86 Kanter, J., Telen, M. J., Hoppe, C., Roberts, C. L., Kim, J. S. & Yang, X. Validation of a novel point of care testing device for sickle cell disease. *BMC Med* **13**, 225, doi:10.1186/s12916-015-0473-6 (2015).
- 87 McGann, P. T., Schaefer, B. A., Paniagua, M., Howard, T. A. & Ware, R. E. Characteristics of a rapid, point-of-care lateral flow immunoassay for the diagnosis of sickle cell disease. *Am J Hematol* **91**, 205-210, doi:10.1002/ajh.24232 (2016).
- 88 Kumar, A. A., Patton, M. R., Hennek, J. W., Lee, S. Y., D'Alesio-Spina, G., Yang, X., Kanter, J., Shevkopyas, S. S., Brugnara, C. & Whitesides, G. M. Density-based separation in multiphase systems provides a simple method to identify sickle cell disease. *Proceedings of the National Academy of Sciences of the United States of America* **111**, 14864-14869, doi:10.1073/pnas.1414739111 (2014).
- 89 Knowlton, S. M., Sencan, I., Aytar, Y., Khoory, J., Heeney, M. M., Ghiran, I. C. & Tasoglu, S. Sickle cell detection using a smartphone. *Sci Rep* **5**, 15022, doi:10.1038/srep15022 (2015).
- 90 Kumar, A. A., Chunda-Liyoka, C., Hennek, J. W., Mantina, H., Lee, S. Y., Patton, M. R., Sambo, P., Sinyangwe, S., Kankasa, C., Chintu, C., Brugnara, C., Stossel, T. P. & Whitesides, G. M. Evaluation of a density-based rapid diagnostic test for sickle cell disease in a clinical setting in Zambia. *PLoS One* **9**, e114540, doi:10.1371/journal.pone.0114540 (2014).

- 91 *Screening Information Dataset: Initial Assessment Report for Sodium Dithionite*
(CAS No.: 7775-14-6), <
<http://www.inchem.org/documents/sids/sids/7775146.pdf> > (2004).
- 92 Asakura, T. & Mayberry, J. Relationship between morphologic characteristics
of sickle cells and method of deoxygenation. *The Journal of laboratory and
clinical medicine* **104**, 987-994 (1984).
- 93 Noguchi, C. T. & Schechter, A. N. The intracellular polymerization of sickle
hemoglobin and its relevance to sickle cell disease. *Blood* **58**, 1057-1068 (1981).
- 94 Horiuchi, K., Ballas, S. K. & Asakura, T. The effect of deoxygenation rate on
the formation of irreversibly sickled cells. *Blood* **71**, 46-51 (1988).
- 95 Nagel, R. L., Fabry, M. E. & Steinberg, M. H. The paradox of hemoglobin SC
disease. *Blood Rev* **17**, 167-178 (2003).
- 96 Ryan, K., Bain, B. J., Worthington, D., James, J., Plews, D., Mason, A., Roper,
D., Rees, D. C., de la Salle, B., Streetly, A. & British Committee for Standards
in, H. Significant haemoglobinopathies: guidelines for screening and diagnosis.
British journal of haematology **149**, 35-49, doi:10.1111/j.1365-
2141.2009.08054.x (2010).
- 97 Edoh, D., Antwi-Bosaiko, C. & Amuzu, D. Fetal hemoglobin during infancy and
in sickle cell adults. *African health sciences* **6**, 51-54,
doi:10.5555/afhs.2006.6.1.51 (2006).
- 98 Illerhaus, G., Wirth, K., Dwenger, A., Waller, C., Garbe, A., Brass, V., Lang, H.
& Lange, W. Treatment and prophylaxis of severe infections in neutropenic
patients by granulocyte transfusions. *Annals of hematology* **81**, 273-281 (2002).

- 99 Sachs, U. J., Reiter, A., Walter, T., Bein, G. & Woessmann, W. Safety and efficacy of therapeutic early onset granulocyte transfusions in pediatric patients with neutropenia and severe infections. *Transfusion* **46**, 1909-1914 (2006).
- 100 Maitta, R. W. Current state of apheresis technology and its applications. *Transfusion and Apheresis Science* **57**, 606-613 (2018).
- 101 Arogundade, F. A., Sanusi, A. A., Oguntola, S. O., Omotoso, B. A., Abdel-Rahman, E. M., Akinsola, A. & Balogun, R. A. Benefits and challenges of starting a new therapeutic apheresis service in a resource-constrained setting. *Journal of clinical apheresis* **29**, 194-198 (2014).
- 102 Pathiraja, V., Matar, A. J., Gusha, A., Huang, C. A. & Duran-Struuck, R. Leukapheresis protocol for nonhuman primates weighing less than 10 kg. *Journal of the American Association for Laboratory Animal Science* **52**, 70-77 (2013).
- 103 Woloskie, S., Armelagos, H., Meade, J. M. & Haas, D. Leukodepletion for acute lymphocytic leukemia in a three-week-old infant. *Journal of Clinical Apheresis: The Official Journal of the American Society for Apheresis* **16**, 31-32 (2001).
- 104 Michon, B., Moghrabi, A., Winikoff, R., Barrette, S., Bernstein, M. L., Champagne, J., David, M., Duval, M., Hume, H. A. & Robitaille, N. Complications of apheresis in children. *Transfusion* **47**, 1837-1842 (2007).
- 105 McLeod, B. C., Sniecinski, I., Ciavarella, D., Owen, H., Price, T. H., Randels, M. J. & Smith, J. W. Frequency of immediate adverse effects associated with therapeutic apheresis. *Transfusion* **39**, 282-288 (1999).

- 106 Rudolph, C. D. *Rudolph's pediatrics*. 1521 (Appleton & Lange Norwalk, CT, 2003).
- 107 Sisson, T. R., Whalen, L. E. & Telek, A. The blood volume of infants: II. The premature infant during the first year of life. *The Journal of pediatrics* **55**, 430-446 (1959).
- 108 Tan, J. K., Park, S.-Y., Leo, H. L. & Kim, S. Continuous separation of white blood cells from whole blood using viscoelastic effects. *IEEE transactions on biomedical circuits and systems* **11**, 1431-1437 (2017).
- 109 Wu, Z., Chen, Y., Wang, M. & Chung, A. J. Continuous inertial microparticle and blood cell separation in straight channels with local microstructures. *Lab on a Chip* **16**, 532-542 (2016).
- 110 Alvankarian, J., Bahadorimehr, A. & Yeop Majlis, B. A pillar-based microfilter for isolation of white blood cells on elastomeric substrate. *Biomicrofluidics* **7**, 014102 (2013).
- 111 Prabhakar, A., Kumar, Y. B. V., Tripathi, S. & Agrawal, A. A novel, compact and efficient microchannel arrangement with multiple hydrodynamic effects for blood plasma separation. *Microfluidics and Nanofluidics* **18**, 995-1006 (2015).
- 112 Singh, R. Introduction to membrane technology. *Membrane technology and engineering for water purification* (2015).
- 113 Nagy, E. in *Basic Equations of Mass Transport Through a Membrane Layer (Second Edition)* (ed Endre Nagy) Ch. Chapter 2, Pages 11-19 (Elsevier Inc., 2019).

- 114 Wei, H., Chueh, B.-h., Wu, H., Hall, E. W., Li, C.-w., Schirhagl, R., Lin, J.-M. & Zare, R. N. Particle sorting using a porous membrane in a microfluidic device. *Lab on a chip* **11**, 238-245 (2011).
- 115 Hosokawa, M., Asami, M., Nakamura, S., Yoshino, T., Tsujimura, N., Takahashi, M., Nakasono, S., Tanaka, T. & Matsunaga, T. Leukocyte counting from a small amount of whole blood using a size-controlled microcavity array. *Biotechnology and bioengineering* **109**, 2017-2024 (2012).
- 116 Li, X., Chen, W., Liu, G., Lu, W. & Fu, J. Continuous-flow microfluidic blood cell sorting for unprocessed whole blood using surface-micromachined microfiltration membranes. *Lab on a Chip* **14**, 2565-2575 (2014).
- 117 Bhagat, A. A. S., Kuntaegowdanahalli, S. S. & Papautsky, I. Enhanced particle filtration in straight microchannels using shear-modulated inertial migration. *Physics of Fluids* **20**, 101702 (2008).
- 118 Ying, Y. & Lin, Y. Inertial focusing and Separation of particles in Similar curved channels. *Scientific reports* **9**, 1-12 (2019).
- 119 Liu, C. & Hu, G. High-throughput particle manipulation based on hydrodynamic effects in microchannels. *Micromachines* **8**, 73 (2017).
- 120 Di Carlo, D. Inertial microfluidics. *Lab on a Chip* **9**, 3038-3046 (2009).
- 121 Kuntaegowdanahalli, S. S., Bhagat, A. A. S., Kumar, G. & Papautsky, I. Inertial microfluidics for continuous particle separation in spiral microchannels. *Lab on a Chip* **9**, 2973-2980 (2009).

- 122 Wu, L., Guan, G., Hou, H. W., Bhagat, A. A. S. & Han, J. Separation of leukocytes from blood using spiral channel with trapezoid cross-section. *Analytical chemistry* **84**, 9324-9331 (2012).
- 123 Nivedita, N. & Papautsky, I. Continuous separation of blood cells in spiral microfluidic devices. *Biomicrofluidics* **7**, 054101 (2013).
- 124 Mutlu, B. R., Smith, K. C., Edd, J. F., Nadar, P., Dlamini, M., Kapur, R. & Toner, M. Non-equilibrium inertial separation array for high-throughput, large-volume blood fractionation. *Scientific reports* **7**, 1-9 (2017).
- 125 Martel, J. M., Smith, K. C., Dlamini, M., Pletcher, K., Yang, J., Karabacak, M., Haber, D. A., Kapur, R. & Toner, M. Continuous flow microfluidic bioparticle concentrator. *Scientific reports* **5**, 1-12 (2015).
- 126 Zhang, J., Yuan, D., Sluyter, R., Yan, S., Zhao, Q., Xia, H., Tan, S. H., Nguyen, N.-T. & Li, W. High-throughput separation of white blood cells from whole blood using inertial microfluidics. *IEEE transactions on biomedical circuits and systems* **11**, 1422-1430 (2017).
- 127 Kim, B., Choi, Y. J., Seo, H., Shin, E. C. & Choi, S. Deterministic Migration-Based Separation of White Blood Cells. *Small* **12**, 5159-5168, doi:10.1002/sml.201601652 (2016).
- 128 Jin, T., Yan, S., Zhang, J., Yuan, D., Huang, X.-F. & Li, W. A label-free and high-throughput separation of neuron and glial cells using an inertial microfluidic platform. *Biomicrofluidics* **10**, 034104 (2016).
- 129 Jeon, H., Jundi, B., Choi, K., Ryu, H., Levy, B. D., Lim, G. & Han, J. Fully-automated and field-deployable blood leukocyte separation platform using

- multi-dimensional double spiral (MDDS) inertial microfluidics. *Lab on a Chip* **20**, 3612-3624 (2020).
- 130 Jain, A. & Munn, L. L. Determinants of leukocyte margination in rectangular microchannels. *PloS one* **4**, e7104 (2009).
- 131 Fedosov, D. A. & Gompper, G. White blood cell margination in microcirculation. *Soft matter* **10**, 2961-2970 (2014).
- 132 Fedosov, D. A., Fornleitner, J. & Gompper, G. Margination of white blood cells in microcapillary flow. *Physical review letters* **108**, 028104 (2012).
- 133 Fay, M. E., Myers, D. R., Kumar, A., Turbyfield, C. T., Byler, R., Crawford, K., Mannino, R. G., Laohapant, A., Tyburski, E. A. & Sakurai, Y. Cellular softening mediates leukocyte demargination and trafficking, thereby increasing clinical blood counts. *Proceedings of the National Academy of Sciences* **113**, 1987-1992 (2016).
- 134 Guo, Q., Duffy, S. P., Matthews, K., Islamzada, E. & Ma, H. Deformability based cell sorting using microfluidic ratchets enabling phenotypic separation of leukocytes directly from whole blood. *Scientific reports* **7**, 1-11 (2017).
- 135 Yamada, M., Seko, W., Yanai, T., Ninomiya, K. & Seki, M. Slanted, asymmetric microfluidic lattices as size-selective sieves for continuous particle/cell sorting. *Lab on a Chip* **17**, 304-314 (2017).
- 136 Huang, L. R., Cox, E. C., Austin, R. H. & Sturm, J. C. Continuous particle separation through deterministic lateral displacement. *Science* **304**, 987-990 (2004).

- 137 Davis, J. A., Inglis, D. W., Morton, K. J., Lawrence, D. A., Huang, L. R., Chou, S. Y., Sturm, J. C. & Austin, R. H. Deterministic hydrodynamics: taking blood apart. *Proceedings of the National Academy of Sciences* **103**, 14779-14784 (2006).
- 138 Salafi, T., Zhang, Y. & Zhang, Y. A review on deterministic lateral displacement for particle separation and detection. *Nano-Micro Letters* **11**, 1-33 (2019).
- 139 Civin, C. I., Ward, T., Skelley, A. M., Gandhi, K., Peilun Lee, Z., Dosier, C. R., D'Silva, J. L., Chen, Y., Kim, M. & Moynihan, J. Automated leukocyte processing by microfluidic deterministic lateral displacement. *Cytometry Part A* **89**, 1073-1083 (2016).
- 140 Campos-González, R., Skelley, A. M., Gandhi, K., Inglis, D. W., Sturm, J. C., Civin, C. I. & Ward, T. Deterministic lateral displacement: the next-generation car t-cell processing? *SLAS TECHNOLOGY: Translating Life Sciences Innovation* **23**, 338-351 (2018).
- 141 Jain, A. & Munn, L. L. Biomimetic postcapillary expansions for enhancing rare blood cell separation on a microfluidic chip. *Lab on a chip* **11**, 2941-2947 (2011).
- 142 Zhou, J., Tu, C., Liang, Y., Huang, B., Fang, Y., Liang, X., Papautsky, I. & Ye, X. Isolation of cells from whole blood using shear-induced diffusion. *Scientific reports* **8**, 1-13 (2018).
- 143 Zhou, J. & Papautsky, I. Size-dependent enrichment of leukocytes from undiluted whole blood using shear-induced diffusion. *Lab on a Chip* **19**, 3416-3426 (2019).

- 144 Gifford, S. C., Spillane, A. M., Vignes, S. M. & Shevkoplyas, S. S. Controlled incremental filtration: a simplified approach to design and fabrication of high-throughput microfluidic devices for selective enrichment of particles. *Lab on a chip* **14**, 4496-4505 (2014).
- 145 Lezzar, D. L., Lam, F. W., Huerta, R., Lu, M., Gifford, S. C. & Shevkoplyas, S. S. Towards centrifugation-free leukapheresis in pediatric patients using high-throughput microfluidic technology. *Nature Biomedical Engineering*, In Press (2021).
- 146 Zhang, J., Yan, S., Yuan, D., Alici, G., Nguyen, N.-T., Warkiani, M. E. & Li, W. Fundamentals and applications of inertial microfluidics: A review. *Lab on a Chip* **16**, 10-34 (2016).
- 147 Molloy, E., Cantilena, C. C. & West, K. A. in *Chimeric Antigen Receptor T-Cell Therapies for Cancer* 7-16 (Elsevier, 2020).
- 148 Korell, F., Laier, S., Sauer, S., Veelken, K., Hennemann, H., Schubert, M.-L., Sauer, T., Pavel, P., Mueller-Tidow, C. & Dreger, P. Current challenges in providing good leukapheresis products for manufacturing of CAR-T cells for patients with relapsed/refractory NHL or ALL. *Cells* **9**, 1225 (2020).
- 149 Mutlu, B. R., Smith, K. C., Edd, J. F., Nadar, P., Dlamini, M., Kapur, R. & Toner, M. Non-equilibrium Inertial Separation Array for High-throughput, Large-volume Blood Fractionation. *Sci Rep* **7**, 9915, doi:10.1038/s41598-017-10295-0 (2017).

- 150 Zeng, F., Huang, H., Fu, D., Huang, Q., Fan, L. & Wei, S. Leukapheresis in 15 patients weighing 20kg or less: A single centre experience. *Transfus Apher Sci* **56**, 889-893, doi:10.1016/j.transci.2017.11.001 (2017).
- 151 Doberschuetz, N., Soerensen, J., Bonig, H., Willasch, A., Rettinger, E., Pfirrmann, V., Salzmann-Manrique, E., Schafer, R., Klingebiel, T., Bader, P. & Jarisch, A. Mobilized peripheral blood stem cell apheresis via Hickman catheter in pediatric patients. *Transfusion* **59**, 1061-1068, doi:10.1111/trf.15113 (2019).
- 152 Ganzel, C., Becker, J., Mintz, P. D., Lazarus, H. M. & Rowe, J. M. Hyperleukocytosis, leukostasis and leukapheresis: practice management. *Blood Rev* **26**, 117-122, doi:10.1016/j.blre.2012.01.003 (2012).
- 153 Cecyn, K. Z., Seber, A., Ginani, V. C., Goncalves, A. V., Caram, E. M., Oguro, T., Oliveira, O. M., Carvalho, M. M. & Bordin, J. O. Large-volume leukapheresis for peripheral blood progenitor cell collection in low body weight pediatric patients: a single center experience. *Transfus Apher Sci* **32**, 269-274, doi:10.1016/j.transci.2004.07.015 (2005).
- 154 Blum, W. & Porcu, P. Therapeutic apheresis in hyperleukocytosis and hyperviscosity syndrome. *Semin Thromb Hemost* **33**, 350-354, doi:10.1055/s-2007-976170 (2007).
- 155 Sigurbjornsson, F. T. & Bjarnason, I. Leukocytapheresis for the treatment of IBD. *Nat Clin Pract Gastroenterol Hepatol* **5**, 509-516, doi:10.1038/ncpgasthep1209 (2008).
- 156 Hanai, H., Takeda, Y., Eberhardson, M., Gruber, R., Saniabadi, A. R., Winqvist, O. & Lofberg, R. The mode of actions of the Adacolumn therapeutic

- leucocytapheresis in patients with inflammatory bowel disease: a concise review. *Clin Exp Immunol* **163**, 50-58, doi:10.1111/j.1365-2249.2010.04279.x (2011).
- 157 Saniabadi, A. R., Tanaka, T., Yamamoto, T., Kruis, W. & Sacco, R. Granulomonocytapheresis as a cell-dependent treatment option for patients with inflammatory bowel disease: Concepts and clinical features for better therapeutic outcomes. *J Clin Apher* **34**, 51-60, doi:10.1002/jca.21670 (2019).
- 158 Takakura, M., Shimizu, M., Mizuta, M., Inoue, N., Tasaki, Y., Ohta, K., Furuichi, K., Wada, T. & Yachie, A. Successful treatment of rituximab- and steroid-resistant nephrotic syndrome with leukocytapheresis. *J Clin Apher* **33**, 409-411, doi:10.1002/jca.21613 (2018).
- 159 Miyazono, A., Abe, J., Ogura, M., Sato, M., Fujimaru, T., Kamei, K. & Ito, S. Successful remission induced by plasma exchange combined with leukocytapheresis against refractory systemic juvenile idiopathic arthritis. *Eur J Pediatr* **173**, 1557-1560, doi:10.1007/s00431-013-2093-5 (2014).
- 160 Padmanabhan, A. Cellular collection by apheresis. *Transfusion* **58 Suppl 1**, 598-604, doi:10.1111/trf.14502 (2018).
- 161 Nikolajeva, O., Mijovic, A., Hess, D., Tatam, E., Amrolia, P., Chiesa, R., Rao, K., Silva, J. & Veys, P. Single-donor granulocyte transfusions for improving the outcome of high-risk pediatric patients with known bacterial and fungal infections undergoing stem cell transplantation: a 10-year single-center experience. *Bone Marrow Transplant* **50**, 846-849, doi:10.1038/bmt.2015.53 (2015).

- 162 Price, T. H., Boeckh, M., Harrison, R. W., McCullough, J., Ness, P. M., Strauss, R. G., Nichols, W. G., Hamza, T. H., Cushing, M. M., King, K. E., Young, J. A., Williams, E., McFarland, J., Holter Chakrabarty, J., Sloan, S. R., Friedman, D., Parekh, S., Sachais, B. S., Kiss, J. E. & Assmann, S. F. Efficacy of transfusion with granulocytes from G-CSF/dexamethasone-treated donors in neutropenic patients with infection. *Blood* **126**, 2153-2161, doi:10.1182/blood-2015-05-645986 (2015).
- 163 Nair, S. K., Driscoll, T., Boczkowski, D., Schmittling, R., Reynolds, R., Johnson, L. A., Grant, G., Fuchs, H., Bigner, D. D., Sampson, J. H., Gururangan, S. & Mitchell, D. A. Ex vivo generation of dendritic cells from cryopreserved, post-induction chemotherapy, mobilized leukapheresis from pediatric patients with medulloblastoma. *J Neurooncol* **125**, 65-74, doi:10.1007/s11060-015-1890-2 (2015).
- 164 Maude, S. L., Laetsch, T. W., Buechner, J., Rives, S., Boyer, M., Bittencourt, H., Bader, P., Verneris, M. R., Stefanski, H. E., Myers, G. D., Qayed, M., De Moerloose, B., Hiramatsu, H., Schlis, K., Davis, K. L., Martin, P. L., Nemecek, E. R., Yanik, G. A., Peters, C., Baruchel, A., Boissel, N., Mechinaud, F., Balduzzi, A., Krueger, J., June, C. H., Levine, B. L., Wood, P., Taran, T., Leung, M., Mueller, K. T., Zhang, Y., Sen, K., Lebwohl, D., Pulsipher, M. A. & Grupp, S. A. Tisagenlecleucel in Children and Young Adults with B-Cell Lymphoblastic Leukemia. *N Engl J Med* **378**, 439-448, doi:10.1056/NEJMoa1709866 (2018).

- 165 Ceppi, F., Rivers, J., Annesley, C., Pinto, N., Park, J. R., Lindgren, C., Mgebroff, S., Linn, N., Delaney, M. & Gardner, R. A. Lymphocyte apheresis for chimeric antigen receptor T-cell manufacturing in children and young adults with leukemia and neuroblastoma. *Transfusion* **58**, 1414-1420, doi:10.1111/trf.14569 (2018).
- 166 Diaz, M. A., Garcia-Sanchez, F., Lillo, R., Vicent, M. G., Vicario, J. L. & Madero, L. Large-volume leukapheresis in pediatric patients: pre-apheresis peripheral blood CD34+ cell count predicts progenitor cell yield. *Haematologica* **84**, 32-35 (1999).
- 167 Karow, A., Wilhelm, A., Ammann, R. A., Baerlocher, G. M., Pabst, T., Mansouri Taleghani, B., Roessler, J. & Leibundgut, K. Peripheral blood progenitor cell collection in pediatric patients optimized by high pre-apheresis count of circulating CD34+ cells and high blood flow. *Bone Marrow Transplant* **54**, 885-893, doi:10.1038/s41409-018-0353-8 (2019).
- 168 Ribeil, J. A., Hacein-Bey-Abina, S., Payen, E., Magnani, A., Semeraro, M., Magrin, E., Caccavelli, L., Neven, B., Bourget, P., El Nemer, W., Bartolucci, P., Weber, L., Puy, H., Meritet, J. F., Grevent, D., Beuzard, Y., Chretien, S., Lefebvre, T., Ross, R. W., Negre, O., Veres, G., Sandler, L., Soni, S., de Montalembert, M., Blanche, S., Leboulch, P. & Cavazzana, M. Gene Therapy in a Patient with Sickle Cell Disease. *N Engl J Med* **376**, 848-855, doi:10.1056/NEJMoa1609677 (2017).
- 169 Thompson, A. A., Walters, M. C., Kwiatkowski, J., Rasko, J. E. J., Ribeil, J. A., Hongeng, S., Magrin, E., Schiller, G. J., Payen, E., Semeraro, M., Moshous, D.,

- Lefrere, F., Puy, H., Bourget, P., Magnani, A., Caccavelli, L., Diana, J. S., Suarez, F., Monpoux, F., Brousse, V., Poirot, C., Brouzes, C., Meritet, J. F., Pondarre, C., Beuzard, Y., Chretien, S., Lefebvre, T., Teachey, D. T., Anurathapan, U., Ho, P. J., von Kalle, C., Kletzel, M., Vichinsky, E., Soni, S., Veres, G., Negre, O., Ross, R. W., Davidson, D., Petrusich, A., Sandler, L., Asmal, M., Hermine, O., De Montalembert, M., Hacein-Bey-Abina, S., Blanche, S., Leboulch, P. & Cavazzana, M. Gene Therapy in Patients with Transfusion-Dependent beta-Thalassemia. *N Engl J Med* **378**, 1479-1493, doi:10.1056/NEJMoa1705342 (2018).
- 170 Sisson, T. R., Whalen, L. E. & Telek, A. The blood volume of infants. II. The premature infant during the first year of life. *J Pediatr* **55**, 430-446, doi:10.1016/s0022-3476(59)80281-x (1959).
- 171 Maitta, R. W. Current state of apheresis technology and its applications. *Transfus Apher Sci* **57**, 606-613, doi:10.1016/j.transci.2018.09.009 (2018).
- 172 Michon, B., Moghrabi, A., Winikoff, R., Barrette, S., Bernstein, M. L., Champagne, J., David, M., Duval, M., Hume, H. A., Robitaille, N., Belisle, A. & Champagne, M. A. Complications of apheresis in children. *Transfusion* **47**, 1837-1842, doi:10.1111/j.1537-2995.2007.01405.x (2007).
- 173 McLeod, B. C., Sniecinski, I., Ciavarella, D., Owen, H., Price, T. H., Randels, M. J. & Smith, J. W. Frequency of immediate adverse effects associated with therapeutic apheresis. *Transfusion* **39**, 282-288, doi:10.1046/j.1537-2995.1999.39399219285.x (1999).

- 174 Woloskie, S., Armelagos, H., Meade, J. M. & Haas, D. Leukodepletion for acute lymphocytic leukemia in a three-week-old infant. *J Clin Apher* **16**, 31-32, doi:10.1002/jca.1006 (2001).
- 175 Sethu, P., Sin, A. & Toner, M. Microfluidic diffusive filter for apheresis (leukapheresis). *Lab Chip* **6**, 83-89, doi:10.1039/b512049g (2006).
- 176 Lombodorj, B., Tseng, H. C., Chang, H.-Y., Lu, Y.-W., Tumurpurev, N., Lee, C.-W., Ganbat, B., Wu, R.-G. & Tseng, F.-G. High-Throughput White Blood Cell (Leukocyte) Enrichment from Whole Blood Using Hydrodynamic and Inertial Forces. *Micromachines* **11**, 275 (2020).
- 177 Gifford, S. C., Spillane, A. M., Vignes, S. M. & Shevkoplyas, S. S. Controlled incremental filtration: a simplified approach to design and fabrication of high-throughput microfluidic devices for selective enrichment of particles. *Lab Chip* **14**, 4496-4505, doi:10.1039/c4lc00785a (2014).
- 178 Xia, H., Strachan, B. C., Gifford, S. C. & Shevkoplyas, S. S. A high-throughput microfluidic approach for 1000-fold leukocyte reduction of platelet-rich plasma. *Sci Rep* **6**, 35943, doi:10.1038/srep35943 (2016).
- 179 Gifford, S. C., Strachan, B. C., Xia, H., Voros, E., Torabian, K., Tomasino, T. A., Griffin, G. D., Lichtiger, B., Aung, F. M. & Shevkoplyas, S. S. A portable system for processing donated whole blood into high quality components without centrifugation. *Plos One* **13**, e0190827, doi:10.1371/journal.pone.0190827 (2018).
- 180 Strachan, B. C., Xia, H., Voros, E., Gifford, S. C. & Shevkoplyas, S. S. Improved expansion of T cells in culture when isolated with an equipment-free, high-

- throughput, flow-through microfluidic module versus traditional density gradient centrifugation. *Cytotherapy* **21**, 234-245, doi:10.1016/j.jcyt.2018.12.004 (2019).
- 181 Voros, E., Lu, M., Lezzar, D. & Shevkoplyas, S. S. Centrifugation-free washing reduces buildup of potassium and free hemoglobin in washed red blood cells after the procedure. *Am J Hematol* **93**, E389-E391, doi:10.1002/ajh.25277 (2018).
- 182 Schwartz, J., Padmanabhan, A., Aqui, N., Balogun, R. A., Connelly-Smith, L., Delaney, M., Dunbar, N. M., Witt, V., Wu, Y. & Shaz, B. H. Guidelines on the Use of Therapeutic Apheresis in Clinical Practice-Evidence-Based Approach from the Writing Committee of the American Society for Apheresis: The Seventh Special Issue. *J Clin Apher* **31**, 149-162, doi:10.1002/jca.21470 (2016).
- 183 Thapa, N., Pham, R., Cole, C., Meinershagen, M., Bowman, P. W. & Ray, A. Therapeutic leukocytapheresis in infants and children with leukemia and hyperleukocytosis: A single institution experience. *J Clin Apher* **33**, 316-323, doi:10.1002/jca.21610 (2018).
- 184 Pagano, D., Milojevic, M., Meesters, M. I., Benedetto, U., Bolliger, D., von Heymann, C., Jeppsson, A., Koster, A., Osnabrugge, R. L., Ranucci, M., Ravn, H. B., Vonk, A. B. A., Wahba, A. & Boer, C. 2017 EACTS/EACTA Guidelines on patient blood management for adult cardiac surgery. *Eur J Cardiothorac Surg* **53**, 79-111, doi:10.1093/ejcts/ezx325 (2018).
- 185 Lake, C. L. & Booker, P. D. *Pediatric cardiac anesthesia*. 4 edn, 228–252 (Lippincott Williams & Wilkins, 2005).

- 186 Alanmanou, E., Deutsch, N., Kartha, V. M. & Schwartz, J. M. in *Critical Heart Disease in Infants and Children* 213-231. e214 (Elsevier, 2019).
- 187 Boasquevisque, C. H., Yildirim, E., Waddel, T. K. & Keshavjee, S. Surgical techniques: lung transplant and lung volume reduction. *Proc Am Thorac Soc* **6**, 66-78, doi:10.1513/pats.200808-083GO (2009).
- 188 Sollier, E., Murray, C., Maoddi, P. & Di Carlo, D. Rapid prototyping polymers for microfluidic devices and high pressure injections. *Lab Chip* **11**, 3752-3765, doi:10.1039/c1lc20514e (2011).
- 189 Lissandrello, C., Dubay, R., Kotz, K. T. & Fiering, J. Purification of Lymphocytes by Acoustic Separation in Plastic Microchannels. *SLAS Technol* **23**, 352-363, doi:10.1177/2472630317749944 (2018).
- 190 Lu, M., Lezzar, D. L., Voros, E. & Shevkoplyas, S. S. Traditional and emerging technologies for washing and volume reducing blood products. *J Blood Med* **10**, 37-46, doi:10.2147/JBM.S166316 (2019).
- 191 Voros, E., Piety, N. Z., Strachan, B. C., Lu, M. & Shevkoplyas, S. S. Centrifugation-free washing: A novel approach for removing immunoglobulin A from stored red blood cells. *Am J Hematol* **93**, 518-526, doi:10.1002/ajh.25026 (2018).
- 192 Rozenberg, G. *Microscopic Haematology: a practical guide for the laboratory*. 106-138 (Elsevier Australia, 2011).